Nuclear structure in odd-odd nuclei, $144 \leqslant A \leqslant 194$

A. K. Jain

Department of Physics, University of Roorkee, Roorkee 247667, India

R. K. Sheline and D. M. Headly

Departments of Chemistry and Physics, Florida State University, Tallahassee, Florida 32306

P. C. Sood

Department of Physics, Banaras Hindu University, Varanasi 221005, India

D. G. Burke

Department of Physics and Astronomy, McMaster University, Hamilton, Ontario, Canada L8S 4M1

I. Hřivnácová, J. Kvasil, and D. Nosek

Department of Nuclear Physics, Charles University, V Holesovickach 2, 180 00 Prague 8, Czech Republic

R. W. Hoff

Isotope Sciences Division, Lawrence Livermore National Laboratory, Livermore, California 94551

A comprehensive review of the present understanding, both theoretical and experimental, of intrinsic and rotational level structures in medium-heavy deformed odd-odd nuclei is presented. A discussion of the various experimental methods is presented, emphasizing the need for a variety of experimental approaches. The odd-odd nuclei that are immediately amenable to fruitful additional study are pointed out. A discussion of the intrinsic level structures, Gallagher-Moszkowski (GM) splittings, Newby (N) shifts, and role of the residual p-n interaction is presented. Currently available data in the rare-earth region allow the empirical determination of 137 GM splittings and 36 N shifts for 25 odd-odd nuclei in the mass region $152 \leqslant A \leqslant 188$. A new parametrization of the residual p-n interaction is presented which also takes into account the 27 GM splittings and 12 N shifts from the actinide region. Newly discovered features of rotational bands, such as odd-even staggering, and other high-spin phenomena, such as signature inversion and delay in bandcrossing frequency, are discussed. The role of higher-order Coriolis coupling is pointed out. Systematics of the two-quasiparticle excitations, shape coexistence, isomers, and four-quasiparticle states are presented. Calculated results of the two-quasiparticle intrinsic excitations using two methods, the intrinsic level spacings for odd-A neighboring nuclei and the quasiparticle-plus-phonon coupling model, are compared with experiment. [S0034-6861(98)00203-7]

CONTENTS

 © 1998 The American Physical Society

I. INTRODUCTION

The level structures of odd-odd deformed nuclei are among the most complex topics in nuclear physics and also among the least studied. The last major review in this area was published more than two decades ago by Boisson *et al.* (1976). It focused upon the parametrization of the residual proton-neutron (p-n) interaction and was based on the empirical knowledge of some 50 Gallagher-Moszkowski (GM) splittings and about 19 Newby (N) shifts in the rare-earth region. A similar but smaller study of rare-earth odd-odd nuclei was also published the same year by Elmore and Alford (1976). Both studies pointed out the scarcity of experimental data as well as the theoretical difficulty of reproducing simultaneously the GM splittings and the N shifts.

Many new data have been reported since then. A compilation of the level structures of odd-odd deformed nuclei in the mass range $144 \leqslant A \leqslant 194$, including energies and suggested configurations, is being published separately by Headly *et al.* (1997). It constitutes the database for the discussion in this review.

In view of the developments over the past two decades, the aims of this review are much broader than those of Boisson *et al.* and Elmore and Alford in 1976. While a major theme of the present review continues to be the parametrization of the residual p-n interaction, using the newer extended database (Headly *et al.*, 1998), and a discussion of the related issues, we also focus upon other important aspects of odd-odd deformed nuclei that have been the topics of recent research. Section II contains a brief discussion of experimental techniques, including the important role of stripping and pickup reactions, and also the newly rediscovered importance of allowed unhindered beta decays in the assignment of configurations. Section III then presents a discussion of the p-n interaction, its parametrization, and the modeling of level structures of well-deformed prolate nuclei. The various unresolved issues related to GM splittings and N shifts are also discussed in this section, as are the level energies of intrinsic two-quasiparticle (2qp) excitations based on calculations using level spacings for odd-A neighboring nuclei.

In Sec. IV the systematics of 2qp states in rare-earth odd-odd nuclei are presented, and other phenomena such as long-lived isomers, shape coexistence (octupole, superdeformed, and oblate-prolate), and four-quasiparticle (4qp) states are examined in the context of odd-odd nuclei. The development of techniques utilizing heavy-ion-induced reactions in high-spin spectroscopy has led to the observation of new rotational features in odd-odd deformed nuclei, including odd-even staggering, signature inversion, and delay in band-crossing frequencies. These phenomena, and the role of high-order Coriolis coupling in explaining them, are discussed in Sect. V.

A fully microscopic understanding of deformed odd-odd nuclei is a cherished dream, and a decent start towards this goal was made by Bennour *et al.* (1987). We present in Sec. VI the brief outlines of a microscopic model based on the quasiparticle-phonon-plus-rotor model; couplings to vibrational phonons of the even-even core are included. We also present the level energies of intrinsic 2qp excitations based on the quasiparticle-plus-phonon model. The experimental picture, including the availability and accessibility of odd-odd nuclei, and suggestions for possible future studies aiming at a complete spectroscopy of odd-odd nuclei are emphasized throughout the review. Conclusions are found in Sec. VII.

II. EXPERIMENTAL TECHNIQUES

A. Need for as many nuclear probes as possible

In order to characterize nuclear states in the detailed manner needed to test available models, it is necessary to make use of many different complementary techniques. Properties such as spins, magnetic dipole moments, and electric quadrupole moments have been obtained from various resonance techniques such as atomic-beam magnetic resonance, electron-spin resonance, nuclear magnetic resonance, etc., and more recently from collinear laser-beam experiments (e.g., see Wallmeroth *et al.*, 1989). Such information is available most commonly for ground states, but also for some isomeric states.

Traditionally, one of the most useful methods of establishing level energies, spins, and parities relative to the ground-state values is the use of standard gamma-ray and conversion-electron spectroscopy, after populating the levels from radioactive decays, nuclear reactions, Coulomb excitation, etc. In order to unravel the collective versus single-particle characteristics of the levels, it is important to have information also on transition probabilities connecting specific initial and final states. Evidence for collective motions is often found from B(Eλ) values, obtained from Coulomb excitation cross sections, or from the many techniques for measuring lifetimes of nuclear states. On the other hand, cross sections for single-nucleon transfer reactions can give quantitatively the percentage admixtures of specific single-particle configurations in a level.

With the level densities observed in heavy deformed nuclei, it is important to strive for the best experimental resolution possible. One class of experiments that has been very productive, because of the excellent resolution attainable, involves the use of curved-crystal gamma-ray spectrometers to observe γ radiation from (n,γ) reactions. Results from such experiments, combined with high-resolution conversion-electron data, have been used to establish complex level schemes.

Especially when performed with epithermal neutrons in so-called averaged resonance capture (ARC) experiments, the (n,γ) reaction is nonselective, in that all the levels within a specific range of spin for each parity can have observable populations, up to a certain excitation energy. It has been stressed (Heyde, 1994) that in order to obtain the best understanding of the structure of a nucleus one should combine results from nonselective methods such as (n,γ) with data from highly selective processes, such as single-nucleon transfer reactions. In practice, this approach has proven to be very successful. Large collaborative studies of ^{166}Ho (Motz *et al.*, 1967) and ^{170}Tm (Sheline *et al.*, 1966) performed in the 1960s proved to be definitive works on the structures of these nuclides for several decades, and only in recent years have the interpretations been extended. More detailed descriptions of some of these processes are given in the following subsections.

B. Particle transfer reactions

One of the most useful techniques for determining nuclear structures for species not too far from stability is the use of single-nucleon transfer reactions such as (d,p), (d,t), $(^3\mathrm{He},d)$, (t,α), etc. In order to obtain adequate resolution for heavy deformed nuclei, a magnetic spectrograph is usually necessary to analyze the reaction products. The spectrum of charged particles obtained is, in principle, relatively easy to analyze because there is a one-to-one correspondence between the peak position in the spectrum and the excitation energy of the level in the residual nucleus. With a properly calibrated spectrograph, reaction Q values and excitation energies can be readily obtained. The cross sections vary with reaction angle in a manner that depends upon the orbital angular momentum ℓ transferred, so measured angular distributions can yield ℓ values. If the incident beam is polarized one can also obtain the total transferred angular momentum j.

These reactions are particularly useful for deformed nuclei because the various members of a rotational band have a characteristic pattern of cross sections, called a "fingerprint," which is determined by the wave function of the transferred nucleon (Vergnes and Sheline, 1963; Elbek and Tjøm, 1969). The cross section for transfer of a single nucleon, starting from the ground state of an odd-mass target nucleus with I_0, K_0 and leading to a rotational band member of spin I_f, K_f in an odd-odd deformed nucleus is (Jones, 1969; Thompson *et al.*, 1975)

$$\frac{d\sigma}{d\Omega}=N\sum_{j,\ell}\left[\sum_i a_i(C_{j\ell})_i P_i\langle I_0K_0 j\Delta K|I_fK_f\rangle\right]^2\left(\frac{d\sigma}{d\Omega}\right)_{\mathrm{DW}}. \tag{1}$$

Here N is a normalization constant for the distorted-wave Born approximation (DWBA) cross sections, $(d\sigma/d\Omega)_{\mathrm{DW}}$. The $C_{j\ell}$ values are expansion coefficients describing the Nilsson orbital of the transferred nucleon. The quantity P_i^2 is a pairing factor, which for a pickup reaction is V_i^2, the occupation probability in the target for the transferred nucleon. For a stripping reaction, $P_i^2=U_i^2=1-V_i^2$, the "emptiness" probability. The final state is assumed to be a Coriolis-mixed configuration, with amplitudes a_i for the various Nilsson orbitals for the transferred nucleon. Here it is assumed that the target ground state is a pure single-particle configuration. A more general expression, valid for the case of mixed target ground states, has recently been given (Garrett and Burke, 1993).

In this description, it is assumed that the odd target nucleon remains unchanged, and the transferred nucleon, $j,\Delta K$, is coupled to I_0,K_0 to form bands with projections on the symmetry axis being $K_f=K_0+|\Delta K|$ and $K_f=|K_0-|\Delta K||$. To first order, before mixing effects are considered, the summed transition strengths for these two bands are the same. The selectivity of the process arises from the fact that the only 2qp states populated are those with the unpaired nucleon of the odd-mass target as one of the two quasiparticles. The transferred nucleon can be a proton or a neutron, depending on the reaction used, and quasiparticle states of hole or particle character can be distinguished. This is because stripping reactions, such as (d,p) or $(^3\mathrm{He},d)$, have larger cross sections for orbitals above the Fermi surface, while pickup reactions, such as (d,t) and (t,α), favor those below the Fermi surface that have a greater "fullness" factor V_i^2.

One of the important aspects of Eq. (1) is that the wave-function amplitudes $C_{j\ell}$ enter directly and can produce vastly different patterns of cross sections for two different transferred nucleons, even though the other quantum numbers such as I_f and K_f are the same. For example, the $1/2^-[521]$ and $1/2^-[510]$ neutrons have quite different wave functions and therefore have markedly different fingerprints. This can be seen clearly in Fig. 1, which compares the sets of (d,t) cross sections at $\theta=90°$ for these two orbitals predicted for the case of an even-even target where the bands would be populated in an odd-N final nucleus. For the $1/2^-[521]$ band the spin-1/2 member is expected to have a cross section an order of magnitude larger than that for spin 3/2, while for the $1/2^-[510]$ band it should be about a factor of 30 *smaller*. Experimental results measured in Yb nuclei for these bands by Burke *et al.* (1966), seen in the lower part of Fig. 1, show that the predicted patterns agree very well with those observed.

A recent case that exemplifies the manner in which this technique can distinguish between different 2qp configurations in an odd-odd final nucleus is that of the well-studied nuclide ^{166}Ho. For some years the K^π

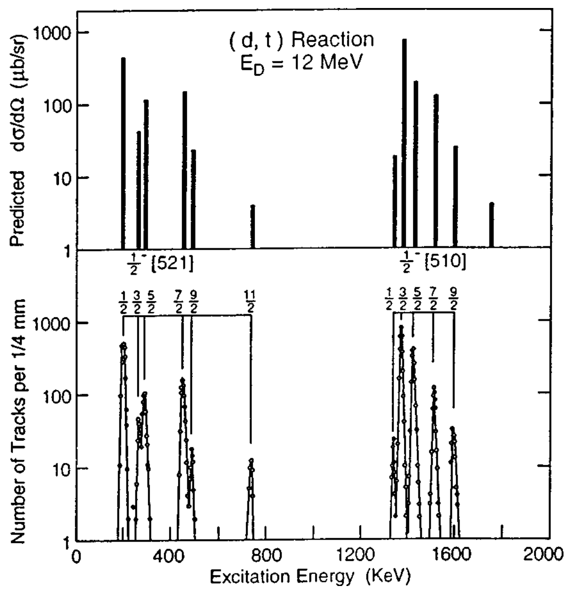

FIG. 1. Comparison of predicted and observed "fingerprints" (patterns of cross sections for various members of rotational bands) for the (d,t) reaction to the $1/2^-[521]$ and $1/2^-[510]$ bands in ytterbium nuclei. Values shown are differential cross sections at $\theta=90°$. It can be seen that the patterns are strikingly different for the two bands, and the predictions for each case are in very good agreement with experimental data.

$=1^+$ band at 426 keV had been assigned as the $7/2^-[523]_p-5/2^-[523]_n$ configuration because of the small logft value of 5.12 observed in beta decay. (In this review we shall always write a 2qp configuration with proton quantum numbers first.) This assignment was problematic from the point of view of energy systematics, and model predictions suggested that the 426-keV band was more likely to be predominantly the $7/2^-[523]_p-5/2^-[512]_n$ configuration, with a small ($\sim$10%) $7/2^-[523]_p-5/2^-[523]_n$ admixture, which would explain the observed logft value. Sood and Burke (1995) recently examined the ^{165}Ho$(d,p)^{166}$Ho data available from an early experiment of Struble *et al.* (1965), and showed that the (d,p) results are inconsistent with the previously adopted assignments. Upon consideration of these data, we should interpret the 426-keV band as predominantly the $7/2^-[523]_p-5/2^-[512]_n$ configuration, and the $K^\pi=1^+$ band at 568 keV probably contains the main $7/2^-[523]_p-5/2^-[523]_n$ component.

In practice, this method has been spectacularly successful in identifying many single-particle excitations in a wide range of nuclei because the cross sections predicted by Eq. (1) are in good agreement with those observed, at least for strongly populated levels (the intensities for weakly populated members of a band are often affected by multistep processes in the reaction mechanism). It is also sometimes found that a band has the expected set of relative intensities among the various members, but that the absolute cross sections are less than predicted by Eq. (1). This can occur because other types of mixing may cause the band to have only a fraction of the 2qp admixture assumed in the calculation. This has proven to be a useful means of extracting percentage admixtures for some of the components in mixed states.

The use of single-nucleon transfer reactions has been very well tested across the deformed rare-earth region by measurements on even-even targets to study odd-mass final nuclei. In many cases, analysis of data for odd-odd nuclides has been aided considerably by the availability of similar reaction data leading to odd-mass neighbors on one or both sides [e.g., the (t,α) data for ^{178}Lu (Burke *et al.*, 1993)]. In such cases, cross sections for various configurations can be predicted with greater confidence.

Particle transfer reactions of other types have been less useful in practice for various reasons. The two-neutron transfer reactions such as (t,p) and (p,t), which have been very important for studies of even-even and some odd-A nuclides, have not been widely applied to odd-odd cases because the required targets are radioactive. (An exception is the target of long-lived ^{176}Lu, on which such experiments have been performed and have provided very useful information for the structure of ^{174}Lu (Struble *et al.*, 1978) and ^{178}Lu (Girshick *et al.*, 1981).)

Other multinucleon transfer reactions, such as (d,α), (p,α), $(^3\text{He},p)$, etc., and charge-exchange reactions such as $(^3\text{He},t)$ have disadvantages of both an experimental and a theoretical character. It is much more difficult to acquire good data because the cross sections are almost two orders of magnitude smaller than for most single-nucleon transfer reactions. Furthermore, since the reaction mechanism is not as well understood, the interpretation of results is more difficult. One exception to this general statement may be the (p,α) reaction. Although the cross sections are small, it is found empirically that the (p,α) cross sections to levels in a specific final nucleus correlate well with the (t,α) ones to the same final states (Shahabuddin *et al.*, 1978). Thus, in some cases the (p,α) data have yielded very useful nuclear structure information where the (t,α) reaction would be difficult because the target needed is unstable. An example of this can be found in the study of ^{158}Tb levels by Burke *et al.* (1989), which exploited the complementarity of different reactions such as (d,t), $(^3\text{He},\alpha)$, and (p,α). Spectra from the (d,t) and (p,α) reactions of that study are shown in Figs. 2 and 3, respectively, where it can be seen that the selectivity of the process causes quite different bands to be populated in the two reactions. The (d,t) reaction removes a neutron from ^{159}Tb, which has its odd proton in the $3/2^+[411]$ orbital, so all the bands populated in ^{158}Tb have the odd proton in this orbital. On the other hand, the ground state of the ^{161}Dy target used for the (p,α) study has an odd neutron in the $5/2^+[642]$ orbital, so all populated bands must have this neutron. Thus, only the $K^\pi=1^+$ and $K^\pi = 4^+$, $3/2^+[411]_p\pm5/2^+[642]_n$ bands are seen in both reactions.

C. Neutron capture gamma-ray spectroscopy

In thermal-neutron capture reactions that produce odd-odd nuclei, s-wave capture populates states with an-

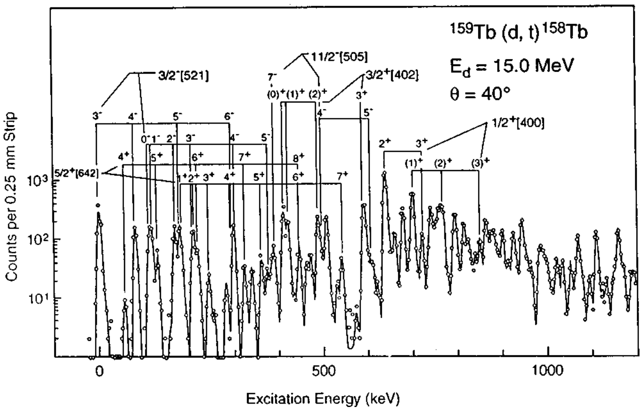

FIG. 2. Spectrum from the ^{159}Tb$(d,t)^{158}$Tb reaction in the study by Burke *et al.* (1989). Each rotational band assignment is labeled by the Nilsson orbital of the transferred neutron, which is coupled to the $3/2^{+}[411]$ proton of the target ground state.

gular momentum $j \pm 1/2$, where j is the angular momentum of the target. As decay proceeds down the γ cascades, the range of angular momenta widens somewhat and low-lying levels within a range of about 4–5 units of angular momentum are populated. Beyond this, thermal-neutron capture is quite unselective with respect to other level characteristics, e.g., configuration. Averaged resonance neutron capture reactions, in which one uses an expressly nonmonoenergetic neutron beam with average energy on the order of several keV, guarantee population of levels within a certain range of spin and parity, given the proper conditions of averaging. Generally, these conditions include the necessity of more than 100 capture states' being populated. This assurance of level population with the ARC technique is unique among the various nuclear reactions.

Neutron capture γ-ray spectroscopy is a particularly important technique due to the high levels of sensitivity and resolution afforded by present day spectrometers installed at high-flux research reactors, e.g., the spectroscopic laboratory for measurements with thermal neutrons at the Institut Laue-Langevin (ILL) in Grenoble, France. In this category of measurement, we include the measurement of both γ rays and conversion electrons arising from the decay of the capture state(s). The ILL is the premier laboratory in the world today for thermal-neutron capture spectroscopy by virtue of the precision and sensitivity of its curved-crystal spectrometers, GAMS1 and GAMS2/3 (Koch *et al.*, 1980). The latter is a double spectrometer that provides for simultaneous diffraction of different parts of the γ-ray beam in opposite directions, thereby improving the resolution of the instrument by compensating for any lateral movement of the sample. The two spectrometers allow measurement of γ energies and intensities in the range 0–1500 keV. Typical resolution (FWHM actually obtained in practice) for GAMS1 with γ rays of 30–500 keV is 5.6 $\times 10^{-6} E_{\gamma}^{2}(\mathrm{keV})/n$, where n is the order of diffraction. Similarly, resolution for GAMS2/3 with γ rays of 150–1500 keV is $2.0\times 10^{-6} E_{\gamma}^{2}(\mathrm{keV})/n$. A second factor in the power of the spectrometers at the ILL is the very high neutron flux in the target region, namely, $5.5\times 10^{14}(\mathrm{n/cm^2})/\mathrm{sec}$. The improved sensitivity of the ILL GAMS spectrometers becomes particularly evident for secondary γ transitions with energies above 200 keV. As an example, in a recent ILL experiment with the reaction ^{169}Tm$(n,\gamma)^{170}$Tm (Hoff, 1994), 422 transitions between 200 keV and 1000 keV were detected in the γ

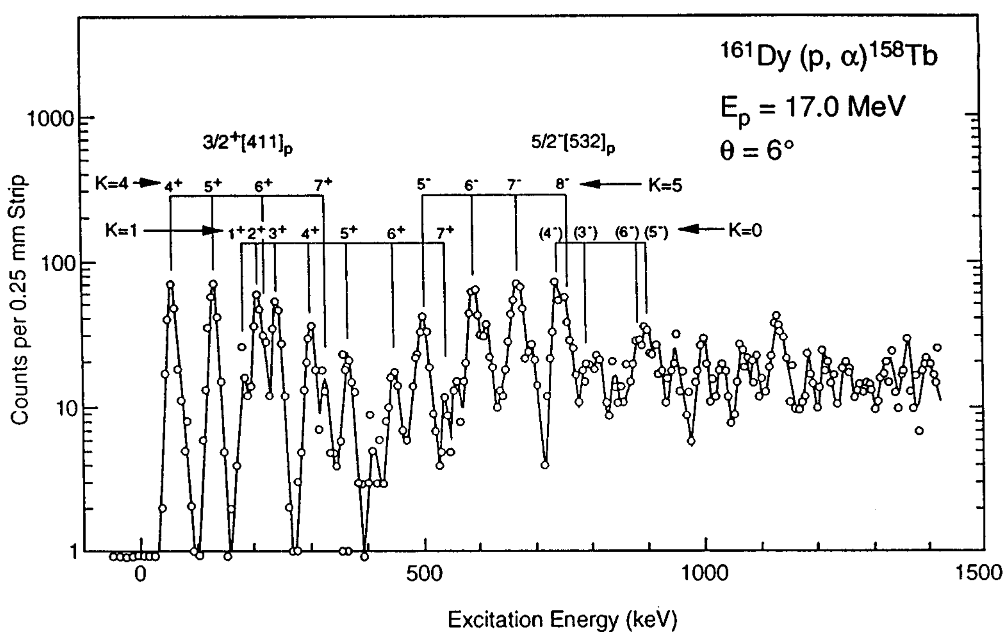

FIG. 3. Spectrum from the ^{161}Dy$(p,\alpha)^{158}$Tb reaction in the study by Burke *et al.* (1989). Each rotational band assignment is labeled by the Nilsson orbital of the transferred proton, which is coupled to the $5/2^{+}[642]$ neutron of the target ground state. Due to the selectivity of the reactions, the only bands populated in the spectra of Fig. 2 *and* Fig. 3 are the $K^{\pi}=1^{+}$ and $K^{\pi}=4^{+}$, $3/2^{+}[411]_{\pi}\pm 5/2^{+}[642]_{\nu}$. Thus the ground-state band is not populated in this spectrum.

spectrum, whereas 115 lines were reported in the same interval from a 1966 measurement in Risø (Sheline *et al.*, 1966). As an example of the gain in precision of the ILL spectrometers, the mean uncertainty of γ transition energies was 11 eV at 500 keV in the ILL study versus 200 eV in that from Risø. Of the twelve odd-odd nuclei that can be readily populated by neutron capture and that are covered in the present paper (from ^{152}Eu to ^{194}Ir), only six have been the subjects of ILL experiments.

Measurements of primary gamma rays in neutron capture studies, those γ transitions that deexcite the capture state(s) and directly populate relatively low-lying levels, are an important source of data on the energies and existence of excited levels in odd-odd nuclei. Ge detectors are usually used in such measurements. In thermal or single-resonance capture, the capture state is generally dominated by compound-nuclear characteristics and decays in a statistical manner, the spread in intensities being described by a Porter-Thomas distribution with one degree of freedom. Two characteristics of this distribution are a large variation in intensities (typically two orders of magnitude or more) and a most probable intensity of zero. Thus, despite the usefulness of these techniques, some primary transitions will be too weak to detect and the corresponding excited levels will not be indicated in the spectra. Nevertheless, thermal-capture measurements provide some very important data for the interpretation of level structure. These measurements have been made for all of the odd-odd nuclei where the requisite target material is available. Many of these nuclei have also been studied using single-resonance capture. When it is possible to measure γ spectra for ten or twenty resonances, the incidence of missed excited levels is somewhat reduced.

With the ARC technique, targets are irradiated using filtered neutron beams with average energies determined by the materials that constitute the filter. For instance, at the Brookhaven National Laboratory's high-flux beam reactor, two ARC beams are obtained with 2- and 24-keV average energy by transmission through Sc and ^{56}Fe filters, respectively. Tens of grams of target are required. Primary γ rays are detected in a three-crystal pair spectrometer. Typical resolution at 5 MeV is 4.5 keV FWHM. At $E_n=2$ keV, ARC spectra are dominated by s-wave capture and $E1$ primary transitions. On the average, primary $E1$ transitions are a factor of 6 more intense than M1 transitions of comparable energy. Therefore, given proper conditions for averaging, i.e., a sufficiently high level density at the neutron binding energy in the product nucleus, one can expect to observe all states in the product nucleus that can be populated by primary $E1$ transitions up to excitation energies of about 1.5 MeV, where resolution of separate γ peaks becomes difficult due to increasing level densities. Of course, these favored states are all of the same parity. Using the ARC tool, one can examine certain aspects of so-called "complete spectroscopy," at least among levels within a restricted range of spin and parity. This property becomes very useful in evaluating the fidelity of nuclear models from many points of view, e.g., models that predict configuration energy, level density, etc., in odd-odd nuclei.

In a recent report (Hoff, 1994), the odd-odd nuclei of the rare-earth region were surveyed to see how thoroughly their structures had been investigated using present-day facilities for neutron capture studies. The most exhaustive and sensitive searches for secondary transitions have been made on the following nuclei: ^{160}Tb, ^{176}Lu, and ^{182}Ta. In this region, certain of the heavier rare-earth nuclei such as ^{166}Ho, ^{186}Re, and ^{188}Re, have moderately large capture cross sections and might very well yield appreciably more data on secondary transitions following capture if further measurements were made with the GAMS spectrometers at the ILL. It was also found that the conversion electron spectra of ^{160}Tb, ^{166}Ho, ^{182}Ta, and ^{188}Re had not been studied with a sensitive β spectrometer. For each of these nuclei, fewer than 15% of the observed secondary transitions have multipolarities assigned from experimental evidence. On the basis of rotational bands assigned, ^{152}Eu, ^{154}Eu, and ^{176}Lu appear to be the most extensively characterized, while ^{160}Tb and ^{186}Re, of the nuclei populated by neutron capture, seem to offer the greatest opportunities for further study.

D. Gamma-ray coincidence measurements

Gamma-gamma coincidence spectroscopy is an experimental technique of considerable importance to the construction of level schemes. Whereas energies of excited levels can be obtained from transition energies using the Ritz combination principle (Ritz, 1908), and the highly precise γ-ray spectrometers such as the GAMS instruments at the ILL have been very important in establishing level schemes using (n,γ) reactions, the measurement of γ-γ coincidence relationships has become extremely important in determining precise details of most decay schemes.

Gamma coincidence studies have been made with neutron capture reactions, involving relationships of low-energy γ rays with both low-energy and high-energy ones. Only a few odd-odd nuclei have been studied in this manner, e.g., ^{170}Tm (Balodis *et al.*, 1995; Hoff *et al.*, 1996). Another approach to the study of odd-odd nuclei has been to populate their excited levels in light charged-ion reactions, as in the studies of ^{174}Lu (Bruder *et al.*, 1987a, 1987b; Drissi *et al.*, 1990) and of ^{166}Tm (Mannanal *et al.*, 1995), where reactions such as $(p,3n\gamma)$, $(^7\mathrm{Li},3n\gamma)$, and $(\alpha,3n\gamma)$ were employed. In these experiments, in-beam γ spectroscopy, including coincidence measurements, formed the basis for construction of the level schemes. Also of interest in the experiments cited is the employment of a curved-crystal spectrometer for in-beam x- and γ-ray spectroscopy, in addition to the usual Ge(Li) detectors (Perny *et al.*, 1988).

E. Beta decay and allowed unhindered transitions

Beta decay, as a means of populating levels in odd-odd rare-earth nuclei, has provided some useful data on level structure, although these data are of limited scope and quantity. Since the parent level ordinarily has $I^{\pi}=0^{+}$, levels directly populated in the daughter nucleus have a limited range of spin values: $I=0$, 1, or 2. Also, many of the better characterized odd-odd nuclei, those that lie close to β stability, are not populated by β decay. Nevertheless, a group of allowed β decays in the rare-earth region, those with log$ft\leqslant 5.2$, have been shown to involve a single-particle spin-flip transition between the proton and neutron orbitals, with all other quantum numbers unaltered (Sood and Sheline, 1989a). It has been demonstrated that such fast beta decays can yield, in many cases, significant new information, particularly regarding the structures in odd-odd deformed nuclei, in view of the rather unambiguous configurational relationship between such beta-connected states.

It has been observed without exception that Alaga selection rules (Alaga 1955, 1957) apply to the beta decays of odd-odd deformed nuclei. The studies of Gallagher (1960) and Zylicz *et al.* (1967) demonstrate that the additional odd nucleon (in odd-odd nuclei) does not appreciably alter the transition rate of the particle undergoing decay and that the even-mass transitions can be classified according to the asymptotic quantum number selection rules with similar log*ft* values. Recent studies by Sood and Sheline (1989a; 1990a, 1990b) identified 122 such allowed unhindered ("au") decays over the mass region $149\leqslant A\leqslant 190$.

As an example we present in Fig. 4 the experimental log*ft* values for all the known "au" transitions connecting the nuclei of the $_{67}$Ho isotopic sequence with $N>82$. The transition shown in Fig. 4 relates to the $p(h_{11/2})\rightarrow n(h_{9/2})$ transformation in spherical nuclei with $82\leqslant N\leqslant 86$, the [532] orbital pair transformation in the $N=87$ transitional nuclei, and the [523] orbital pair transformation in the well-deformed nuclei with $N>88$. One may view the gradual onset of deformation in this domain by noting that the experimental spin parities for the 67th proton are $11/2^{-}$ in the $N\leqslant 86$ nuclides, $5/2^{-}$ in the $N=87$ nuclides, and $7/2^{-}$ in the $N\geqslant 89$ nuclides. The high-spin isomers, both in ^{152}Ho and in ^{158}Ho, have $I^{\pi}=9^{+}$; however, in ^{152}Ho it results from the coupling of an $11/2^{-}$ proton with a $7/2^{-}$ neutron, while in ^{158}Ho it arises from the coupling of a $7/2^{-}$ proton with an $11/2^{-}$ neutron! Our 30 log*ft* values shown in Fig. 4 include 11 odd-mass and 19 even-mass cases. No systematic or significant difference is observed in the transition rates for "au" decays of the odd-mass and the even-mass nuclei, in agreement with the earlier studies (Gallagher, 1960; Zylicz *et al.*, 1967).

Bunker and Reich (1971) had pointed out that only two orbital pairs, namely, [523] and [514], give rise to "au" transitions in the odd-mass rare-earth nuclei. Examination of the even-mass decays by Sood and Sheline (1989a,b) revealed two more orbital pairs, namely, [532] and [505], which are involved in the even-mass "au" decays of $A\leqslant 154$ and $A\approx 190$ nuclei, respectively. Thus the underlying "au" transitions in decays of odd-odd deformed nuclei may be explicitly written in terms of the asymptotic quantum numbers $\Omega[Nn_3\Lambda\Sigma]$ with $N=5$ for rare-earths as follows:

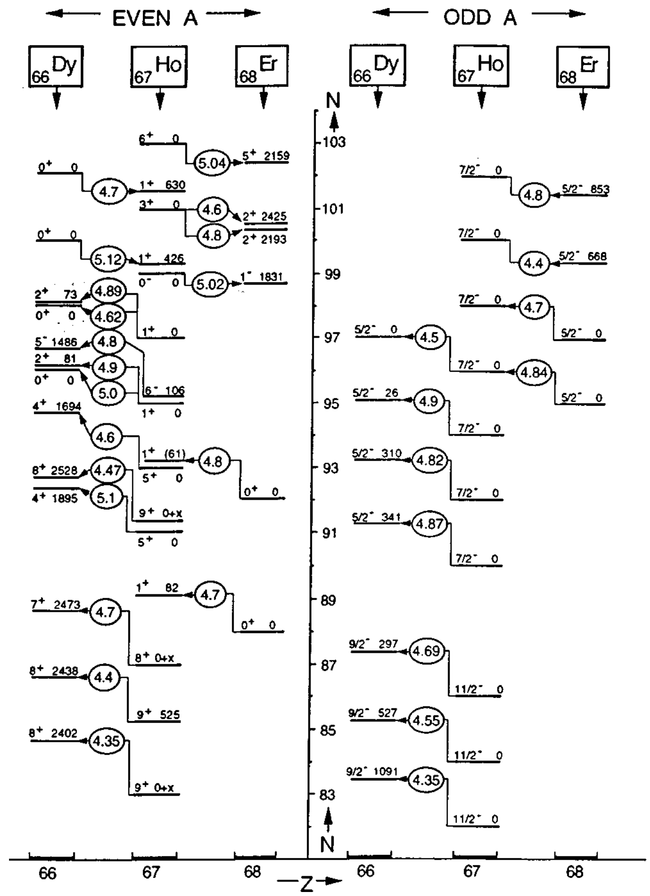

FIG. 4. Beta decays with log$ft\leqslant 5.2$ involving $_{67}$Ho isotopes with $82\leqslant N\leqslant 103$. Numbers on the lines, representing energy levels, denote spin parity I^{π} and level energy in keV. The level position approximately indicates the excitation energy. Circled numbers denote log*ft* values. Arrows towards the right represent β^{-} and those to the left represent β^{+}/EC decays.

$$p:\ (\Lambda+1/2)[5(5-\Lambda)\Lambda\uparrow]\rightleftharpoons n:\ (\Lambda-1/2)[5(5-\Lambda)\Lambda\downarrow],$$
$$\text{with } \Lambda=2 \text{ to } 5. \qquad (2)$$

These allowed, unhindered transitions come about through the interchange of a proton with $\Omega_p=\Lambda+1/2$ and a neutron with $\Omega_n=\Lambda-1/2$. In the case of a deformed, even-even parent, a pair of nucleons is broken in β decay and, for a spin-flip transition, a 1^{+} state in the daughter nucleus may be created (this state lies lower than that with parallel coupling of the angular momenta of the unpaired nucleons). The orbitals [523], [514], [532], and [505] are the transforming orbitals of the nuclei reported to undergo spin-flip transitions in this region. Twenty-two instances of levels being populated by spin-flip β transitions have been identified in which either parent or daughter is an odd-odd nucleus (Sood and Sheline, 1990a). Such "au" decays have provided undisputed configuration assignments to states in many odd-odd nuclei.

Many of the odd-odd nuclei that lie close to β stability either do not have a beta-decaying parent or are populated by decay with low values of Q_β, e.g., $\leqslant 500$ keV. An interesting exception to this situation is the 61.5-min, β-decaying isomer in ^{182}Hf. The isomer is an 8^- level that has a Q_{β^-} value of approximately 1600 keV. Analysis of the γ rays from this decay has led to the identification of five high-spin ($I=7-10$) levels in ^{182}Ta with a range of excitation of 500–1350 keV (Ward *et al.*, 1974).

F. Heavy-ion reactions leading to high-spin states

To study higher-spin states ($I>10$), one must use a reaction in which a larger amount of angular momentum can be transferred to the nucleus. Many experiments have been performed in which higher rotational band members were populated by (d,xn), (α,xn), etc., reactions. There are now several laboratories with large arrays of Compton-suppressed Ge gamma-ray detectors designed to measure cascades of transitions following the population of high-spin states by heavy-ion-induced reactions. The use of heavy ions increases the angular momentum attainable, while the large number of detectors increases the detection efficiency and provides additional information such as multiplicities and angular correlations. Rotational bands have been extended up to spin values as high as $\sim 65\hbar$. Level schemes established from such experiments provide information on moments of inertia, signature splittings, band crossings, etc., which give indications of the single-particle configurations on which the bands are based as well as insights into changes that take place in the structure as a result of the nucleus' being stressed by the high spin. As an example, in a recent study of odd-odd Ho isotopes with the Gammasphere array (Yu *et al.*, 1996), high-spin states up to $42\hbar$ were populated and studied. Such measurements have also led to the discovery of superdeformation and "identical bands" in many nuclides.

The nature of these reactions is such that the residual nuclei populated most favorably are somewhat neutron deficient, and therefore many nuclides not easily studied by other techniques can be reached by this means. Also, due to inherent selectivity, bands that are yrast or near yrast tend to be strongly fed in the deexcitation of the states formed by neutron evaporation, and above a minimal spin value the yrast bands are likely to involve high-j orbitals, e.g., protons from the $h_{11/2}$ shell or neutrons from the $i_{13/2}$ shell, which have large moments of inertia. Low-Ω orbitals from such shells can have steep negative slopes in the Nilsson diagram and thus can be "deformation driving," i.e., the nucleus gains a lower total energy by moving to a larger deformation.

III. LEVEL STRUCTURES IN WELL-DEFORMED PROLATE NUCLEI AND THE RESIDUAL *p-n* INTERACTION

Odd-odd nuclei show a daunting complexity due to the high density of states and the larger number of couplings and interactions possible. For a description of all their features, it will therefore be necessary to consider many effects. However, as we shall see, even a simple model is good enough to bring out the rudimentary features, which may then be further refined. Our survey of data on odd-odd nuclei (Headly *et al.*, 1998) covering $A=144$–194 mostly includes well-deformed nuclei with $156\leqslant A\leqslant 186$ in which nuclear shapes are considered to be prolate deformed. The low-lying level structures of these nuclei can therefore be understood mostly in terms of the simple and straightforward 2qp-plus-axially-symmetric-rotor model. The intrinsic (nonrotational) 2qp states are taken to correspond to the valence proton and neutron single-particle configurations. The residual p-n interaction plays a crucial role in determining the splitting and ordering of the 2qp intrinsic excitations; a rotational band may be built upon each 2qp excitation. In this section, we introduce the basic definitions and the models upon which rests most of the discussion. In particular, we concentrate upon the residual p-n interaction, its parametrization, and calculation of low-lying level structures.

A. Two-quasiparticle rotor model

A detailed description of the two-quasiparticle rotor model may be found in several recent papers such as those of Jain *et al.* (1988, 1989) and Ragnarsson and Semmes (1988). Here, we present a brief description of the 2qp-plus-rotor model for an axially symmetric and reflection-symmetric core. The total Hamiltonian for the odd-odd system is usually written as (Motz et al., 1967)

$$H=H_{\mathrm{intr}}+H_{\mathrm{rot}}. \tag{3}$$

The intrinsic part of the Hamiltonian consists of a deformed axially symmetric average field H_{av} (assumed to be the Nilsson-model Hamiltonian in this review), a short-range proton-neutron interaction V_{pn}, a short-range residual interaction H_{pair} and a long-range residual interaction H_{vib} so that

$$H_{\mathrm{intr}}=H_{\mathrm{av}}+V_{pn}+H_{\mathrm{pair}}+H_{\mathrm{vib}}. \tag{4}$$

The effect of pairing and the vibrational interaction will be mostly ignored in the discussions in this section and the next. The rotational part of the Hamiltonian may be further written as

$$H_{\mathrm{rot}}=\frac{\hbar^2}{2\Im}(I^2-I_3^2)+H_{\mathrm{rpc}}+H_{\mathrm{ppc}}+H_{\mathrm{irrot}}, \tag{5}$$

where the rotation-particle coupling (or the Coriolis term), particle-particle coupling, and the irrotational (often called the recoil) terms are given by

$$H_{\mathrm{rpc}}=-\frac{\hbar^2}{2\Im}(I_+j_-+I_-j_+), \tag{6a}$$

$$H_{\mathrm{ppc}}=\frac{\hbar^2}{2\Im}(j_{p_+}j_{n_-}+j_{p_-}j_{n_+}), \tag{6b}$$

$$H_{\mathrm{irrot}}=\frac{\hbar^2}{2\Im}[(j_p^2-j_{p_3}^2)+(j_n^2-j_{n_3}^2)]. \tag{6c}$$

Here I_3 is the component of I along the symmetry axis. The operators $I_\pm=I_1\pm iI_2$, $j_\pm=j_1\pm ij_2$,

$j_{n\pm}=j_{n_1}\pm ij_{n_2}$, and $j_{p\pm}=j_{p_1}\pm ij_{p_2}$ are the usual shifting operators. $\mathfrak{I}$ is the moment of inertia with respect to the rotation axis.

The single-particle orbitals $|\rho_p\Omega_p\rangle$ or $|\rho_n\Omega_n\rangle$ for the axially symmetric quadrupole-deformed shapes are normally described (Bohr and Mottelson, 1975) in terms of the Nilsson-model asymptotic quantum numbers $\Omega^\pi[Nn_3\Lambda\Sigma]$ or their abbreviated notation $\Omega[Nn_3\Lambda]$, wherein parity $\pi=(-1)^N$ and the spin projection Σ are determined using the relation $\Omega=\Lambda+\Sigma$.

In the strong-coupling formalism, a first approximation to the excitation spectra of odd-odd nuclei is obtained by coupling the single quasiproton and quasineutron states of the odd-mass neighbors. Normally this coupling is additive for both the energy and the angular momentum projection quantum numbers. Thus the angular momenta vector relation of the 2qp-plus-rotor model,

$$\vec{I}=\vec{j}_p+\vec{j}_n+\vec{R}, \tag{7}$$

gives rise to a pair of bands with band quantum numbers

$$K_{><}=|\Omega_p\pm\Omega_n| \tag{8}$$

in odd-odd nuclei for each proton-neutron (2qp) configuration (Ω_p, Ω_n). Each of these bands has a set of rotational levels with spins $I=K,\ K+1,\ K+2,\ldots$ and with level spacings obeying the $I(I+1)$ law. The unperturbed level energies of a rotational band for each 2qp configuration are given by

$$E_{IK}=E^p_{\text{qp}}+E^n_{\text{qp}}+\frac{\hbar^2}{2\mathfrak{I}}[I(I+1)-K^2]. \tag{9}$$

Here the effect of pairing on single-particle energy has been approximately included by replacing the single-particle energies with the respective quasiparticle energies for the odd proton and the odd neutron $[E_{\text{qp}}=\sqrt{(\epsilon_{\text{sp}}-\lambda)^2+\Delta^2}-\Delta$, where Δ is the pairing gap parameter]. In the 2qp-plus-rotor calculations, it is usually assumed that the quasiparticle energies also absorb the diagonal contributions from H_{irrot}; the nondiagonal part is neglected.

The set of basis eigenfunctions for the unperturbed Hamiltonian $H_{\text{av}}+(\hbar^2/2\mathfrak{I})(I^2-I_3{}^2)$ may be written in the form of the symmetrical product of the rotational wave functions D^I_{MK} and the intrinsic wave functions $|K\alpha_\rho\rangle$ as

$$|IMK\alpha_\rho\rangle=\left[\frac{2I+1}{16\pi^2(1+\delta_{K0})}\right]^{1/2}[D^I_{MK}|K\alpha_\rho\rangle+(-1)^{I+K}D^I_{M-K}R_i|K\alpha_\rho\rangle], \tag{10}$$

where the index α_ρ characterizes the 2qp configuration ($\alpha_\rho\equiv\rho_p\rho_n$) of the odd proton and the odd neutron. Choice of an appropriate basis is crucial to the success and usefulness of these calculations (see Jain *et al.*, 1989 for more details).

B. Gallagher-Moszkowski splittings and Newby shifts

Degeneracy of the bandheads of the $K_{><}$ pair is lifted by inclusion of the contribution $\langle V_{pn}\rangle$ of the residual proton-neutron interaction and also by the zero-point rotational energy; characterization of the residual interaction is generally sought on the basis of phenomenological considerations, as described later in this section. Relative energy ordering of the $K_{><}$ bands is determined by the empirical Gallagher-Moszkowski (GM) rule. This rule places the spin-parallel (triplet K_T) band lower in energy than its spin-antiparallel (singlet K_S) counterpart (Gallagher and Moszkowski, 1958). In consideration of the observed universal applicability of the GM rule, each pair of 2qp bands is referred to as a GM doublet. Their energy separation, appropriately corrected for the zero-point rotational energy, is referred to as the GM splitting energy or GM splitting. Further, the established validity of the GM rule has led to the inclusion of an explicitly spin-spin-dependent interaction term $(\sigma_p\cdot\sigma_n)$ in almost every adopted characterization of the residual p-n interaction (see, for example, Pyatov, 1963; Boisson *et al.*, 1976; Nosek *et al.*, 1994). The GM rule has now been extended to multi-quasiparticle states and generalized rules proposed (Jain and Jain, 1992).

Another important consequence of the residual interaction is the observed shift of the odd- and even-spin rotational levels relative to each other in $K=0$ bands; this feature is generally referred to as the Newby (N), or odd-even shift (Newby, 1962). It is therefore necessary to correct the energy separation of a GM pair for the Newby shift in the case of $K=0$ bands, in order to obtain the GM splitting.

The Newby shift arises from the special nature of the wave function for a $K=0$ band, which may be written as

$$|IMK=0,\alpha_\rho\rangle=\left[\frac{2I+1}{32\pi^2}\right]^{1/2}D^I_{M0}[|K=0,\alpha_\rho\rangle+(-1)^I R_i|K=0,\alpha_\rho\rangle], \tag{11}$$

where R_i is the rotation operator $\exp^{-i\pi j_1}$ with eigenvalue $\exp^{-i\pi\alpha}$, α is the signature quantum number with values $\alpha=0$ or 1 (or, alternatively, R_i has eigenvalues $r=\pm1$), and

$$|K=0,\alpha_\rho\rangle=\frac{1}{\sqrt{2}}[|\rho_p\Omega\rangle|\rho_n-\Omega\rangle-r|\rho_p-\Omega\rangle|\rho_n\Omega\rangle]. \tag{12}$$

The total wave function is nonvanishing when $\alpha=0$ (or $r=+1$), $I=0,2,4,6\ldots$ and $\alpha=1$ (or $r=-1$), $I=1,3,5,7\ldots$; in other words, $r=(-1)^I$. This splits the $K=0$ band into two chains: $r=+1$ and $r=-1$. The residual p-n interaction V_{pn} gives rise to a different diagonal contribution for $r=\pm1$ members of the $K=0$ band, causing an odd-even shift given by the expression

$$\mathcal{E}_{\text{N}}=(-1)^I\langle\rho_p\Omega;\rho_n-\Omega|V_{pn}|\rho_p-\Omega;\rho_n\Omega\rangle=(-1)^I B_{\text{N}}. \tag{13}$$

This definition of B_{N} is identical to the quantity B of Elmore and Alford (1976) but differs by a phase factor $(-\pi)$ with the quantity E_{N} of Boisson et al. (1976). It is also opposite in sign to the similar quantity discussed by Jain *et al.* (1988, 1989), Hoff *et al.* (1990), Goel *et al.* (1991), and Frisk (1988).

We can now evaluate the uncorrected empirical values of the GM splittings and N shifts from available experimental data. These uncorrected values, as will be clear from the following, do not take into account the effect of nondiagonal contributions from the Coriolis and the p-n interaction. Neglecting these contributions, the energy of a particular state in an odd-odd nucleus can be written as

$$E_{IK}=E_{\rm qp}^{p}+E_{\rm qp}^{n}+\frac{\hbar^2}{2\Im}[I(I+1)-K^2]+E_{\rm int}^{K}+(-)^{I}\delta_{K,0}[E_{\rm int}^{K=0}+E_a]. \quad (14)$$

$E_{\rm int}^{K}$ and $E_{\rm int}^{K=0}$ are the diagonal contributions of the p-n residual interaction and E_a is the diagonal contribution of the rotation-particle coupling term, which contributes only when $\Omega_p=\Omega_n=1/2$ and depends on the decoupling parameters a_p and a_n of the proton and neutron configurations as

$$E_a=-\frac{\hbar^2}{2\Im}a_p a_n \delta_{\Omega_p,1/2}\delta_{\Omega_n,1/2}\delta_{K,0}. \quad (15)$$

The GM splitting energy and N shift are then defined for a given pure 2qp configuration by the relations

$$\Delta E_{\rm GM}=E_{\rm int}^{K_<}-E_{\rm int}^{K_>} \quad (16)$$

and

$$B_{\rm N}=E_{\rm int}^{K=0}. \quad (17)$$

It should be emphasized that these quantities represent bare-particle effects arising from a diagonal estimate of the p-n interaction. Further, it has been shown by Boisson *et al.* (1976) that the pairing interaction does not modify these quantities.

C. The residual p-n interaction and its parametrization

Early calculations of GM splittings and N shifts were based on a central force with zero range, the delta force (Pyatov, 1963; Neiburg *et al.*, 1972). The spin-spin part of the force (the Bartlett force) was found to be mainly responsible for the lowering of the spin-triplet state and led to the GM rule. A finite-range Gaussian radial shape was introduced by De Pinho and Picard (1965) and Jones *et al.* (1971). Later Massmann *et al.* (1974) also fitted 12 GM splittings with a parameter set quite different from that of Jones *et al.* (1971). Two studies of the p-n interaction based on GM splittings and N shifts appeared in 1976 (Boisson, Piepenbring, and Ogle, 1976; Elmore and Alford, 1976). The more comprehensive study of Boisson *et al.* used a delta force, a Gaussian shape, and a Yukawa shape and also included spin-exchange, tensor, and polarization effects.

Several attempts were made to improve the description of observed features with the residual interaction (Lasijo *et al.*, 1977; Tanaka *et al.*, 1979; Nosek *et al.*, 1985). Sood and Singh (1982) used the delta interaction to obtain the spectra of doubly odd deformed nuclei. The Newby shift became the focus of studies by Frisk (1988), Hoff *et al.* (1990), and Goel *et al.* (1991).

Elmore and Alford (1976) used 42 empirical GM splittings and 16 N shifts to parametrize the residual p-n interaction. Boisson *et al.* (1976) used 50 empirical GM splittings and 19 N shifts from 16 nuclei and obtained several sets of parameters of the residual p-n interaction. Since then many new data have been reported in the literature (Headly *et al.*, 1998). The data from the actinide region (Hoff *et al.*, 1990; Sood *et al.*, 1994) were not considered in most of the previous studies except for the study of the N shift (Frisk, 1988). The analysis presented in this section is based on 164 values of the GM splittings and 48 values of the N shifts taken from the rare-earth and actinide regions (Nosek *et al.*, 1994).

1. Empirical analysis

Extraction of the uncorrected empirical values of the GM splittings and N shifts from available experimental data is based on Eq. (14). Individual rotational bands were parametrized by a parameter that represents the sum of $(E_{\rm qp}^{p}+E_{\rm qp}^{n}+E_{\rm int}^{K})$ and an inertial parameter $\hbar^2/2\Im$. For $K=0$ rotational bands, the N shift $E_{\rm int}^{K=0}$ was also included. A least-squares fitting was done to obtain the parameters and their errors. The GM energy splittings $\Delta E_{\rm GM}$ were calculated as the difference between the energy parameters $(E_{\rm qp}^{p}+E_{\rm qp}^{n}+E_{\rm int}^{K})$ of the two rotational bands constituting the GM pair; the contribution from $E_{\rm qp}^{p}+E_{\rm qp}^{n}$ cancels out when the difference is taken.

The 137 empirical values of the GM splittings and 36 empirical values of the N shifts from the rare-earth region and their errors are collected in Table I together with assignments of Nilsson configurations. These values correspond to 25 nuclei lying in the mass region $152\leqslant A\leqslant 188$ and are based on the data in Headly *et al.*, 1998.

2. Theoretical analysis

We use a phenomenological form of the p-n interaction (Boisson *et al.*,1976),

$$V_{pn}=V_{pn}(r)[u_0+u_1\vec{\sigma}_p\cdot\vec{\sigma}_n+u_2P_{\rm M}+u_3\vec{\sigma}_p\cdot\vec{\sigma}_nP_{\rm M}+V_{\rm T}S_{12}+V_{\rm TM}S_{12}P_{\rm M}]. \quad (18)$$

Here $V_{pn}(r)$ is the radial shape of the p-n interaction depending on the distance $r=|\vec{r}_p-\vec{r}_n|$ and additional parameters describing the radial shape. The p-n interaction contains contributions from six different types of forces and corresponding strength parameters. The constant or Wigner(1), spin-spin $(\vec{\sigma}_p\cdot\vec{\sigma}_n)$, space-exchange $(P_{\rm M})$, spin-spin-space-exchange $(\vec{\sigma}_p\cdot\vec{\sigma}_nP_{\rm M})$, tensor (S_{12}), and tensor-space-exchange $(S_{12}P_{\rm M})$ forces are included. It should be pointed out that the constant term gives no contribution to the GM splitting energies or N shifts. The tensor operator S_{12} is given by the relation

$$S_{12}=\frac{(\vec{\sigma}_p\cdot\vec{r})(\vec{\sigma}_n\cdot\vec{r})}{r^2}-\frac{1}{3}(\vec{\sigma}_p\cdot\vec{\sigma}_n). \quad (19)$$

The polarization of the intrinsic operators was also considered by Boisson *et al.* (1976) and is included in our calculations. Then the intrinsic spin-dependent terms, the spin-spin, and spin-spin-space-exchange terms are replaced by the intrinsic spin-parallel and perpendicular terms as follows:

$$u_1\vec{\sigma}_p\cdot\vec{\sigma}_n \rightarrow u_{1\parallel}\sigma_{pz}\sigma_{nz}+u_{1\perp}[\sigma_{p+}\sigma_{n-}+\sigma_{p-}\sigma_{p+}], \tag{20}$$

$$u_3\vec{\sigma}_p\cdot\vec{\sigma}_n P_{\mathrm{M}} \rightarrow u_{3\parallel}\sigma_{pz}\sigma_{nz}P_{\mathrm{M}} + u_{3\perp}[\sigma_{p+}\sigma_{n-}+\sigma_{p-}\sigma_{p+}]P_{\mathrm{M}}. \tag{21}$$

Boisson *et al.* also considered the effects of the long-range forces and the intrinsic spin-orbit force originating in the relative motion of the two valence particles. While the spin-orbit force was found to be unimportant, the long-range forces were found to improve the fitting of GM splittings only. These effects, however, are not considered in the present review.

In the special case of the zero-range delta interaction, the p-n interaction reduces to the relation introduced by Pyatov (1963):

$$V_{pn}^{\delta}=-4\pi g\,\delta(\vec{r}_p-\vec{r}_n)[(1-\alpha)+\alpha(\vec{\sigma}_p\cdot\vec{\sigma}_n)], \tag{22}$$

where g is the strength of the p-n interaction and α is a parameter (not to be confused with signature quantum number α) describing the relative strength of the constant and spin-spin forces. The constant and spin-spin parameters are written as

$$u_0=4\pi g(1-\alpha), \quad u_1=4\pi g\alpha. \tag{23}$$

One often comes across a parameter $u_1=\alpha W$, where W, written as

$$W=g\left[\frac{2}{\pi}\left(\frac{m\omega_0}{\hbar}\right)^3\right]^{1/2}=(\mathrm{const})A^{1/2}, \tag{24}$$

is dependent on the mass number A. This dependence is usually omitted and the spin-spin parameter $u_1=\alpha W$ is assumed to be constant for all nuclei.

For finite-range forces we use the Gaussian-shape potential written

$$V_{np}^{\mathrm{G}}(r)=\exp\left(\frac{-r^2}{r_g^2}\right), \tag{25}$$

where r_g is the finite-range parameter. Both central and tensor forces remain active in this case.

The theoretical matrix elements of the residual p-n interaction can be written in general as

$$\Delta E_{\mathrm{GM}}^{\mathrm{theor}}=u_c+\sum_i W_i[\langle K_<|\mathcal{O}_i|K_<\rangle-\langle K_>|\mathcal{O}_i|K_>\rangle], \tag{26}$$

$$B_{\mathrm{N}}^{\mathrm{theor}}=u_c+\sum_i W_i[\langle K=0|\mathcal{O}_i|\overline{K=0\rangle}, \tag{27}$$

where W_i are the force parameters (to be determined by fitting of data) as given in Eq. (18) and $\langle K|\mathcal{O}_i|K\rangle$ are expectation values of corresponding operators. An additional constant paramter u_c has been added to the theoretical values of the GM splitting and N-shift matrix elements. We have found that the introduction of this parameter improves the fitting and gives a better agreement between experimental and theoretical values. It should be emphasized that this parameter has no physical significance. On the other hand, a significant value of this parameter in a particular fit would indicate that the parametrization of the residual p-n interaction was not good. It could even imply that some important effects were missing in the analysis or in the interaction.

Theoretical matrix elements of the residual p-n interaction were calculated by using Nesbet's transformation method (Nesbet, 1963). The intrinsic wave functions used were approximated by the eigenfunctions of the modified harmonic-oscillator potential (Nilsson potential) with dynamic parameters as recommended by Soloviev (1971). An axially symmetric quadrupole-hexadecapole deformed average field was assumed. Deformation parameters were chosen individually for every nucleus (Jain *et al.*, 1990). All shells with N = 3–7 were included.

3. Fitting of the parameters of the residual p-n interaction

In the p-n interaction parameter analysis, we included 162 empirical values of the GM splittings and 34 empirical values of the N shifts from the rare-earth and the actinide regions. Two values of the GM splittings and 14 values of Newby shifts were not included in our analysis as these were found to be admixed by nondiagonal terms of either the Coriolis interaction or the p-n interaction, and/or were tentative in assignment. Two sets of parameters were obtained for a given choice of p-n interaction: one corresponds to the GM splitting and the other corresponds to the N shifts. Most of the earlier calculations carried out a simultaneous fitting to both the GM splittings and the N shifts from the rare-earth region (see, for example, Elmore and Alford, 1976 and Boisson *et al.*, 1976). Boisson *et al.* also fitted the parameters to only GM splittings. Frisk (1982), however, fitted the parameters to N shifts only from the rare-earth and the actinide region. Our calculations (Nosek *et al.*, 1994), more rigorous in nature, used the generalized weighted multiple linear regression method (Arnold, 1990). We also address the question of which parameters of the p-n interaction are significant and well determined by available experimental data.

We obtained four parameter sets for the zero-range delta force with and without polarization effects; two sets for GM splittings and two for Newby shifts. We then obtained eight parameter sets for finite-range Gaussian potential with only central forces, central-plus-tensor forces, central plus intrinsic spin polarization, and finally central plus tensor plus intrinsic spin polarization (Nosek *et al.*, 1994).

Some of the important parameter sets obtained with the Gaussian-shaped potential with $r_g=1.4$ fm are summarized in Table II together with previously deduced parameters of Boisson *et al.* (1976) and Frisk (1988). The parameters of our analysis that have been found to

TABLE I. Empirical values of the GM splitting energies and N shifts. The nucleus under consideration is given in the first column, followed by the proton and the neutron Nilsson configurations $\Omega[Nn_3\Lambda]$. The empirical values of the GM splitting energies are given in the second column together with their experimental errors (in the last significant places) given in smaller fonts; the theoretical values of the GM splittings from the present analysis are given in the same column, separated by a comma. If the error is not given, it is in the second decimal place. Similarly, the third column contains empirical values, errors in smaller fonts, and theoretical values of the N shifts, respectively, for $K=0$ bands. If the Nilsson quantum number Λ for neutron and proton is same, it corresponds to a central (singlet) term, and if the Nilsson quantum number Λ differs, it corresponds to a tensor (triplet) term, for the N shift. In the fourth column are given the number of experimentally known rotational band members of $K_<$ and $K_>$, respectively, which were included in the analysis. A "− −" in place of $\Delta E_{\mathrm{GM}}^{\mathrm{exp}}$ or $B_{\mathrm{N}}^{\mathrm{exp}}$ indicates that these GM pairs were placed in the table after empirical parameters were determined for the whole data set, so that only theoretical values were calculated for these examples using the fixed set of parameters. Experimental data are from the compilation of Headly *et al.* (1998).

Nucleus Proton Neutron $\Omega[Nn_3\Lambda]$ $\Omega[Nn_3\Lambda]$	ΔE_{GM} Expt., Theor. (keV)	B_{N} Expt., Theor. (keV)	Numbers of band members
^{152}Pm			
5/2[532] 3/2[521]	− −, 103.0		
^{152}Eu			
5/2[413] 11/2[505]	-87.8_{56}, -107.6		5/9
5/2[413] 3/2[521]	-103.5_{18}, -70.4		3/1
5/2[413] 5/2[523]	192.6, 171.9	-3.2, -13.3	3/1
5/2[413] 3/2[532]	95.8_{23}, 84.7		3/1
5/2[413] 1/2[530]	-58.6_{30}, -27.7		3/2
5/2[413] 3/2[402]	182.1, 198.0		2/2
5/2[413] 1/2[400]	-223.4, -108.3		1/1
5/2[413] 1/2[521]	131.8, 153.9		2/2
5/2[413] 3/2[651]	− −, -30.3		
5/2[532] 3/2[521]	163.8, 120.3		2/1
5/2[532] 3/2[532]	-84.2_{13}, -89.6		3/1
3/2[411] 3/2[521]	96.1, 122.1	5.7, -2.5	3/2
3/2[411] 5/2[523]	-181.2_{5}, -77.3		3/1
3/2[411] 3/2[532]	-127.3_{16}, -31.4	-19.1_{11}, 10.7	4/2
3/2[411] 1/2[530]	114.9_{48}, 57.2		3/3
3/2[411] 1/2[521]	-142.3_{49}, -89.6		3/2
^{154}Eu			
5/2[413] 1/2[400]	-188.2_{65}, -112.8		3/1
5/2[413] 3/2[402]	45.6_{72}, 195.3		4/3
5/2[413] 3/2[651]	-141.6_{129}, -31.8		6/3
5/2[413] 5/2[642]	-60.7_{110}, -62.7	-9.5_{115}, 5.3	4/1
5/2[413] 1/2[530]	-86.1, -34.3		2/1
5/2[413] 3/2[521]	-114.3_{84}, -80.4		6/2
5/2[413] 3/2[532]	30.6_{101}, 88.4		5/3
5/2[413] 5/2[523]	72.8, 190.5	8.4_{100}, 7.4	4/1
5/2[413] 11/2[505]	-74.6_{226}, -103.5		3/1
5/2[532] 3/2[402]	-83.6_{5}, -48.9		4/1
5/2[532] 3/2[651]	153.8, 102.9		1/1
5/2[532] 3/2[521]	97.9, 129.9		2/2
5/2[532] 3/2[532]	-150.0_{26}, -91.1		4/1
3/2[411] 3/2[651]	108.8_{73}, 71.9	-36.7,[a]	3/3
3/2[411] 3/2[521]	78.6_{59}, 130.1	-6.327,[b]	4/3
^{156}Eu			
5/2[413] 5/2[642]	$-102._{27}$, -67.7	-4.0_{5}, 4.5	6/1
5/2[413] 5/2[523]	125.1_{24}, 195.4	-14.0_{16},[a]	1/1

TABLE I. (*Continued*).

Nucleus Proton Neutron $\Omega[Nn_3\Lambda]$ $\Omega[Nn_3\Lambda]$	ΔE_{GM} Expt., Theor. (keV)	B_N Expt., Theor. (keV)	Numbers of band members
5/2[413] 3/2[521]	-97.3_{9}, -86.8		4/2
5/2[532] 3/2[521]	145.3_{3}, 133.7		4/2
5/2[532] 5/2[642]	$--$, 168.8	$--$, -32.3	
3/2[411] 3/2[521]	170.1, 122.3		1/2
^{154}Tb			
3/2[411] 3/2[521]	$--$, 121.9	$--$, -9.5	
^{156}Tb			
3/2[411] 3/2[521]	123.0_{43}, 122.3	11.6_{25}, 5.4	4/2
^{158}Tb			
3/2[411] 3/2[521]	133.5_{13}, 120.3	7.9_{9}, 4.1	6/5
3/2[411] 3/2[402]	-110.7, -160.7	-32.3, -21.0	3/1
3/2[411] 1/2[400]	74.9_{64}, 163.6		3/2
3/2[411] 5/2[642]	149.8_{24}, 100.0		7/5
3/2[411] 11/2[505]	134.2, 122.6		2/1
5/2[532] 5/2[642]	201.4_{238}, 168.8	-48.9_{92},[a,c]	4/4
7/2[404] 3/2[521]	$--$, -51.7		
5/2[402] 3/2[521]	$--$, 76.3		
^{160}Tb			
3/2[411] 3/2[521]	126.0_{12}, 123.2	-18.0_{8},[b]	5/3
3/2[411] 5/2[642]	91.6_{45}, 100.0		4/2
3/2[411] 5/2[523]	-161.5_{51}, -81.2		5/2
3/2[411] 1/2[521]	$--$, -91.5		
5/2[413] 5/2[642]		0.5_{16},[a,d]	5/$-$
^{162}Tb			
3/2[411] 5/2[523]	$--$, -81.7		
^{156}Ho			
7/2[523] 3/2[521]	82.2, 133.4		1/1
^{158}Ho			
7/2[404] 3/2[521]	-59.7, -45.5		1/1
7/2[523] 3/2[521]	167.1, 132.7		1/1
7/2[523] 5/2[642]	$--$, 120.1		
^{162}Ho			
7/2[523] 5/2[642]	$--$, 118.5		
^{164}Ho			
7/2[523] 5/2[523]	-146.0_{9}, -142.1		5/2
7/2[523] 3/2[521]	163.7_{30}, 88.0		4/3
7/2[523] 3/2[402]	-79.7, -94.2		2/1
7/2[523] 1/2[400]	106.1, 128.9		2/1
7/2[523] 5/2[642]	41.5_{37}, 137.4		2/4
7/2[523] 1/2[660]	$--$, 37.2		
^{166}Ho			
7/2[523] 7/2[633]	83.517, 160.3	-30.6_{8}, 2.9	7/3
7/2[523] 1/2[521]	-168.7_{6}, -105.5		5/3
7/2[523] 5/2[512]	316.8_{4}, 140.7		5/2

TABLE I. (*Continued*).

Nucleus Proton Neutron $\Omega[Nn_3\Lambda]$ $\Omega[Nn_3\Lambda]$	ΔE_{GM} Expt., Theor. (keV)	B_{N} Expt., Theor. (keV)	Numbers of band members
7/2[523] 1/2[510]	266.0, 149.1		1/1
7/2[523] 3/2[521]	− −, 121.9		
1/2[411] 7/2[633]	−160.9$_{14}$, −98.0		4/3
7/2[404] 7/2[633]	32.3$_{20}$,[a,e]	−77.7$_{14}$, −37.5	6/1
3/2[411] 7/2[633]	195.8$_{18}$, 129.2		4/3
3/2[411] 5/2[512]	− −, 198.6		
5/2[413] 7/2[633]	−66.6$_{24}$, −115.9		5/2
1/2[411] 1/2[521]	223.3$_{78}$, 113.2	−37.5$_{13}$, −14.7	6/5
3/2[411] 1/2[521]	−173.2$_{41}$,−80.6		5/1
^{168}Ho			
7/2[523] 5/2[512]	− −, 141.4		
^{170}Ho			
7/2[523] 5/2[512]	− −, 140.6		
^{160}Tm			
7/2[523] 3/2[521]	− −, 141.3		
^{168}Tm			
1/2[411] 7/2[633]	−139.3$_{17}$, −96.4		5/4
1/2[411] 1/2[521]	194.7$_{68}$, 108.7	−31.5$_{21}$, −18.8	5/4
1/2[411] 3/2[521]	−66.7$_{160}$, −47.3		4/3
1/2[411] 5/2[523]	60.9$_{89}$, 120.7		4/3
1/2[411] 3/2[402]	335.7$_{204}$, 198.3		3/2
1/2[411] 1/2[400]	−258.8$_{44}$, −169.3	−24.5$_{31}$, −40.5	4/2
1/2[541] 7/2[633]	−128.1$_{189}$, −32.4		4/4
5/2[402] 7/2[633]	138.2$_{18}$, 105.6		3/1
1/2[530] 7/2[633]	60.0$_{155}$, 104.3		3/3
1/2[411] 5/2[512]	−236.0, −115.2		1/1
1/2[411] 1/2[510]	−61.0, −185.6	2.9,[c,d]	2/1
7/2[404] 7/2[633]	− −, −75.1	− −, −42.4	
^{170}Tm			
1/2[411] 1/2[521]	192.8$_{21}$, 98.3	−41.4$_{5}$, −27.2	6/7
1/2[411] 3/2[521]	− −, −41.2		
1/2[411] 7/2[633]	− −, −93.4		
3/2[411] 1/2[521]	−131.9, −70.8		2/2
1/2[411] 5/2[512]	−239.6$_{2}$, −109.1		3/1
5/2[402] 1/2[521]	−141.5, −25.2		1/1
5/2[413] 1/2[521]	174.5$_{28}$, 147.3		3/2
7/2[404] 1/2[521]	140.3, 101.7		1/1
7/2[523] 1/2[521]	−9.2, −92.6		2/2
^{172}Tm			
1/2[411] 1/2[521]	97.6, 83.0	−29.0, −37.6	2/2
1/2[411] 5/2[512]	−231.7, −99.5		3/1
^{166}Lu			
7/2[404] 5/2[523]	− −, 133.7		
^{170}Lu			
7/2[404] 1/2[521]	13.1, 101.7		1/1
1/2[411] 1/2[521]	193.8, 98.3	−30.3, −27.2	2/2
1/2[541] 1/2[521]	158.0, 82.6	−93.5,[c,d]	2/1
7/2[404] 7/2[633]		−42.3$_{8}$, −34.8	4/−

TABLE I. (*Continued*).

Nucleus Proton Neutron $\Omega[Nn_3\Lambda]$ $\Omega[Nn_3\Lambda]$	ΔE_{GM} Expt., Theor. (keV)	B_N Expt., Theor. (keV)	Numbers of band members
^{172}Lu			
7/2[404] 1/2[521]	76.9_{8}, 97.1		5/4
1/2[541] 1/2[521]	89.7_{56}, 73.2	-21.7_{46},[a,d]	5/3
9/2[514] 1/2[521]	−147.0, −46.3		2/2
7/2[404] 5/2[512]	−121.7, −96.1		1/1
5/2[402] 1/2[521]	−97.0, −20.3		2/1
7/2[404] 7/2[633]		−55.5, −36.5	3/−
1/2[411] 1/2[521]	− −, 85.2	− −, −53.1	
^{174}Lu			
7/2[404] 5/2[512]	-114.9_{13}, −95.4		9/4
7/2[404] 7/2[633]	-64.2_{100}, −79.4	-40.0_{32}, −36.5	10/4
7/2[404] 1/2[521]	79.5_{50}, 96.6		5/4
7/2[404] 1/2[510]	− −, −115.8		
1/2[541] 5/2[512]	−149.8, 8.3		2/1
5/2[402] 5/2[512]	130.2_{21}, 147.3	29.0_{11}, 48.8	4/4
9/2[514] 5/2[512]	135.3_{31}, 162.3		5/3
7/2[404] 3/2[521]	-94.9_{57}, −47.6		4/3
1/2[530] 5/2[512]	42.3_{42}, 43.9		1/4
^{176}Lu			
7/2[404] 7/2[514]	250.7_{20}, 242.5	69.2_{6}, 64.6	8/4
7/2[404] 9/2[624]	-115.9_{32}, −117.7		6/2
9/2[514] 7/2[514]	-66.7_{51}, −178.4		6/2
5/2[402] 7/2[514]	-101.0_{16}, −103.4		6/2
5/2[402] 1/2[510]	− −, 112.3		
1/2[411] 7/2[514]	127.4_{61}, 202.7		3/3
7/2[523] 7/2[514]	12.5_{88},[a,e]	-155.5_{12},[a,c]	5/2
7/2[404] 5/2[512]	-65.2_{10}, −91.2		5/2
7/2[404] 3/2[512]	228.7, 172.1		2/2
7/2[404] 1/2[510]	-109.8_{16}, −113.2		4/2
5/2[402] 9/2[624]	195.3_{5}, 135.6		3/1
1/2[541] 7/2[514]	103.1, 33.3		3/2
9/2[514] 1/2[510]	241.8, 157.2		1/2
9/2[514] 9/2[624]	− −, 161.6	− −, 35.5	
7/2[404] 1/2[521]	56.6, 88.0		2/1
^{178}Lu			
7/2[404] 9/2[624]	− −, −117.0		
1/2[411] 9/2[624]	− −, −107.5		
^{180}Lu			
9/2[514] 1/2[510]	− −, 153.8		
^{176}Ta			
7/2[404] 7/2[633]		−41.9, −35.2	3/−
^{178}Ta			
9/2[514] 7/2[514]	− −, −176.6		
^{180}Ta			
7/2[404] 9/2[624]	-99.9_{67}, −119.0		5/3
9/2[514] 9/2[624]	121.2, 158.7	1.2, 40.3	3/2
7/2[404] 5/2[512]	-87.5_{54}, −83.6		4/2

TABLE I. (*Continued*).

Nucleus Proton Neutron $\Omega[Nn_3\Lambda]$ $\Omega[Nn_3\Lambda]$	ΔE_{GM} Expt., Theor. (keV)	B_{N} Expt., Theor. (keV)	Numbers of band members
7/2[404] 1/2[521]	66.5_{11}, 71.6		2/3
5/2[402] 9/2[624]	254.5, 135.9		1/1
^{182}Ta			
7/2[404] 1/2[510]	-92.6_{83}, -98.5		5/3
7/2[404] 3/2[512]	128.0_{7}, 169.4		5/2
7/2[404] 7/2[503]	-122.0_{31}, -154.1	23.1_{21},[a,d]	6/1
9/2[514] 1/2[510]	147.2_{6}, 129.4		4/3
9/2[514] 3/2[512]	-111.1_{124}, -123.4		4/1
5/2[402] 1/2[510]	114.7_{6}, 94.5		4/3
9/2[514] 11/2[615]	301.2, 223.9		2/1
^{184}Ta			
7/2[404] 3/2[512]	$--$, 168.1		
^{180}Re			
5/2[402] 1/2[521]	$--$, 12.6		
1/2[541] 7/2[514]	$--$, 8.6		
9/2[514] 7/2[514]	$--$, -175.9		
^{182}Re			
5/2[402] 9/2[624]	$--$, 132.4		
9/2[514] 9/2[624]	$--$, 161.5	$--$, 32.1	
^{184}Re			
5/2[402] 1/2[510]	85.0_{46}, 95.1		4/4
5/2[402] 3/2[512]	-209.3_{70}, -114.3		3/3
5/2[402] 7/2[503]	168.8_{8}, 244.0		4/1
5/2[402] 11/2[615]	352.5_{24}, 160.1		3/2
^{186}Re			
5/2[402] 1/2[510]	127.8_{90}, 87.6		4/4
5/2[402] 3/2[512]	-130.0_{29}, -112.8		6/3
5/2[402] 7/2[503]	207.4_{15}, 243.6		5/1
5/2[402] 11/2[615]	242.0_{24}, 159.8		3/1
9/2[514] 1/2[510]	156.0, 120.1		1/1
9/2[514] 3/2[512]	-169.3_{88}, -121.7		4/1
^{188}Re			
5/2[402] 1/2[510]	93.5_{11}, 77.4		3/3
5/2[402] 3/2[512]	-138.7_{14}, -109.6		5/2
5/2[402] 7/2[503]	209.4_{2}, 244.2		3/1
5/2[402] 3/2[501]	275.8_{23}, 258.9		3/1
1/2[411] 3/2[512]	197.2_{573}, 181.8		3/2
9/2[514] 9/2[505]		-54.3_{4}, -70.2	5/$-$
9/2[514] 3/2[512]	$--$, -118.5		
^{184}Ir			
1/2[541] 1/2[510]	$--$, 31.6	$--$, -54.3	
^{186}Ir			
3/2[402] 1/2[510]	$--$, -24.6		
^{190}Ir			
3/2[402] 1/2[510]	$--$, 4.8		
3/2[402] 11/2[615]	$--$, -121.4		
3/2[402] 9/2[505]	$--$, 266.1		

TABLE I. (*Continued*).

Nucleus Proton Neutron $\Omega[Nn_3\Lambda]$ $\Omega[Nn_3\Lambda]$	ΔE_{GM} Expt., Theor. (keV)	B_{N} Expt., Theor. (keV)	Numbers of band members
3/2[402] 3/2[512]	− −, 179.6	− −, 10.5	
1/2[400] 3/2[512]	− −, −58.7		
^{192}Ir			
3/2[402] 1/2[510]	− −, 41.1		
3/2[402] 3/2[512]	− −, 174.8	− −, 5.6	
1/2[400] 1/2[510]	− −, 7.7	− −, −58.0	
1/2[400] 3/2[512]	− −, −56.1		
11/2[505] 11/2[615]	− −, 185.9	− −, 90.0	
^{194}Ir			
3/2[402] 1/2[510]	− −, 67.4		

[a]Strongly perturbed rotational bands.
[b]Mixed neutron orbits.
[c]Tentative assignments.
[d]Strong configurational mixing. Values are strongly dependent on shapes of intrinsic wave functions.
[e]Anomalous values of GM splitting energies.

be statistically significant are underlined. We also list the estimated errors below them in parentheses.

The theoretical values of 137 GM splittings and 25 N shifts in the rare-earth region, obtained with the parameter set G_{TP}, are given in Table I. GM splittings and N shifts may be said to be satisfactorily described. The N shifts, as expected, are not so well described as GM splittings.

A detailed discussion of the quality of fits, parameter significance, estimated errors, and the stability of the p-n interaction parameters appears in Nosek *et al.* (1994). We present here some salient features of this discussion.

It was found that among the 162 GM splittings from the rare-earth and the actinide regions, only seven calculated values were considerably different from the empirical values in the G_{TP} fit. Out of 34 N shifts, four were calculated to be very different from the empirical values in the G_{TP} fit. In a few cases opposite signs of GM splittings or N shifts were calculated as compared to empirical values; this was found to be independent of the type of parametrization. It was also found that GM splittings and N shifts of certain configurations were quite sensitive to the shape of the average nuclear potential. Overall consideration of all the statistical indicators suggests that the new experimental data (included in our analysis) do not significantly improve the quality of fits of the new sets of empirical parameters.

It may be remarked that, in almost all the cases, our values of GM splittings and N shifts match reasonably well with those of Boisson *et al.* However, in about eight cases, the values of ΔE_{GM} or B_{N} differ significantly (from 50 to 125 keV) from the values obtained by Boisson *et al.* This may be due to different approaches adopted in extracting the empirical matrix elements. Also, our database (Headly *et al.*, 1998) is different and contains new or additional data in many of these cases, which may result in different values. Values may differ particularly when the bands are highly perturbed.

4. Parameters of GM splittings and N Shifts

The extended set of GM splitting energies used in this study yields an optimal spin-spin parameter $\alpha W = 0.805$ for the delta interaction, which is very close to the value obtained in previous studies (Pyatov, 1963; Sood and Singh, 1982). In agreement with the GM rule, the spin-spin term is the leading term. The constant term u_c introduced in our study has a value $u_c = 25$ keV, which is much smaller than the average absolute value of 125 keV for the 162 empirical GM splittings; it slightly improves the agreement between empirical and calculated values.

The parameters of the residual interaction with the Gaussian shape, presented in Table II, also confirm the importance of the spin-spin force (u_1 parameter). In the case of fits with intrinsic spin-polarization effects included, the spin-spin force with perpendicular spin polarization ($u_{1\perp}$) is very well determined. Further, we found that the tensor-space-exchange term (V_{TM}) plays a significant role in the description of GM splittings (see fits G_{T} and G_{TP}). Jones *et al.* (1971) and Lasijo *et al.* (1977) also emphasized the importance of tensor forces. However, Boisson *et al.* (1976) concluded that the tensor forces are not well determined by the GM splittings, contrary to our findings.

As expected, the delta interaction was found incapable of a satisfactory description of the Newby shifts. The parameter value $\alpha W = 0.191$ obtained by fitting N shifts only is quite different from the one for GM split-

TABLE II. Empirical parameters of the residual *p*-*n* interaction with the Gaussian potential (r_g =1.4 fm) extracted from experimental data of GM splitting energies and N shifts, respectively. The constant term (u_C) is given in keV; the other empirical parameters (u_1, $u_{1\parallel}$, $u_{1\perp}$, u_2, u_3, $u_{3\parallel}$, $u_{3\perp}$, V_T, and V_{TM}) are given in MeV. The most significant parameters of our analysis are underlined, with their estimated errors given below the *p*-*n* parameters. The parameters from the fittings carried out by Boisson *et al.* (1976) using harmonic-oscillator wave functions and Frisk (1988) are also given for comparison with similar parameter sets from our calculations, wherever possible. The number of GM and/or N values used in each fit is displayed in the two rightmost columns. Parameter set G refers only to central forces assumed; G_P, spin-polarized force included; G_T, central and tensor forces included; G_{TP}, central intrinsic spin-polarized and tensor forces included.

	u_C	u_1	u_2	u_3	M_{GM}	M_N
G	$\underline{20.0}$	$\underline{-16.0}$	-2.4	4.7	162	-
	(9.0)	(2.4)	(4.2)	(4.4)		
Boisson		-9.22	-0.52	-6.2	50	-
G	$\underline{-69.0}$	2.4	$\underline{75.6}$	$\underline{-13.5}$	-	34
	(13.0)	(2.5)	(18.3)	(2.3)		

	u_C	u_1	u_2	u_3	V_T	V_{TM}	M_{GM}	M_N
G_T	$\underline{22.0}$	$\underline{-10.1}$	-3.0	4.1	-9.9	$\underline{-51.8}$	162	-
	(8.0)	(3.0)	(4.1)	(4.3)	(8.9)	(18.4)		
G_T	-28.0	3.8	$\underline{62.4}$	$\underline{-12.1}$	$\underline{-13.5}$	-4.8	-	34
	(24.0)	(2.8)	(19.0)	(2.6)	(6.6)	(10.4)		
Frisk		-2.1	-43.1	-1.5	-46.2	-36.0	-	20

	u_C	$u_{1\parallel}$	$u_{1\perp}$	u_2	$u_{3\parallel}$	$u_{3\perp}$	V_T	V_{TM}	M_{GM}	M_N
G_P	$\underline{17.0}$	41.6	-33.6	-2.9	-37.0	19.9			162	-
	(9.0)	(31.8)	(9.8)	(4.1)	(46.3)	(13.5)				
Boisson		-7.3	-21.7	-1.2	-4.4	13.0			50	-
G_{TP}	$\underline{20.0}$	40.0	$\underline{-24.5}$	-3.0	-12.5	13.7	-16.8	$\underline{-62.5}$	162	-
	(8.0)	(32.5)	(10.4)	(4.0)	(47.0)	(14.0)	(9.1)	(18.5)		
G_{TP}	-32.0	7.6	3.1	$\underline{56.9}$	-0.9	$\underline{-12.2}$	-12.5	3.8	-	34
	(29.0)	(55.2)	(5.4)	(27.2)	(45.8)	(2.9)	(8.3)	(11.8)		

tings. Considerable improvement in the N-shift description was achieved with the inclusion of intrinsic spin polarization. Both parallel and perpendicular components ($\alpha W_\parallel$ and $\alpha W_\perp$) were found to be significant. However, a large negative constant ($u_c=-80$ keV) implies that the N-shift parametrization is not good. Compare this with the average absolute value of $|B_N|_{av}=30$ keV for the 34 empirical N shifts.

Introduction of the Gaussian-shape potential does not improve the picture for describing N shifts with central forces. We also found that the tensor-force terms are not well determined (see fits G_T and G_{TP} in Table II). This is contrary to the conclusions of earlier studies, which suggested that the tensor term played an important role for N shifts (Newby, 1962; Boisson *et al.*, 1976). In agreement with Frisk (1988), we found that the N shifts were well parametrized by the space-exchange force (u_2). The spin-spin-space-exchange force (u_3) or its perpendicular polarized component $u_{3\perp}$ was also very well determined by the data. The best results were obtained in the fits G_P and G_{TP}, which included the intrinsic spin-polarization effects.

It is clear from these remarks that the N-shift parameters remain poorly determined compared to the GM splitting parameters. It was a general observation of the earlier studies that the central force parameters fitted to reproduce the GM splittings often gave the wrong sign for the N shifts in triplet configurations (neutron and proton spins are opposite in $K=0$), whereas a correct sign was obtained in singlet configurations but the magnitude of the N shifts became large. Based on this observation, Sood and Ray (1986) introduced an *ad hoc* phase factor dependent on spin and were able to obtain reasonable fits to the N shifts by using delta force only. Others invoked a tensor force as suggested by Newby (1962); however, this did not resolve the problem completely. It was pointed out by Goel *et al.* (1991) that the empirical value of the N shift might sometimes acquire an opposite sign due to Coriolis effects; it is therefore necessary to obtain corrected values of N shifts before a fitting of the p-n interaction is carried out. Such cases will, however, be few in number. Thus an understanding of the N shift of $K=0$ states in odd-odd nuclei remains one of the challenging problems in nuclear structure physics.

One may speculate on some points that may help clear up this issue. While the GM splitting is the difference of two diagonal contributions in the first approximation, the N shift is a typical signature effect originating in the R symmetry of the $K=0$ intrinsic proton-neutron wave function. When $r=+1$, the intrinsic wave function $|K=0,\alpha=0\rangle$ [see Eq. (11)] acquires a symmetric character (if we disregard the difference between neutron and proton), and when $r=-1$ it becomes antisymmetric in character; the two are energetically separated because of different self-contributions to energy. It is therefore expected that an exchange force might play a crucial role. Our calculations, in agreement with those of Frisk (1988), confirm the role of the space-exchange force (u_2) and spin-spin-space-exchange force (u_3) in determining the N shift. A simple rule for determining the sign of the N shift was therefore proposed by Frisk (1988) according to which the favored angular momenta I_F in a $K=0$ band primarily composed of proton-neutron angular momenta (j_p, j_n) are given by $I_F=(j_p+j_n)$ mod 2. The rule seems to work in a majority of cases; however, its validity in general cannot be taken for granted (Goel *et al.*, 1991).

Some important effects that have not been considered in the calculations so far are (i) inclusion of nondiagonal Coriolis mixing effects into the GM splittings and N shifts and (ii) inclusion of nondiagonal contributions to the p-n interaction. The importance of the latter has been demonstrated in a calculation of ^{160}Tm (Nosek *et al.*, 1989), where a zero-range p-n interaction was considered; this resulted in significant $\Delta K=0$ mixings of many 2qp configurations, which also helped in explaining the data on transition probabilities. Any future attempts at parametrizing the residual p-n interaction must take these two effects into account.

5. Proposed violations of the GM rule

The GM coupling rule is a "strong" empirical rule, in that any apparent violation of it, with the energy of the triplet state E_T becoming greater than the energy of the singlet state E_S, must occur under unusual circumstances. In fact a true violation can only be said to have occurred when one looks at the rule in light of the additional rotational energy term in Eq. (9). In particular, the bandhead ($I=K$) rotational energy is directly proportional to K and yields an energy difference between $K_<$ and $K_>$ of

$$\frac{\hbar^2}{2\Im}(K_> - K_<) = \frac{\hbar^2}{2\Im}(2\Omega_<)\delta_{K,K_<}, \tag{28}$$

where $\Omega_<$ is the smaller of the Ω_p, Ω_n values. Since E_{int}^K favors K_T and E_{rot} favors $K_<$, if $K_T=K_<$ then no "violation" of the GM rule is possible (Singh and Sood, 1982). If $K_T=K_>$ and $(K_>-K_<)$ is large enough to compensate for the GM term then $E_S<E_T$ is possible (i.e., the GM rule appears to be violated).

Although there are 12 cases (^{156}Pm, ^{160}Eu, ^{154}Tb, ^{154,166}Ho, ^{156}Tm, ^{182}Re, and ^{184,188,190,192,196}Ir) in which violations of the GM rule are suspected, the evidence for violations in most instances is not very strong (Headly *et al.*, 1998). In 8 of the 12 cases the triplet energy is not known but the singlet state is proposed as the ground state, which in itself is a violation; the spin and parity of several proposed K_S states is tentative (as is the proposed energy for ^{182}Re). A puzzling example is that of ^{192}Ir, where the $I^\pi=3^-$ level at 84.3 keV is populated in the (d,t) reaction with an $\ell=5$ transition strength, in excellent agreement with that expected if the level were the $K^\pi=3^-, 3/2^+[402]_p-9/2^-[505]_n$ bandhead. However, according to the GM rule, the $K^\pi=6^-$ bandhead formed by parallel coupling of the same particles should be found at a lower excitation energy. It should have a stronger $\ell=5$ transition, but there is no evidence for such a level below about 200 keV. Thus there must be additional effects that are not taken into account. Finally, for N and Z near the transition region between deformed and spherical shapes (e.g., ^{154}Ho, ^{154}Tb, ^{156}Tm), the GM rule loses its validity. The quasiparticle-plus (vibrational)-phonon model calculations (see Sec. VI) actually favor a GM rule violation only in ^{154}Tb.

In only four of these nuclei, ^{166}Ho, ^{182}Re, ^{184}Ir, and ^{190}Ir, have both E_T and E_S configurations been observed (in ^{182}Re both E_S and I_S are very tentative), and only in ^{166}Ho has the situation been studied in detail (see Sood *et al.*, 1987, and references therein). In ^{184}Ir, $K_T=K_<$ and therefore at least one of the proposed assignments must be incorrect (no GM rule violation is possible); for the same reason the ground state in ^{156}Pm should not be assigned as 5/2[413] +3/2[521]. Although $K_T=K_>$ in ^{190}Ir so that a violation is possible, the extremely large anomalous GM splitting of 404 keV suggests that other interactions or mixings are taking place.

D. Level structures in well-deformed prolate nuclei

Theoretical treatments of the level structure of odd-odd deformed nuclei have taken many forms. However, they can logically be divided into two main types. The first of these is more nearly phenomenological and uses either theoretical or experimental energies of the odd-proton and odd-neutron orbitals to give a zeroth-order approximation for the energy of each configuration. The rotational and residual interactions are then added (see Sec. III.A).

The second modeling type involves a much wider variety of techniques, all of which might be classified under the category of microscopic modeling. It includes the Hartree-Fock-Bogolyubov and Soloviev methods.

In the following we give a description of the phenomenological approach. A microscopic model based on the Soloviev model will be described in Sec. VI.

1. Modeling the level structure of odd-odd deformed nuclei with the Pyatov-Struble phenomenological method (example ^{166}Ho)

One can effectively predict the excitation energies of 2qp configurations in an odd-odd deformed nucleus by use of a modeling technique first described by Pyatov (1963) and later described in detail by Struble, Kern, and Sheline (1965). The basic idea behind this model is that, if the *p-n* residual interaction energy in an odd-odd nucleus is small compared with the energy with which the odd nucleons are bound to the core, the excitations can be calculated by a simple extension of the odd-*A* model and the interaction energy treated as a perturbation. Thus the excitation of a given level is calculated as the sum of the two odd-nucleon excitations plus terms for the rotational energy and the residual interaction, as given by the following expression:

$$E_{IK}=E^{p}_{\rm qp}+E^{n}_{\rm qp}+\frac{\hbar^2}{2\Im}[I(I+1)-K^2 +(-1)^{I+1}a_p a_n\delta_{K,0}\delta_{\Omega_p,1/2}\delta_{\Omega_n,1/2}] -(\tfrac{1}{2}-\delta_{\Sigma,0})\Delta E_{\rm GM}+\delta_{K,0}(-1)^I B_{\rm N}. \quad (29)$$

The quasiparticle energies for the odd proton and the odd neutron can be obtained theoretically by the use of a single-particle average potential. One can obtain more accurate predictions by employing empirical values for these energies that are derived from experimental data in neighboring odd-mass nuclei (Jain *et al.*, 1990). Best results are obtained if one averages the neighboring isotopic odd-*A* experimental nuclear energies on both sides of the odd-odd nucleus and does the same for the isotonic odd-*A* nuclear energies. Effective moments of inertia may be obtained for each band in a manner proposed by Peker (1960), Struble *et al.* (1965), and Scharff-Goldhaber *et al.* (1967), as follows:

$$\Im_{\text{odd-odd}}=\Im_{\text{o-e}}+\Im_{\text{e-o}}-\Im_{\text{e-e}}. \quad (30)$$

Calculations reported in Table III, in the column labeled $E2$, used the values for the matrix elements of the *p-n* interaction from Boisson *et al.* (1976) and Frisk (1988), respectively. For configurations where calculations have not been performed, a mean value for all of the currently measured $\Delta E_{\rm GM}$'s in odd-odd rare-earth nuclei of 120 ± 30 keV was assumed. This modeling technique has been found to be most effective for the well-deformed nuclei of the rare-earth region, e.g., for nuclei included in the range from ^{156}Eu to ^{186}Re. Deviations from experiment of modeled bandhead energies average ±50 keV and of modeled rotational parameters average $\pm8\%$ for a selected group of nuclei accessible by use of neutron capture gamma-ray spectroscopy (Hoff *et al.*, 1990).

In order to demonstrate the use of this phenomenological model and to compare the theoretical and experimental level schemes we have chosen $^{166}_{67}$Ho$_{99}$. This nucleus offers one of the best known level schemes among odd-odd deformed nuclei. Over 330 energy levels and 20 rotational bands have been identified. Fifteen of the known bands have been assigned reasonably firm 2qp Nilsson-model configurations based on (d,p) and (t,α) reaction studies. However, for the other bands detailed assignments could only be suggested on the basis of plausibility arguments or model considerations.

The resulting experimental level scheme below 1250 keV is shown in Fig. 5 with the assigned 2qp configurations indicated under each pair of GM bands. All of the bands shown have either the ground-state proton or neutron configuration, except those in the shaded rectangle, which have both excited proton and excited neutron configurations. The theoretical level scheme for energies below 1250 keV is shown in Fig. 6. To facilitate comparison with the experimental level scheme, the sequence and the number of band members in the theoretical level scheme is purposely kept the same as in the experimental level scheme. The first thing to be noticed is the excellent gross overall agreement. We note, however, that the $K=0^-$ band is not the ground state in the theoretical level scheme. This failure of the GM coupling rule was discussed in Sec. III.C.5. Furthermore, the Newby splittings in the three $K=0$ bands are well reproduced only for the $K=0^-$, 1/2[411] −1/2[521] band.

Perhaps the most surprising feature of the theoretical spectrum of ^{166}Ho is that a vast number of configurations and rotational bands are predicted that are not experimentally observed. Specifically, 70 bandheads of 2qp states in ^{166}Ho are predicted below 1200 keV, whereas experimentally only 20 have been observed, and this is one of the best studied odd-odd cases. Thus it is quite clear that we are very far from having a complete experimental spectroscopy of odd-odd deformed nuclei, even in the low-energy region. It stands, therefore, as a special challenge to experimentalists to achieve a complete spectroscopy of a few odd-odd deformed nuclei at least in the low-energy region.

E. Level structure in heavy transitional nuclei

As one approaches the shape-transitional region near $A\sim190$ by considering nuclides of increasing mass, the spectra (Headly *et al.*, 1998), have usually been interpreted in terms of rotational bands built on 2qp configurations, usually specified in the language of the Nilsson model or the shell model. The competition between prolate and oblate deformations can also be seen in the data. For the iridium nuclei, most of the assignments are made in terms of prolate Nilsson orbitals. For gold nuclei of mass $A\geqslant186$ there are many bands interpreted as oblate. These appear as excited states in ^{186}Au but also as ground states in ^{188}Au to ^{192}Au. One of the well-known islands of superdeformation also occurs near the $A\sim190$ region.

As one proceeds from the very-neutron-deficient nuclei to those near the line of beta stability, experimental data are available from a greater variety of studies. As a result, the level schemes are much more complex, and more demanding tests of the models can be made. In recent years there have been several projects involving many collaborators, using complementary experimental

TABLE III. Experimental and theoretical bandhead energies and [singlet (K_S)-triplet (K_T)] energy splittings for the observed two-quasiparticle (2qp) configurations in medium-heavy odd-odd deformed nuclei. The left two columns list the Nilsson configuration of each state, using the appropriate asymptotic quantum numbers. The fourth column lists the nuclides in which the 2qp states appear, in order of increasing Z, A. E_T and E_S are experimental bandhead energies in keV. Parentheses and question marks come from Headly *et al.* (1998) and are carried over to ΔE(S−T) (in keV). Parentheses denote uncertain spin-parity assignments. A question mark indicates tentative K value and, therefore, characterization. The theoretical portion (col 8–15) lists results from three different calculational methods (see text for explanation): E_1, zeroth order estimate from odd-A nuclei, $E_T = E_S = E_{qp}(p) + E_{qp}(n)$; E_2, Pyatov-Struble phenomenological model; E_3, quasiparticle-plus-phonon model. The columns labeled "$\{p+n\}$ (%)" list first the percentage contribution of the major 2qp configuration (columns 1 and 2) in the quasiparticle-plus-phonon model to the total wave function for that state. If minor components contribute ⩾10%, their characterization (2qp or phonon, $Q_{\lambda\mu}$) and percentage are then listed and separated by a semicolon. A key at the end of the table identifies the abbreviations, p#±n#, used in these columns. An asterisk next to E_3 indicates that the 2qp configuration of columns 1 and 2 is calculated as a minor component of that wave function. "NA" in the quasiparticle-plus-phonon model columns means not available.

				Expt			Theory							
							K_T				K_S			
Proton $\Omega[Nn_3\Lambda\Sigma]$	Neutron $\Omega[Nn_3\Lambda\Sigma]$	K_T^π/K_S^π	^AX	E_T	E_S	ΔE(S−T)	E_1	E_2	E_3	$\{p+n\}$ (%)	E_1	E_2	E_3	$\{p+n\}$ (%)
1/2[550↑]	3/2[532↓]	$1^+/2^+$	^{144}La	603.4?										
	3/2[651↑]	$2^-/1^-$	^{148}La	(0.0)					4	89			0	89
3/2[541↑]	1/2[530↑]	$2^+/1^+$	^{148}La		56.1				48	87			67	72 ;$p1+n3$,12
			^{154}Ho		26.9?				806	84			819	84
			^{156}Tm		115.2?				1489*	2;$p8+n3$-Q_{22},98			1483*	2;$p8$-$n3$-Q_{22},98
	5/2[523↓]	$1^+/4^+$	^{152}Pm	0.0 or 294.6?					300	83;$p6$-$n4+Q_{30}$,11			347	82;$p6+n4+Q_{30}$,12
5/2[532↑]	3/2[532↓]	$1^+/4^+$	^{148}La	109.9					111	65;$p1$-$n1$,33			212	77;$p3+n2+Q_{30}$,16
			^{152}Pm	0.0 or 294.6?					0	72;$p3$-$n5$,20			49	52;$p3+n5$,36
			^{154}Pm	(850.2)					840	48;$p3+n3$-Q_{22},40			903	44;$p3$-$n3+Q_{22}$,42
			^{152}Eu	78.2	196.9?	118.7?			229	84			288	83
			^{154}Eu	249.4	(428.7)?	(179.3)?	301	306	376	84	301	439	442	85
			^{154}Ho		26.9?				42	95			148	94
			^{156}Tm	115.2?					1592*	5;$p7$-$n1+Q_{30}$,87			1621*	5;$p7+n1+Q_{30}$,88
	3/2[651↑]	$4^-/1^-$	^{152}Pr	(0.0)					0	81			0	80
			^{154}Eu	425.8	(549.6)	(123.8)	142	181	395	80	142	252	459	79
			^{156}Tb	(378.9(6^-))?					265	88			266	88
	3/2[521↑]	$4^+/1^+$	^{152}Pm		0.0 or 294.6?				208	51;$p3+n1$,41			182	67;$p3$-$n1$,23
			^{154}Pm	(0.0)?	(20(12))?	(20(12))?			0	85			37	84
			^{152}Eu	178.9?	(307.5)	(128.6)?			116	77;$p3+n2+Q_{30}$,10			161	76;$p3$-$n2+Q_{30}$,10
			^{154}Eu	326.9	(402.8)	(759.0)	108	123	307	73;$p3+n2+Q_{30}$,17	108	241	375	73;$p3$-$n2+Q_{30}$,16
			^{156}Eu	175.2	291.3	116.1			442	80			550	78
			^{158}Tb	459(5^+)	662(4^+)?				399	100			451	100
			^{160}Tb		(478.2)?		420	411	416	90	420	527	488	89

TABLE III. (*Continued*).

				Expt			Theory							
							K_T				K_S			
Proton $\Omega[Nn_3\Lambda\Sigma]$	Neutron $\Omega[Nn_3\Lambda\Sigma]$	K_T^π/K_S^π	^AX	E_T	E_S	ΔE(S−T)	E_1	E_2	E_3	$\{p+n\}$ (%)	E_1	E_2	E_3	$\{p+n\}$ (%)
5/2[532↑]	5/2[523↓]	$0^+/5^+$	^{154}Pm	(151.7(1^+))					134	90			220	90
			^{152}Eu	(177.7(1^+))?					212	89			31	88
	5/2[642↑]	$5^-/0^-$	^{152}Eu	180.6					64	84			200	82
			^{156}Eu	149.7	217.8	68.1			240	87			399	85
			^{152}Tb	342.2?					1638	76			1633	75
			^{154}Tb		(0.0)?				548	83;$p3+n9+Q_{22}$,13			543	82;$p3$-$n9$-Q_{22},13
			^{158}Tb	501	(780(3^-))?				518	87			516	86;$p3$-$n9$-Q_{22},10
	11/2[505↑]	$8^+/3^+$	^{152}Eu		221.2				222	87			232	87
			^{154}Eu		319.2		152	198	365	97	152	301	406	97
			^{152}Tb	501.7?					510	97			551	97
			^{154}Ho	320(110)					365	97			406	97
	3/2[402↓]	$1^-/4^-$	^{154}Eu	362.6	(467.5)	(104.9)	389	390	381	80	389	530	498	79
	7/2[633↑]	$6^-/1^-$	^{166}Ho	(1560)					1539	41;$p1+n12+Q_{22}$,28; $p3+n2+Q_{22}$,15			1495	41;$p1$-$n12$-Q_{22},29; $p3$-$n2$-Q_{22},15
5/2[413↓]	3/2[651↑]	$1^+/4^+$	^{152}Pm	0.0?					199	73;$p4$-$n5+Q_{30}$,15			259	72;$p4+n5+Q_{30}$,15
			^{152}Eu	158.0	227.7?	69.7			110	87			179	88
			^{154}Eu	71.9	203.8	131.9			139	89			209	90
	3/2[521↑]	$1^-/4^-$	^{152}Pm		170(130)				119	87			191	94
			^{156}Pm		(0.0)				0	90			118	89
			^{152}Eu	65.3	203.2	137.9			32	80;$p4$-$n2+Q_{30}$,10			322	75;$p4+n2+Q_{30}$,13
			^{154}Eu	82.8	235.3	152.5			10	80;$p4$-$n2+Q_{30}$,12			333	75;$p4+n2+Q_{30}$,17
			^{156}Eu	87.5	214.9	127.4			33	88			444	84
			^{158}Eu	(0.0)					0	55;$p4$-$n7+Q_{30}$,23; $p4$-$n2+Q_{30}$,20			93	50;$p4+n7+Q_{30}$,29; $p4+n2+Q_{30}$,19
			^{160}Eu	(0.0)?					46	52;$p4$-$n7+Q_{30}$,40			77	51;$p4+n7+Q_{30}$,40
	11/2[505↑]	$3^-/8^-$	^{150}Eu	1223.8					1730	74;$p4+n11$,14			1818*	25;$p7+n6+Q_{20}$,75
			^{152}Eu	0.0	147.8	147.8			0	93			165	93
			^{154}Eu	0.0	145.3	145.3			0	95			163	95
			^{156}Eu	434.2					433	94			592	93
	3/2[402↓]	$4^+/1^+$	^{152}Eu	89.8	(249.3)	159.5			86	84			191	83
			^{154}Eu	100.9	134.8	33.9			85	86			199	85
	5/2[642↑]	$0^+/5^+$	^{152}Eu		108.1				50	89			158	88
			^{154}Eu	(286.9)	415.7	(128.8)			318	86			429	86

TABLE III. (*Continued*).

				Expt			Theory							
							K_T				K_S			
Proton $\Omega[Nn_3\Lambda\Sigma]$	Neutron $\Omega[Nn_3\Lambda\Sigma]$	K_T^π/K_S^π	^AX	E_T	E_S	$\Delta E(\mathrm{S-T})$	E_1	E_2	E_3	$\{p+n\}$ (%)	E_1	E_2	E_3	$\{p+n\}$ (%)
5/2[413↓]	5/2[642↑]	$0^+/5^+$	^{156}Eu	0.0	145.7	145.7			0	93			106	92
			^{158}Tb		(587 or 665)?				480	87			587	86;$p4+n9+Q_{22}$,10
			^{160}Tb	222.6			320	289	224	81	320	440	330	79
	1/2[660↑]	$2^+/3^+$	^{152}Eu		114.0 or 146.1?				NA				NA	
	3/2[532↓]	$4^-/1^-$	^{152}Eu	141.8	203.1	61.3			133	90			198	89
			^{154}Eu	129.7	162.4	32.7			109	93			187	93
	1/2[400↑]	$2^+/3^+$	^{152}Eu	(249.0)	(483.3)	(234.3)			99	78;$p4$-$n3+Q_{30}$,17			545	71;$p4+n3+Q_{30}$,22
			^{154}Eu	282.8	(486.4)	(203.6)			128	79;$p4$-$n3+Q_{30}$,18			665	70;$p4+n3+Q_{30}$,24
	1/2[530↑]	$2^-/3^-$	^{152}Eu	(283.7)	(359.8)	(76.1)			166	80			359	78;$p4+n9+Q_{30}$,10
			^{154}Eu	419.7	515.9	96.2			340	73;$p4$-$n9+Q_{30}$,14			558	70;$p4+n9+Q_{30}$,19
			^{152}Tb	0.0?					0	100			4	100
	5/2[523↓]	$5^-/0^-$	^{152}Eu		(341.2(1^-))?				285	90			283	89
			^{154}Eu	364.0	(414.7)?	(50.7)?			397	92			410	90
			^{156}Eu	368.5	(513.3(1^-))?				364	94			381	94
			^{160}Eu		(0.0)?				0	94			17	93
			^{152}Tb	342.2?					342	99			303	99
	1/2[521↓]	$3^-/2^-$	^{152}Eu	(345.6)?	(482.9)	(137.3)?			NA				NA	
			^{170}Tm	1213(6)	1382	169			1299	85			1373	92
	7/2[633↑]	$1^+/6^+$	^{166}Ho	(1150)	(1272)	(122)	1045	989	1103	75;$p4$-$n2$-Q_{22},11	1045	1152	1230	74;$p4+n2+Q_{22}$,11
7/2[404↓]	3/2[651↑]	$2^+/5^+$	^{152}Pm	(119.2)?					152	76;$p5$-$n5+Q_{30}$,13			208	75;$p5+n5+Q_{30}$,13
			^{158}Ho	(408.8)					268	55;$p5+n9$-Q_{22},30; $p5$-$n12+Q_{22}$,10			327	54;$p5$-$n9+Q_{22}$,31; $p5+n12$-Q_{22},10
	3/2[521↑]	$2^-/5^-$	^{158}Tb	709	817	108			678	74;$p6+n3$,22			792	99
			^{158}Ho	67.2	(156.9)?	(89.7)?			80	96			150	88
			^{160}Ho	60.0			202	214	34	50;$p9+n5$,31	202	325	159	92
			^{158}Tm	0.0					0	90			158	93
			^{162}Tm	66.9					57	67;$p9+n5$,17			142	91
			^{166}Tm		($334<E<354$)?				306	93			349	93
			^{164}Lu	(0.0)?					0	94			88	86
			^{174}Lu	(1178 or 1185)	(1305 or 1312)				1185	73			1289	72
			^{166}Ta	(0.0)?					0	97			41	97
	3/2[532↓]	$5^-/2^-$	^{154}Ho		0.0?				48	100			389	77;$p5$-$n5$,22
			^{156}Tm		0.0?				0	100			0	100
	5/2[642↑]	$1^+/6^+$	^{158}Ho	315.8					356	54;$p5$-$n9$-Q_{22},34			459	84;$p8+n4$,14

TABLE III. (*Continued*).

				Expt			Theory							
							K_T				K_S			
Proton $\Omega[Nn_3\Lambda\Sigma]$	Neutron $\Omega[Nn_3\Lambda\Sigma]$	K_T^π/K_S^π	^AX	E_T	E_S	ΔE(S−T)	E_1	E_2	E_3	$\{p+n\}$ (%)	E_1	E_2	E_3	$\{p+n\}$ (%)
7/2[404↓]	5/2[642↑]	$1^+/6^+$	^{162}Tm		$E>81$?				169	82;$p5$-$n9$-Q_{22},10			275	80;$p5+n9+Q_{22}$,11
			^{164}Tm	(97.2)?	?		126	130	89	79;$p5$-$n9$-Q_{22},17	126	228	196	78;$p5+n9+Q_{22}$,18
			^{166}Tm		$211<E<231$				163	85			270	84
			^{166}Lu		(190)				77	54;$p5$-$n9$-Q_{22},39			177	52;$p5+n9+Q_{22}$,42
			^{170}Lu	785.5			596	611	771	74;$p5$-$n9$-Q_{22},24	596	724	879	73;$p5+n9+Q_{22}$,25
	7/2[633↑]	$0^+/7^+$	^{166}Ho	803.4	(915)	(112)	842	800	776	62;$p5$-$n2$-Q_{22},17	842	933	925	60;$p5+n2+Q_{22}$,18
			^{168}Tm	(17)	312	(295)	208	220	91	82;$p5$-$n2$-Q_{22},11	208	351	242	81;$p5+n2+Q_{22}$,11
			^{170}Tm	(719.2(1^+))?			585	576	722	68;$p5$-$n2$-Q_{22},24	585	719	867	66;$p5+n2+Q_{22}$,25
			^{170}Lu	0.0			0	0	0	85	0	139	150	84
			^{172}Lu	65.8			127	78	58	98	127	215	211	98
			^{174}Lu	281.2	431.4	150.2	286	292	265	88	286	409	414	88
			^{176}Lu		854.7		1017	1013	708	87	1017	1150	857	86
			^{176}Ta	100.2					114	90			264	89
	5/2[523↓]	$6^-/1^-$	^{164}Tm	$E<40$			6	40	37	94	6	126	33	94
			^{166}Tm	109-129					190	94			180	75;$p9+n11$,25
			^{166}Lu	(0.0)	(57.2)	(57.2)			7	96			0	91
			^{168}Lu	0.0					10	96				80;$p5$-$n13$,16
			^{170}Lu		801.7		568	617	799	95	568	680	799	95
	1/2[521↓]	$4^-/3^-$	^{166}Tm	($E>235$)?					478	92			515	91
			^{170}Tm	644	774.6	130.6	437	447	589	87	437	578	692	64;$p9+n11+Q_{22}$,22
			^{170}Lu	92.9	148.1	55.2	43	92	120	97	43	161	238	97
			^{172}Lu	0.0	68	68	0	0	0	100	0	69	114	100
			^{174}Lu	365.2	432.9	67.7	284	313	342	100	284	427	448	98
			^{176}Lu	908.3	957.9	49.6	954	975	913	95	954	1088	954	94
			^{180}Ta	719	780	61	541	584	686	86	541	691	785*	36;$p5+n17$-Q_{22},55
	5/2[512↑]	$1^-/6^-$	^{170}Tm	590.2					804	74			878	73
			^{166}Lu		(144.8)				100	89			172	89
			^{170}Lu	164.7			114	113	95	64;$p9+n11$,36	114	286	240	95
			^{172}Lu	41.9	213.6	171.7	90	39	89	98	90	210	164	98
			^{174}Lu	0.0	170.8	170.8	0	0	0	93	0	162	76	93
			^{176}Lu	637.9	765.7	127.8	659	646	674	88	659	795	748	88
			^{176}Ta	0.0					0	97			74	97
			^{180}Ta	414	571	157	454	479	440	55;$p5$-$n16$-Q_{32},33	454	622	518	57;$p5+n16$-Q_{32},28
	7/2[514↓]	$7^-/0^-$	^{174}Lu	523 or 877?			475	494	486	87	475	628	489	87

TABLE III. (*Continued*).

				Expt			Theory							
							K_T				K_S			
Proton $\Omega[Nn_3\Lambda\Sigma]$	Neutron $\Omega[Nn_3\Lambda\Sigma]$	K_T^π/K_S^π	^AX	E_T	E_S	ΔE(S−T)	E_1	E_2	E_3	$\{p+n\}$ (%)	E_1	E_2	E_3	$\{p+n\}$ (%)
7/2[404↓]	7/2[514↓]	$7^-/0^-$	^{176}Lu	0.0	237.1	237.1	0	0	0	97	0	143	21	96
			^{178}Lu	136(5)			163	175	137	96	163	344	152	95
			^{180}Lu	500?					1084	93			1080	91
			^{178}Ta	⩾0			0	0	1	100	0	162	0	100
			^{180}Ta	465			313	391	456	83;$p5+n17+Q_{22}$,12	313	423	445	91
			^{182}Ta	1116.0			1033	1097	1100*	31;$p5+n23+Q_{33}$,54; $p5+n16$-Q_{31},13	1033	1100	1056*	31;$p5$-$n23$-Q_{33},68
	1/2[510↑]	$3^-/4^-$	^{174}Lu	(1085(5))	(1204)	(119)	971	994	1124	96	971	1114	1157	96
			^{176}Lu	658.6	723.0 or 788.2		543	555	710	94	543	674	729	93
			^{180}Lu	13.9			0	0	33	89	0	114	53	89
			^{180}Ta		(659)		457	494	580	96	457	617	623	94
			^{182}Ta	0.0	114.3	114.3	0	0	0	97	0	121	56	97
			^{184}Ta	(47.9)					50	85			112	94
			^{186}Ta	(0.0)					0	89			66	88
	9/2[624↑]	$1^+/8^+$	^{176}Lu	339.0	424.9	230.4	260	250	235	90	260	427	400	89
			^{178}Lu	0.0	187	187	0	0	0	93	0	202	164	93
			^{180}Lu	562.0			33	5	662	76;$p12$-$n16+Q_{31}$,15	33	170	820*	1;$p12+n16$-Q_{31},99
			^{180}Ta	0.0	176	176	0	0	0	91	0	191	160	90
			^{182}Ta	593.0			571	541	523	83	571	747	682	81
			^{184}Ta	(617.2)					632	74;$p5+n13$-Q_{32},10			781	73;$p5+n13+Q_{32}$,10
	3/2[512↓]	$5^-/2^-$	^{176}Lu	834.8	1029.7	194.9	834	883	940	75;$p5+n15$-Q_{22},12	834	931	926	76
			^{182}Ta	173.2	270.4	97.2	212	244	25	95	212	323	431	90
			^{184}Ta	(0.0)	(89.3)	(89.3)			0	91			411	96
	11/2[615↑]	$2^+/9^+$	^{180}Lu	453.2			282	260	504	97	282	459	713	97
			^{182}Ta	402.6			311	294	396	99	311	505	607	99
	7/2[503↑]	$0^-/7^-$	^{182}Ta	583.3	776.4	193.1	510	467	614	76;$p5$-$n16$-Q_{31},11; $p5$-$n23$-Q_{13},11	510	691	736	75;$p5+n23+Q_{33}$,13
			^{184}Ta	(272.3)					278	84			394	81
3/2[411↑]	3/2[532↓]	$0^-/3^-$	^{152}Eu	45.6	220.8	175.2			200	82			259	83
	3/2[521↑]	$3^-/0^-$	^{152}Eu	77.3	161.0(1^-)?				156	76;$p6+n2+Q_{30}$,10			186	75;$p6$-$n2+Q_{30}$,11
			^{154}Eu	239.3	(279.0)	(39.7)			279	74;$p6+n2+Q_{30}$,15			319	72;$p6$-$n2+Q_{30}$,16
			^{156}Eu	353.4	513(1^-)?				448	79			490	76
			^{154}Tb	>0	0.0?				12	99			0	99
			^{156}Tb	0.0	(100(1^-))?		0	0	0	95	0	102	17	95
			^{158}Tb	0.0	109.4	109.4			0	100			25	100
			^{160s}Tb	0.0	79.1	79.1	4	4	0	93	4	92	42	94
	11/2[505↑]	$7^-/4^-$	^{152}Eu		(287.1)?				NA				NA	
			^{154}Eu		(471.9)				NA				NA	
			^{154}Tb	>0					284	100			277	100
			^{156}Tb	(>50)			107	142	100	98	107	254	93	98
			^{158}Tb	388.4	495	106.6			450	99			443	99
	1/2[530↑]	$2^-/1^-$	^{152}Eu	328.1?	(436.2)?	108.1			NA				NA	

TABLE III. (*Continued*).

				Expt			Theory							
							K_T				K_S			
Proton $\Omega[Nn_3\Lambda\Sigma]$	Neutron $\Omega[Nn_3\Lambda\Sigma]$	K_T^π/K_S^π	^AX	E_T	E_S	ΔE(S−T)	E_1	E_2	E_3	$\{p+n\}$ (%)	E_1	E_2	E_3	$\{p+n\}$ (%)
3/2[411↑]	1/2[530↑]	$2^-/1^-$	^{152}Tb	0.0?					110	97			103	97
			^{158}Tb	(678)					678	82			713	87
	1/2[521↓]	$1^-/2^-$	^{152}Eu	(361.7)?	(519)?	(157)?			NA				NA	
			^{160}Tb	381.3	515.0	133.7	414	394	396	99	414	524	503	98
			^{166}Ho	373.1?	562.9 or 638.8	189.8 or 265.7?	515	461	446	86;$p3+n11$-Q_{32},12	515	590	536	98
			^{168}Ho	(143.5)					145	96			188	97
			^{170}Tm	(720)			611	598	757	96	611	729	780	59;$p9$-$n11+Q_{22}$,18 $p9$-$n4$,11
	5/2[523↓]	$1^-/4^-$	^{152}Eu	221.5(2)	(434.7)				NA				NA	
			^{160}Tb	63.7	257.5	193.8	41	0	123	99	41	189	195	99
			^{162}Tb	0.0	216	216			0	94			75	94
	3/2[651↑]	$3^+/0^+$	^{154}Eu	281.7	(342.2)?	(60.5)?			336	81			326	80
			^{154}Tb		0.0?				402	80;$p6$-$n9+Q_{22}$,14			392	80;$p6$-$n9$-Q_{22},14
			^{156}Tb	49.6(4)?					37	89			30	89
	5/2[642↑]	$4^+/1^+$	^{156}Eu	260.2					NA				NA	
			^{156}Tb	49.6			35	50	263	87;$p6+n9+Q_{22}$,10	35	125	274	86;$p6$-$n9$-Q_{22},11
			^{158}Tb	55.0	180	125			119	91			130	90
			^{160}Tb	64.1	138.7	74.6	0	13	93	82	0	77	104	82
	3/2[402↓]	$0^+/3^+$	^{156}Tb	(88.4)			289	243	91	91	289	437	230	92
			^{158}Tb	(420)	590	(170)			447	93			586	91
	1/2[400↑]	$2^+/1^+$	^{158}Tb	639	(699)	(60)			278	96			1090	60;$p6$-$n5+Q_{31}$,33
	7/2[633↑]	$5^+/2^+$	^{164}Tb	(0.0)					0	91			34	91
			^{166}Ho	263.8	430.0	166.2	330	295	234	41;$p8+n5$,30	330	416	283	49;$p8$-$n5$,14; $p8$-$n12+Q_{32}$,11; $p1+n12$-Q_{32},10
	5/2[512↑]	$4^-/1^-$	^{166}Ho	599.4	740.9	141.5	599	576	576	79	599	665	764	48;$p6$-$n4$,34
			^{170}Tm		863.4		693	715	973	58;$p9$-$n13+Q_{22}$,25	693	801	1040	54;p9+n13-Q_{22},27
	7/2[514↓]	$2^-/5^-$	^{176}Lu		1395				1401*	0;$p8$-$n15+Q_{32}$,100			1466*	3,$p8+n15$-Q_{32},87
5/2[402↑]	3/2[521↑]	$4^-/1^-$	^{158}Tb	962	1068	106			974	73			1021	67;$p4$-$n5+Q_{20}$,12
			^{158}Ho		139.2?				117	74;$p12+n5$-Q_{32},14			160	73;$p12$-$n5$-Q_{32},15
			^{160}Lu	(>0)?					209	83			246	81
	1/2[530↑]	$3^-/2^-$	^{154}Ho		0.0?				0	99			42	99
			^{156}Tm		0.0?				0	66;$p7+n24+Q_{20}$,10			7	66;$p7$-$n24+Q_{20}$,11

TABLE III. (*Continued*).

				Expt			Theory							
							K_T				K_S			
Proton $\Omega[Nn_3\Lambda\Sigma]$	Neutron $\Omega[Nn_3\Lambda\Sigma]$	K_T^π/K_S^π	^AX	E_T	E_S	$\Delta E(S-T)$	E_1	E_2	E_3	$\{p+n\}$ (%)	E_1	E_2	E_3	$\{p+n\}$ (%)
5/2[402↑]	7/2[633↑]	$6^+/1^+$	^{168}Tm	732	818	86	628	662	746	72;$p8+n13$,24	628	744	760	57;$p9$-$n12$-Q_{22},24; $p7$-$n2$-Q_{22},10
			^{170}Lu		349.0		367	408	331	74	367	476	347	65
			^{172}Lu		179.8?		465	463	523	90	465	508	538	90
			^{172}Ta	(<40)					14	93			32	92
			^{174}Ta	(131.3)					155	90			173	89
			^{176}Ta		184.3				164	88			181	88
			^{176}Re	(>0)?					268	67;$p7+n2+Q_{22}$,11			273	66;$p7$-$n2$-Q_{22},11
	1/2[521↓]	$2^-/3^-$	^{170}Tm	716	862.8	147	821	820	759	63;$p14$-$n11$-Q_{33},10; $p9+n5$,10	821	952	833	61;$p8$-$n11+Q_{30}$,12
			^{172}Lu	(406)	(513)	(107)	338	310	405	86;$p12$-$n11$-Q_{32},10	338	415	498	87
			^{180}Re	(78.1)?	(25.0)?	(−53.1)?			63	97			92	97
			^{182}Re	~260 or ~656?			421	381	656	94	421	514	708	93
	5/2[523↓]	$0^-/5^-$	^{166}Lu	(42.9)					36	86			108	86
	5/2[512↑]	$5^-/0^-$	^{174}Lu	456	553	97	362	376	492	69;$p14+n13$-Q_{32},10	362	491	506	69;$p14$-$n13$-Q_{33},10
			^{176}Re	>0					317	72			343	71
	7/2[514↓]	$1^-/6^-$	^{176}Lu	386.7	563.9	177.2			419	71;$p12$-$n15$-Q_{32},11			537	72;$p12+n15$-Q_{32},10
			^{178}Ta		>289		169	159	193	97	169	341	292	97
			^{180}Re	(0.0)	(>0)				0	93			110	93
			^{182}Re	~287 or ~403?			385	333	229	99	385	529	320	94
			^{176}Lu	734.0	866.4	132.4	616	664	760	75	616	725	790	74
	9/2[624↑]	$7^+/2^+$	^{178}Lu	(499)?			570	640	489	78;$p8+n16$-Q_{31},13	570	701	516	71;$p8$-$n16+Q_{31}$,19
			^{180}Ta	361	563	202	376	440	437	84;$p12+n13$,14	376	502	460	79;$p12$-$n13$,18
			^{180}Re	(25.0 or >79)?					260	95			290	95
			^{182}Re	0.0	~24?	~24?	0	0	0.0	90	0	67	25	89
			^{184}Re	(590)?			441	516	586	90	441	551	611	90
	1/2[510↑]	$3^-/2^-$	^{176}Lu	(1040)?	(1133)	(93)?	899	907	1164	74	899	1012	1172	73
			^{182}Ta	547.1	647.6	100.5	484	483	526	75;$p14$-$n14$-Q_{32},18	484	585	618	59;$p12$-$n14$-Q_{32},22
			^{182}Re		~260?		349	330	240	88	349	430	262	88
			^{184}Re	0.0	(74)	(74)	0	0	0.0	96	0	103	31	96
			^{186}Re	99.4	210.7	111.3	20	69	101	96	20	101	98	96
			^{188}Re	169.4	256.9	87.5			207	85			204	97
	3/2[512↓]	$1^-/4^-$	^{182}Ta	443.6			697	647	641	53;$p12$-$n17$-Q_{32},28	697	861	891	46;$p12+n17$-Q_{32},24; $p8+n17$-Q_{31},11
		$1^-/4^-$	^{182}Re	~287 or ~403?			744	669	401	86	744	879	511	84

TABLE III. (*Continued*).

				Expt			Theory							
							K_T				K_S			
Proton $\Omega[Nn_3\Lambda\Sigma]$	Neutron $\Omega[Nn_3\Lambda\Sigma]$	K_T^π/K_S^π	^AX	E_T	E_S	$\Delta E(S-T)$	E_1	E_2	E_3	$\{p+n\}$ (%)	E_1	E_2	E_3	$\{p+n\}$ (%)
5/2[402↑]	3/2[512↓]	$1^-/4^-$	^{184}Re	(56)	(311)	(255)	148	103	127	96	148	317	238	95
			^{186}Re	0.0	173.9	173.9	0	0	0	93	0	201	95	93
			^{188}Re	0.0	(182.7)	(182.7)			0	90			82	89
	11/2[615↑]	$8^+/3^+$	^{182}Ta		(749.1)?		795	825	1000	65;$p12+n18-Q_{32}$,22	795	949	1062	64;$p12-n18+Q_{32}$,21
			^{184}Re	188.0	381.0	193?	232	248	250	97	232	384	304	97
			^{186}Re	149(37)	314.0?	165?	179	248	202	95	179	381	253	94
			^{188}Re		(439.8)				380	96			431	82
	7/2[503↑]	$6^-/1^-$	^{184}Re	(348)?	(440)?	(92)?	227	331	339	96	227	371	445	95
			^{186}Re	186	316.5	130	129	181	205	94	129	321	275	92
			^{188}Re	172.1	290.7	118.6			219	90			240	90
			^{190}Re	(∼170)?					818	90			800	90
	9/2[505↓]	$2^-/7^-$	^{186}Re	577.7			746	781	571	91	746	959	740	91
			^{188}Re	205.3					100	91			271	92
			^{190}Re	0.0					0.0	95			174	95
	3/2[501↑]	$4^-/1^-$	^{188}Re	325.9	(556.8)?	(230.9)?			408	72			461	70;$p7-n17-Q_{22}$,10
7/2[523↑]	5/2[523↓]	$1^+/6^+$	^{162}Tb	442.1					299	$p6-n4-Q_{32}$,18			1038	
			^{156}Ho	82.1					86	73;$p17+n4-Q_{22}$,12; $p8-n4-Q_{22}$,10			192	71;$p2+n4+Q_{22}$,17
			^{160}Ho	67.1			226	192	61	88	226	391	179	86
			^{162}Ho	0.0					0	89			123	88
			^{164}Ho	0.0	(191)	(191)			0	96			123	92
			^{166}Ho	567.6			605	533	466	55;$p8-n13$,31	605	733	568	87
			^{168}Ho	630.4					648	92			785	92
			^{160}Tm	215.8					215	98			336	98
			^{162}Tm	163.4					151	94			272	93
			^{164}Tm	0.0			97	69	0	94	97	256	124	92
			^{166}Tm	82.3					104	91			230	90
			^{162}Lu	(0.0)?					128	83;$p2-n4-Q_{22}$,12			242	82;$p2+n4+Q_{22}$,13
			^{166}Lu	136.0					142	86			265	85
			^{168}Ta		178.5				179	91			304	89
	3/2[521↑]	$5^+/2^+$	^{156}Ho	(0.0)?	52.2				8	70;$p1+n5+Q_{22}$,14			13	94
			^{158}Ho	0.0	118 or 137	118 or 137			0	85			35	96
			^{160}Ho	0.0			0	0	0	86	0	127	65	86
			^{164}Ho	(343)	(486)	(143)			370	85			456	84
			^{160}Tm	70(20)?	(174.4)	104(30)?			113	97			175	97

TABLE III. (*Continued*).

				Expt			Theory							
							K_T				K_S			
Proton $\Omega[Nn_3\Lambda\Sigma]$	Neutron $\Omega[Nn_3\Lambda\Sigma]$	K_T^π/K_S^π	^AX	E_T	E_S	ΔE(S−T)	E_1	E_2	E_3	$\{p+n\}$ (%)	E_1	E_2	E_3	$\{p+n\}$ (%)
7/2[523↑]	3/2[521↑]	$5^+/2^+$	^{162}Tm	67≤E≤192					94	88			158	87
	$5/2^+$[642↑]	$6^-/1^-$	^{158}Ho	(227.8)?	139.2 or 378.2				328	52;$p8+n9+Q_{22}$,35			320	51;$p8$-$n9$-Q_{22},36
			^{160}Ho	118.4			348	386	103	59;$p8+n9+Q_{22}$,30	348	472	97	58;$p8$-$n9$-Q_{22},31
			^{162}Ho	106	179.9	74			131	64;$p8+n9+Q_{22}$,25			128	63;$p8$-$n9$-Q_{22},25
			^{164}Ho	140	$(234(3^-))$?				176	61;$p8+n9+Q_{22}$,29			176	60;$p8$-$n9$-Q_{22},30
			^{162}Tm	230<E<355					275	77;$p8+n9+Q_{22}$,11			230	77;$p8$-$n9$-Q_{22},11
			^{166}Tm	231<E<251					192	81			190	80
	3/2[651↑]	$5^-/2^-$	^{158}Ho		(143.5)?				224	48;$p8$-$n9+Q_{22}$,28; $p8+n7$,10			214	53;$p8+n9$-Q_{22},32; $p8$-$n12+Q_{22}$,10
			^{166}Ho		543.7?				579	33;$p8+n12$-Q_{22},31; $p8+n15$-Q_{32},15; $p8$-$n9+Q_{22}$,10			551	29;$p8$-$n12+Q_{22}$,26 $p8$-$n7$,18; $p8$-$n15+Q_{32}$,16
	3/2[402↓]	$2^-/5^-$	^{158}Ho		(156.9)?				93	73			182	61
			^{164}Ho	(620)	(733)	(113)			622	64;$p8$-$n5+Q_{30}$,11 $p8+n5+Q_{33}$,11			718	62;$p8+n5+Q_{30}$,15; $p8$-$n5+Q_{33}$,10
	11/2[505↑]	$9^+/2^+$	^{158}Ho	180					225	90			270	89
			^{160}Ho	(<225)?					202	81			262	80
	1/2[521↓]	$3^+/4^+$	^{164}Ho	188.6					194	92			326	92
			^{166}Ho	190.9	372.0	181.1	184	128	163	86	184	296	307	91
			^{168}Ho	0.0					0	98			153	97
			^{170}Tm	402.7 or 891(5)?	$(829(7))(5^+)$		371	352	498	83	371	529	639	82
	1/2[400↑]	$4^-/3^-$	^{164}Ho	(833)?	(925)?	(92)?			702	88			109.9	77
	1/2[660↑]	$4^-/3^-$	^{164}Ho	(833)?	(925)?	(92)?			835	38;$p8$-$n2+Q_{22}$,37; $p8+n8$-Q_{22},17			848*	36;$p8+n2$-Q_{22},41; $p8$-$n8+Q_{22}$,16
	7/2[633↑]	$7^-/0^-$	^{166}Ho	6.0	0.0	−6	0	0	0	72;$p8+n2+Q_{22}$,10	0	47	2	71;$p8$-$n2$-Q_{22},10
			^{170}Tm		683.6		520	560	718	67;$p8+n2+Q_{22}$,23	520	598	711	65;$p8$-$n2$-Q_{22},24
	1/2[510↑]	$4^+/3^+$	^{166}Ho	558.6	815.1	256.5	693	666	434	83	693	777	950	76
	5/2[512↑]	$6^+/1^+$	^{166}Ho	295.1	426.0	130.9	268	261	354	66;$p8+n8+Q_{30}$,15	268	334	362	44;$p8$-$n4$,28; $p8$-$n8+Q_{30}$,14
			^{168}Ho	(59)	192.5	(133)			115	98			134	98
			^{170}Ho	(0.0)	(120(70))	(120(70))			0	99			18	99
			^{170}Tm		661.9		454	459	762	72	454	589	877	59;$p10+n11$,15
			^{172}Tm		610.1		341	434	588	82	341	508	572	78

TABLE III. (*Continued*).

				Expt			Theory							
							K_T				K_S			
Proton $\Omega[Nn_3\Lambda\Sigma]$	Neutron $\Omega[Nn_3\Lambda\Sigma]$	K_T^π/K_S^π	^AX	E_T	E_S	ΔE(S−T)	E_1	E_2	E_3	$\{p+n\}$ (%)	E_1	E_2	E_3	$\{p+n\}$ (%)
7/2[523↑]	5/2[512↑]	$6^+/1^+$	^{174}Tm		(58.5)?				647	61;$p2+n13+Q_{22}$,19			655	60;$p2$-$n13$-Q_{22},20
	9/2[624↑]	$8^-/1^-$	^{174}Tm		(58.5)?				4	62;$p8+n8+Q_{22}$,24; $p2+n16+Q_{22}$,11			81	60;$p8$-$n8$-Q_{22},26; $p2$-$n16$-Q_{22},12
	7/2[514↓]	$0^+/7^+$	^{176}Lu	(1057(8))	1273	(216)			1092	67			1257	62;$p8+n19+Q_{20}$,10
1/2[411↓]	3/2[521↑]	$1^-/2^-$	^{156}Ho	87.5					60	74			138	44;$p18$-$n5+Q_{22}$,15; $p5$-$n5$,11;$p6$-$n5+Q_{22}$,11
			^{158}Ho	139.2?					133	85			172	58;$p19+n5+Q_{20}$,14; $p4+n5$-Q_{22},13
			^{160}Tm	0.0					0	97			39	97
			^{162}Tm	0.0					0	91			20	73;$p5$-$n5$,18
			^{168}Tm	(614)	(700)	(86)	717	717	631	74	717	848	659	74
			^{170}Tm	648.7	854.3	205.6	797	753	668	54;$p9+n11$-Q_{22},33	797	944	696	84;$p7$-$n11$,12
			^{160}Lu	(⩾0)?					0	85			44	85
			^{162}Lu	(0.0)?					0	87			37	85
			^{164}Lu	(0.0)?					37	86			60	76;$p9$-$n4$,11
	5/2[523↓]	$3^-/2^-$	^{160}Ho		60.0?		467	468	160	94	467	579	180	91
			^{164}Ho	(>0)?			0	0	431	93	0	130	477	93
			^{164}Tm	<40?					13	94			17	94
			^{166}Tm	109.4					2	94			10	96
			^{168}Tm	(849)?	(897)	(48)?	620	639	875	88;$p7+n11$,10	620	749	873	96
			^{166}Lu	(34.4)					38	94			52	94
	1/2[521↓]	$1^-/0^-$	^{166}Ho	350.6 or 595.7?	525.4 or 759.5(2^-)?	174.8?	627	586	416	69;$p4+n11$-Q_{22},17	627	670	530	87
			^{168}Ho	(187.3)					184	100			348	99
			^{168}Tm	3	167	164	139	152	13	98	139	235	185	97
			^{170}Tm	0.0	149.7	149.7	0	0	0	96	0	83	153	94
			^{172}Tm	407.3	475.4?	681.0?	320	382	358	90	320	465	488	92
			^{174}Tm	(767 or 773)?					779	80;$p9$-$n5$-Q_{22},12			892	76;$p9+n5$-Q_{22},13
			^{170}Lu	244.9	407.5	162.6	238	244	305	62;$p5$-$n13$,38	238	331	396	98
			^{172}Lu	(237.4)?	(237.4)?		356	316	78	100	356	400	224	100
	5/2[642↑]	$2^+/3^+$	^{160}Tm	(140.3)					140	98			211	98
			^{164}Tm	(97.2)?			121	118	91	78;$p9$-$n9+Q_{22}$,19	121	222	162	77;$p9+n9+Q_{22}$,20
			^{166}Tm	0.0	423.6(6^+)?		61	35	0	88	61	157	71	94
			^{168}Tm	(769(4^+))?					584	83;$p9+n5+Q_{30}$,10			644	62;$p9+n9+Q_{22}$,31
	7/2[633↑]	$3^+/4^+$	^{166}Ho	592.5 or 721.1?	(719.4) or (891.6)?	(126.9) or (170.5)?	443	392	202	70;$p9$-$n2+Q_{22}$,12	443	545	284	70;$p9+n2+Q_{22}$,12
			^{168}Tm	0.0	148.4	148.4	0	0	0	83;$p9$-$n2+Q_{22}$,11	0	152	83	80;$p9+n2+Q_{22}$,11
			^{170}Tm	183.2	355.0	171.8	148	137	217	78;$p9$-$n2+Q_{22}$,18	148	283	296	76;$p9+n2+Q_{22}$,19
	5/2[512↑]	$2^-/3^-$	^{168}Tm	325(3^-)	499		268	220	273	82;$p6+n11$,18	268	468	484	76;$p5$-$n11$,22

TABLE III. (*Continued*).

				Expt			Theory							
							K_T				K_S			
Proton $\Omega[Nn_3\Lambda\Sigma]$	Neutron $\Omega[Nn_3\Lambda\Sigma]$	K_T^π/K_S^π	^AX	E_T	E_S	ΔE(S−T)	E_1	E_2	E_3	$\{p+n\}$ (%)	E_1	E_2	E_3	$\{p+n\}$ (%)
1/2[411↓]	5/2[512↑]	$2^-/3^-$	^{170}Tm	204.4	447.1	242.7	82	22	267	82	82	271	340	81
			^{172}Tm	0.0	239.9	239.9	0	0	0	99	0	247	77	90
			^{172}Lu	(196.6)?			446	359	215	97	446	580	291	96
	1/2[510↑]	$0^-/1^-$	^{168}Tm	(792(1^-))?	(885(2^-))?				655	93			964	81;$p9+n11+Q_{20}$,12
	1/2[400↑]	$0^+/1^+$	^{168}Tm	1056	1347	291			1114	75;$p9$-$n5$-Q_{31},11			1153	62;$p9$-$n5+Q_{30}$,30
	3/2[402↓]	$2^+/1^+$	^{168}Tm	1115	1426	311			1261*	28;$p9$-$n4+Q_{30}$,58			1215	34;$p9+n10$,26; $p9+n5$-Q_{31},23
	7/2[514↓]	$4^-/3^-$	^{174}Tm	0.0					0	66;$p9+n17+Q_{22}$,12			94	63;$p9$-$n17+Q_{22}$,13
			^{176}Lu	723.0?	843.4	120.4?	643	562	776	89	643	871	792	89
	9/2[624↑]	$4^+/5^+$	^{176}Tm	(0.0)					0	89			45	88
			^{176}Lu	985.6			903	870	1065	74;$p9$-$n19+Q_{31}$,15	903	1097	1114	71;$p9+n19+Q_{31}$,16
			^{178}Lu	656	834	178	621	610	707	78;$p9$-$n19+Q_{31}$,12	621	837	758	74;$p9+n19+Q_{31}$,14
	3/2[512↓]	$2^-/1^-$	^{182}Ta	740.1?			875	859	737	83	875	966	1073	62;$p9$-$n23+Q_{31}$,18
			^{188}Re	(582.2)?	(745)?	(163)?	672	706	569	59;$p16+n17$,16; $p7+n17$-Q_{22},16	672	813	734	82;$p16$-$n17$,10
1/2[541↓]	7/2[633↑]	$3^-/4^-$	^{166}Ho		771.5		714	693	635	47;$p9$-$n12+Q_{30}$, 19;$p7$-$n12+Q_{32}$,15	714	777	730	45;$p9+n12+Q_{30}$, 18;$p7+n12$-Q_{32},17
			^{168}Tm	193.3	337.7	144.4	257	290	187	72	257	375	286	71
			^{170}Tm	715.6			711	727	733	54;$p9$-$n12+Q_{30}$,13	711	809	852	53;$p9+n12+Q_{30}$,14
			^{170}Lu	(96.0)?			93	117	128	79	93	199	232	77
			^{172}Ta		(<40)				1	90			117	88
			^{174}Ta		(>98(6^-))?				221	87			227	87
	1/2[521↓]	$1^+/0^+$	^{170}Tm	604.0	661.9(1^+)		563	592	477	80;$p8$-$n13$,16	563	615	568	58;$p9$-$n11+Q_{30}$, 14;$p20+n11$-Q_{22},10
			^{170}Lu	160 or 198.4?	(436.9)?	(320.9 or 238.5)?	136	176	297		136	194	324	89
			^{172}Lu	109.4	(232.5)?	123.1	142	133	152	89	142	151	175	88
			^{182}Re	(~751)?			1015	996	1148	90	1015	1033	1154	96
	5/2[512↑]	$2^+/3^+$	^{170}Tm	758.3			645	694	782	95	645	710	798	55;$p9+n13+Q_{30}$,14
			^{174}Lu	278?	414.4	136?	305	350	290	57;$p15+n13$-Q_{32},13; $p7$-$n13+Q_{32}$,10	305	384	364	75;$p7+n13$-Q_{32},10
	5/2[523↓]	$3^+/2^+$	^{166}Lu	(60.5)					73	83			125	82
			^{168}Lu	220(130)					229	81			269	80
			^{168}Ta	(0.0)?					0	84			46	84
			^{170}Ta	(0.0)					0	90			33	89
			^{170}Re	(0.0(5^+))					0	91			45	91
	7/2[514↓]	$4^+/3^+$	^{176}Lu	635.3	734.4	99.1	445	463	683	69;$p7+n15$-Q_{32},16	445	545	675	68;$p7$-$n15+Q_{32}$,18
			^{180}Re	(25.0)?	(78.1)?	(53.1)?			60	89			54	88
			^{182}Ir	84.4(6^+)					8	70;$p10+n19$,18			0	65;$p10$-$n19$,21
	5/2[642↑]	$2^-/3^-$	^{168}Ta	(0.0)?					367	38;$p10$-$n9+Q_{22}$,37; $p10$-$n13+Q_{30}$,16			400*	36;$p10+n9+Q_{22}$,39; $p10+n13+Q_{30}$,16
	9/2[624↑]	$4^-/5^-$	^{182}Re	(~485)?			595	587	484	82;$p7$-$n16+Q_{32}$,10	595	665	494	80;$p7$-$n16$-Q_{32},12
			^{180}Ir		(0.0)?				0	91			11	91
			^{182}Ir		(>127)				163	89			175	89
			^{184}Ir	70.8	0.0	−70.8			0	88			13	88
	1/2[510↑]	$0^+/1^+$	^{192}Au		306.5?				NA				NA	

TABLE III. (*Continued*).

				Expt			Theory							
							K_T				K_S			
Proton $\Omega[Nn_3\Lambda\Sigma]$	Neutron $\Omega[Nn_3\Lambda\Sigma]$	K_T^π/K_S^π	^AX	E_T	E_S	ΔE(S−T)	E_1	E_2	E_3	$\{p+n\}$ (%)	E_1	E_2	E_3	$\{p+n\}$ (%)
1/2[530↑]	7/2[633↑]	$4^-/3^-$	^{168}Tm	1389	1434	45			1375*	12;p9-n12+Q_{31},75			1718	94
	5/2[512↑]	$3^+/2^+$	^{174}Lu	(1261)	(1293)	(32)			1107	57;p7+n13-Q_{32},22			1391	53;p7-n13+Q_{32},35
9/2[514↑]	3/2[521↑]	$6^+/3^+$	^{166}Lu	(83.5)					252	87;p7+n5+Q_{32},11			333	86
			^{168}Re	(0.0)					14	99			0	99
	5/2[642↑]	$7^-/2^-$	^{166}Lu	(287.2)					286	64;p12+n9+Q_{22},26			281	62;p12-n9-Q_{22},27
			^{168}Ta	(>0(10$^-$))?					1060	37;p12+n9+Q_{22},37; p12+n13+Q_{30},16			1050*	35;p12-n9-Q_{22},39; p12-n13+Q_{30},16
	1/2[521↓]	$4^+/5^+$	^{172}Lu	(581(5$^+$))?	(640)		455	449	483	79;p7-n11+Q_{32},21	455	539	650	76;p7+n11+Q_{32},24
			^{174}Ta		(82.8)				54	93			89	92
	5/2[512↑]	$7^+/2^+$	^{174}Lu	531	(635)	(104)	413	448	537	75;p7+n13+Q_{32},16	413	557	571	71;p22+n13-Q_{22},11; p7-n13+Q_{32},11
			^{176}Lu	(709.2)?			1045	1053	1115	63;p7+n13+Q_{32},36	1045	1174	1134	63;p7-n13+Q_{32},34
			^{176}Ta	(>0)					80	90			98	89
	7/2[633↑]	$8^-/1^-$	^{174}Lu	(772.0)			699	730	840	73;p7+n12+Q_{32},14	699	809	841	73;p7-n12-Q_{32},14
			^{174}Ta	(>190)					263	88			290	88
			^{176}Ta	(>187)					230	89			232	89
	7/2[514↓]	$1^+/8^+$	^{176}Lu	194.5	487.8	293.3	386	360	311	77;p7-n15-Q_{32},22	386	574	515	76;p7+n15+Q_{32},23
			^{178}Lu	390.8			244	240	138	99	244	462	340	98
			^{180}Lu	981.6					979	89			1158	86
			^{178}Ta	⩾0	(⩾220)	?	43	58	6	96	43	207	211	95
			^{180}Re	20.1	(>0)?				39	92			234	91
			^{182}Re	510.1			738	675	570	93	738	912	743	92
			^{182}Ir		>446?				265	80;p7-n15-Q_{32},14			428	78;p7+n15+Q_{32},16
	9/2[624↑]	$9^-/0^-$	^{176}Lu	642.0	646.1 or (780.2)?	4.1 or (138.2)?	646	698	666	83;p7+n16+Q_{32},10	646	749	702	82;p7-n16-Q_{32},10
			^{178}Lu	120			81	157	124	98	81	205	164	98
			^{178}Ta	⩾393			369	402	409	97	369	476	422	97
			^{180}Ta	75.3	134(1$^-$)		9	76	104	75;p7+n16+Q_{32},20	9	127	113	75;p7-n16-Q_{32},20
			^{182}Ta	652.4			602	652	680*	23;p7+n16+Q_{32},76	602	689	686*	22;p7-n16-Q_{32},77
			^{180}Re	(>79)?					306	95			345	94
			^{182}Re	443.1	(∼293)?		353	354	356	84;p7+n16+Q_{32},13	353	416	388	82;p7-n16-Q_{32},14
	1/2[510↑]	$5^+/4^+$	^{176}Lu	657.1	871.3?	214.2?	929	940	1119	80;p7+n14+Q_{32},16	929	1079	1111	80;p7-n14+Q_{32},16
			^{180}Lu	0.0	(102.8)	(102.8)	141	140	7	86	141	273	0	86
			^{182}Ta	16.3	150.1	133.8	32	30	33	64;p7+n14+Q_{32},36	32	169	176	60;p7-n14+Q_{32},39
			^{184}Re	(348)?	(348)?		404	407	351	95	404	546	345	95
			^{186}Re	(330)?	(471)?	(141)?	280	330	461	90;p7+n14+Q_{32},10	280	470	456	90;p7-n14+Q_{32},10
			^{188}Re	360.9			289	359	429	83;p7+n14+Q_{32},16	289	494	423	83;p7-n14+Q_{32},16
	3/2[512↓]	$3^+/6^+$	^{180}Lu	442.3					425	68;p12-n22+Q_{30},15			495	66;p12+n22+Q_{30},15; p12+n23+Q_{31},10
			^{182}Ta	250.0	(390.1)	(140.1)	244	230	152	54;p7+Q_{32},45	244	416	412	54;p7+n17+Q_{32},45
			^{186}Re	314.0 or (351.2)?	(562)?	(211) or (248)?	260	292	373	88	260	469	439	89
			^{188}Re	(230.9)	(486)?	(255)?	187	218	233	82;p7-n17+Q_{32},33	187	397	292	82;p7+n17+Q_{32},12
	11/2[615↑]	$10^-/1^-$	^{182}Ta	519.6	740.1(2$^-$)?		342	418	531	67;p7+n18+Q_{32},33	342	432	580	66;p7-n18−Q_{32},,34

TABLE III. (*Continued*).

				Expt			Theory							
							K_T				K_S			
Proton $\Omega[Nn_3\Lambda\Sigma]$	Neutron $\Omega[Nn_3\Lambda\Sigma]$	K_T^π/K_S^π	^AX	E_T	E_S	ΔE(S−T)	E_1	E_2	E_3	$\{p+n\}$ (%)	E_1	E_2	E_3	$\{p+n\}$ (%)
9/2[514↑]	7/2[503↑]	$8^+/1^+$	^{184}Ta		(453.3)				484	89			441	77;p7-n19-Q_{32},22
			^{186}Re		601.6		390	505	630	92	390	534	574	93
			^{188}Re		(482.2)		437	543	470	86	437	578	441	90
	9/2[505↓]	$0^+/9^+$	^{188}Re	(207.9)					289	92			513	91
			^{190}Re	(162.1)					167	93			392	93
3/2[532↓]	5/2[512↑]	$1^+/4^+$	^{174}Lu		(672.0)				639	58;p9+n13-Q_{32},16			677	80
	9/2[624↑]	$3^+/6^+$	^{186}Au	0.0					0	74			60	73
	1/2[510↑]	$1^+/2^+$	^{192}Au	306.5?					NA				NA	
11/2[505↑]	3/2[521↑]	$7^+/4^+$	^{168}Re	(162.1)?					181	100			160	100
			^{170}Re	(210.4)?					213	99			199	99
			^{172}Ir	(140(11))?					148	97			120	97
			^{174}Ir	(193(11))?					197	97			169	97
	5/2[523↓]	$3^+/8^+$	^{168}Re	⩾349?					369	100			450	100
			^{170}Re	(224.7)?					222	99			320	99
			^{172}Ir	(0.0)?					0	99			79	99
			^{174}Ir	(0.0)?					0	97			78	97
	9/2[505↓]	$1^+/10^+$	^{190}Re	319.7?					334	96			680	95
			^{192}Ir	(193.5)					39	100			385	100
	7/2[514↓]	$2^+/9^+$	^{182}Ir	(>907)?					76	93			194	93
	11/2[615↑]	$11^-/0^+$	^{190}Ir	175.0					260	100			296	100
			^{192}Ir	(212)	(226)?	(14)?			196	100			230	100
			^{194}Ir	(240<E<440)?					341	100			373	100
	3/2[512↓]	$4^+/7^+$	^{190}Ir	465					366	100			399	100
			^{192}Ir	(217)					294	100			321	100
			^{194}Ir	270.9					145	100			177	100
3/2[402↓]	7/2[503↑]	$2^-/5^-$	^{186}Ir	<1.5					30	88			154	94
	1/2[510↑]	$1^-/2^-$	^{186}Ir	(~55)?	~111	(~56)?			93	96			113	92
			^{188}Ir	0.0?					0	90			16	90
			^{190}Ir	⩾26	(⩾220)	(194)			118	95			126	99
			^{192}Ir	56.7	192.9	136.2			117	98			131	99
			^{194}Ir	0.0 or 161.0?	112.2 or 501.8?	112.2 or (340.8)?			0	98			14	98
			^{192}Au	0.0?					0	96			24	96
	11/2[615↑]	$4^+/7^+$	^{188}Ir	(354.2)?					348	94			480	93
			^{190}Ir	0.0	26.3				0	100			133	100
			^{192}Ir	0.0					0	100			134	100
			^{194}Ir	147.1					192	100			324	100
	9/2[505↓]	$6^-/3^-$	^{190}Ir	(⩾442)	⩾38	(−404)			181	100			297	100
			^{192}Ir		84.3				11	100			132	85;p15+n17,15
	3/2[512↓]	$3^-/0^-$	^{190}Ir	⩾83.0	⩾183.2	100.2			132	100			134	100

TABLE III. (*Continued*).

				Expt			Theory							
							K_T				K_s			
Proton $\Omega[\mathrm{Nn},\Lambda\Sigma]$	Neutron $\Omega[\mathrm{Nn},\Lambda\Sigma]$	K_T^π/K_S^π	${}^AX$	E_T	E_S	$\Delta E(S-T)$	E_1	E_2	E_3	$\{p+n\}$ (%)	E_1	E_2	E_3	$\{p+n\}$ (%
3/2[402↓]	3/2[512↓]	$3^-/0^-$	^{192}Ir	118.8	128.7	9.9			116	89;$p15$-$n20$,11			125	100
			^{194}Ir	148.9	(245.5)?	(96.6)?			34	99			15	99
			^{192}Au	(66.8)?	(157.3)?				1286	87			1267	86
	5/2[503↓]	$4^-/1^-$	^{192}Ir						513	97			675	97
1/2[400↑]	3/2[521↑]	$2^-/1^-$	^{188}Ir		0.0?				NA				NA	
	3/2[512↓]	$1^-/2^-$	^{188}Re	(556.8) or (582.2)					539	51;$p7$-$n17$-Q_{22},34			704	44;$p7+n17$-Q_{22},31; $p9+n17$,18
			^{190}Ir	⩾144.0	⩾225.0	81			128	98			239	95
			^{192}Ir	104.8 or (212.8)?	311.0	206.2 or (98.2)?			176	96			266	96
			^{194}Ir	82.3					124	97			186	96
			^{194}Tl		0.0?				0	100			62	100
	9/2[505↓]	$4^-/5^-$	^{192}Ir	(66.8)?					156	98			178	97
	11/2[615↑]	$6^+/5^+$	^{192}Ir		(178)				154	96			171	96
	1/2[10↑]	$1^-/0^-$	^{192}Ir	235.8	(264)	(28)			180	89			241	95
			^{194}Ir	138.7?	(143.6)	(4.9)?			91	96			155	96

Table III Key

P-1 1/2[550↑]	P-5 7/2[404↓]	P-9 1/2[411↓]	P-13 3/2[532↓]	P-16 1/2[400↑]	P-19* 1/2[651↓]
P-2 3/2[541↑]	P-6 3/2[411↑]	P-10 1/2[541↓]	P-14 11/2[505↑]	P-17*[b] 1/2[510↑]	P-20*[b] 11/2[615↑]
P-3 5/2[532↑]	P-7 5/2[402↑]	P-11 1/2[530↑]	P-15 3/2[402↓]	P-18* 3/2[651↑]	P-21*[b] 3/2[512↓]
P-4 5/2[413↓]	P-8 7/2[523↑]	P-12 9/2[514↓]			

N-1 3/2[532↓]	N-5 3/2[521↑]	N-9 1/2[660↑]	N-13 5/2[512↑]	N-17 3/2[512↓]	N-21[b] 3/2[501↑]
N-2 3/2[651↑]	N-6 11/2[505↑]	N-10 1/2[400↑]	N-14 1/2[510↑]	N-18 11/2[615↑]	N-22 3/2[642↓]
N-3 1/2[530↑]	N-7 3/2[402↓]	N-11 1/2[521↓]	N-15 7/2[514↓]	N-19 7/2[503↑]	N-23* 1/2[651↓]
N-4 5/2[523↓]	N-8 5/2[642↑]	N-12 7/2[633↑]	N-16 9/2[624↑]	N-20 9/2[505↓]	N-24*[a] 1/2[541↓]

*Not in Headly *et al.*, 1998; present calculations only.

[a]1/2[541↓] appears before N-1 in a Nilsson diagram (in energy).

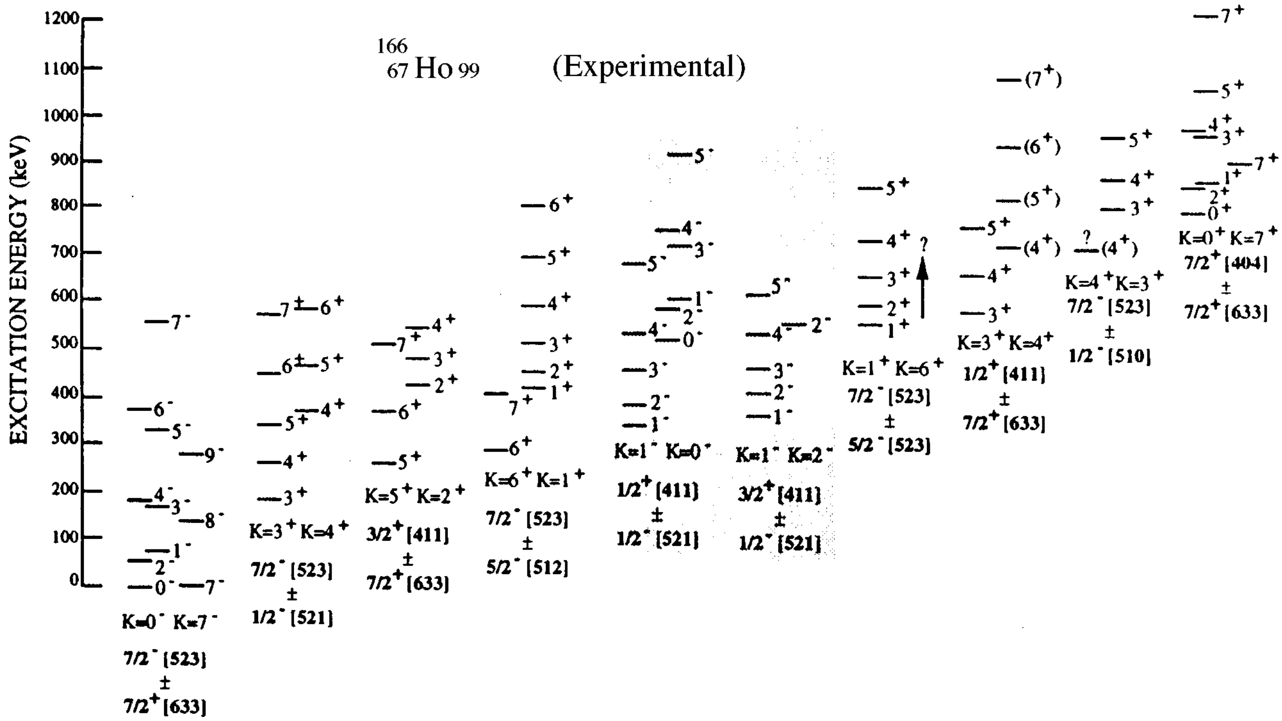

FIG. 5. The experimental structure of ^{166}Ho below 1250 keV. All the bands shown have either ground-state proton or neutron partial configurations except those in the shaded area, which have both excited proton and neutron partial configurations.

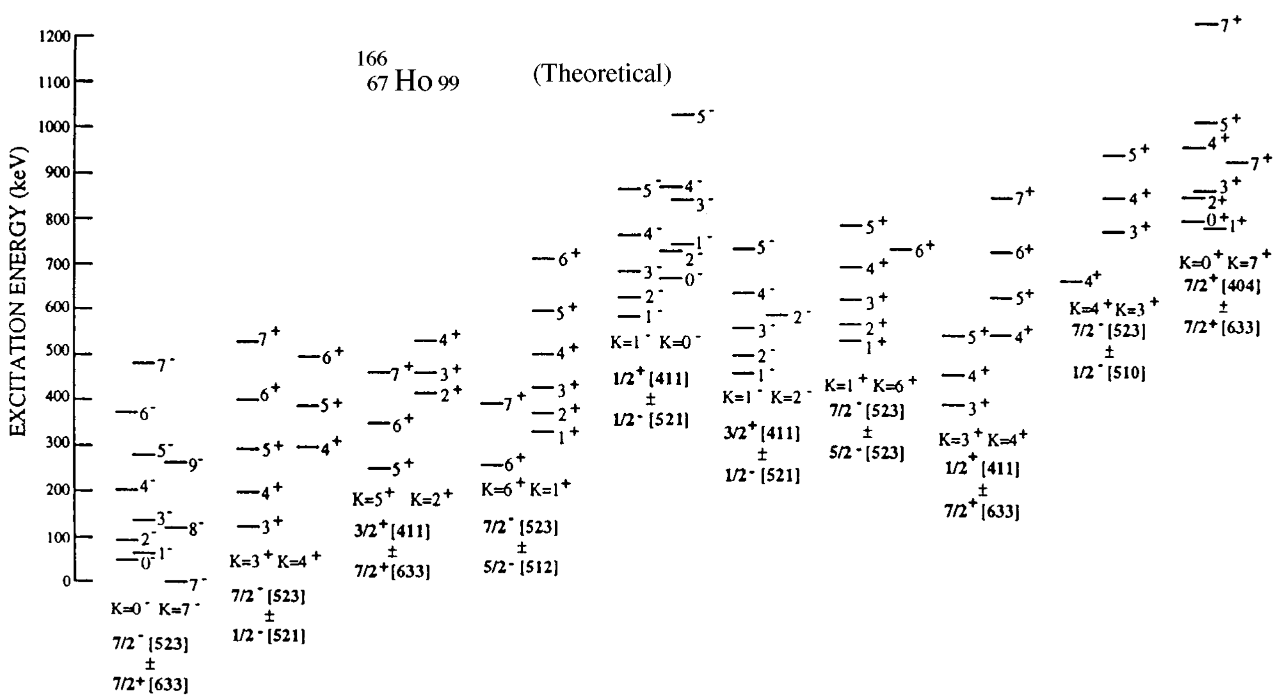

FIG. 6. Partial calculated band structure for ^{166}Ho below 1250 keV. Only those bands which correspond to the experimental level structure in Fig. 5 are given. Furthermore the ordering of the bands is the same as that in Fig. 5.

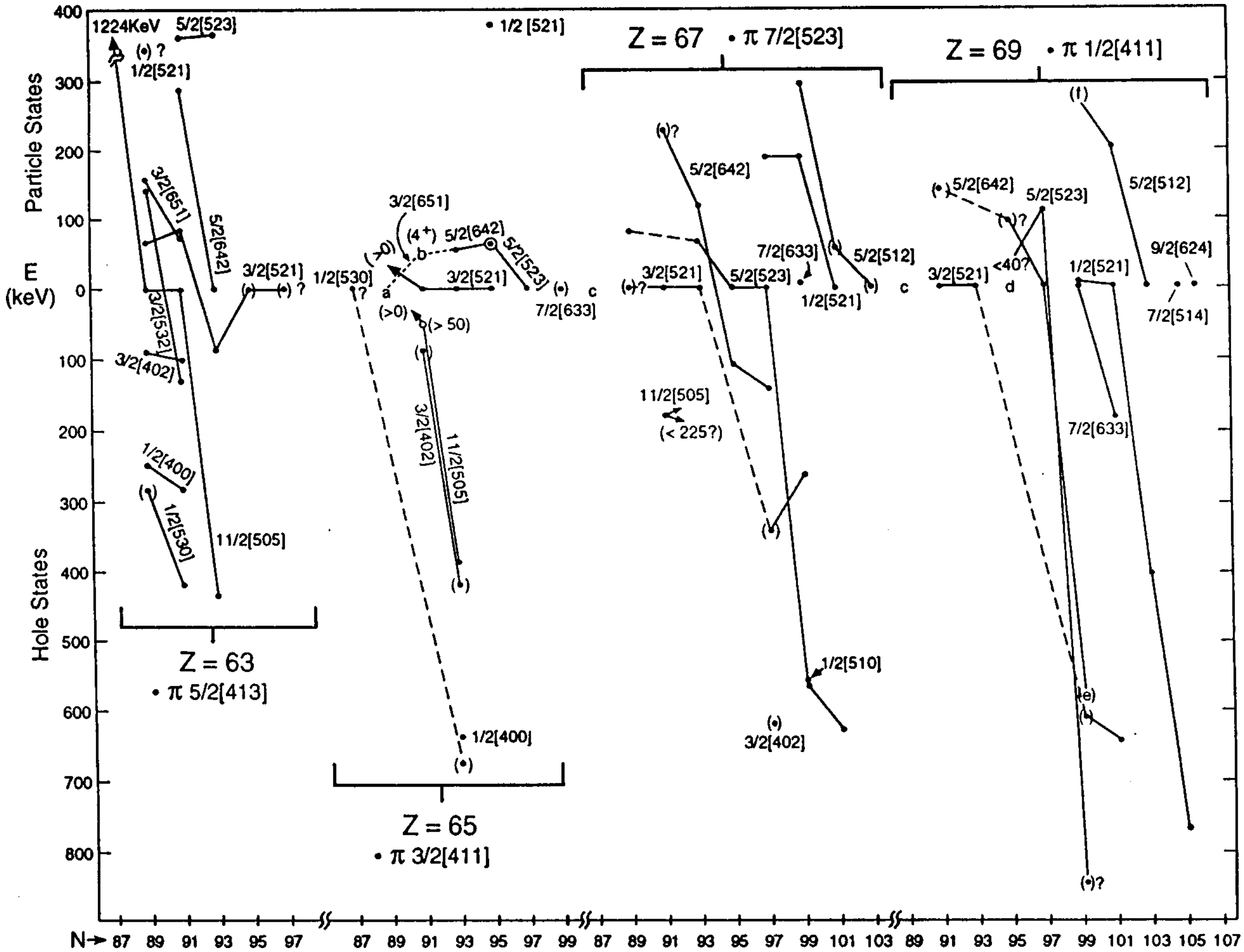

FIG. 7. Systematics of various 2qp configurations in odd-odd nuclei with the proton part of the configuration fixed, for various neutron configurations, as a function of neutron number and particle and hole excitation energy (keV). The systematics are shown for proton numbers $Z=63$, 65, 67, and 69. Key: (a) ^{154}Tb ground state proposed as 0^+ singlet state or 5/2[532]-5/2[642]; (b) either $3/2[651]_\nu(K=3)$ or $5/2[642]_\nu$; (c) $5/2[402]_\pi$ or $7/2[404]_\pi$; (d) $7/2[523]_\pi$; (e) theory ($E[4^+]=769$ keV expt); (f) theory ($E[3^-]=325$ keV expt).

techniques to study the structures of ^{190}Ir (Garrett and Burke, 1995; Garrett *et al.*, 1996), ^{192}Ir (Kern *et al.*, 1991; Garrett and Burke, 1994), and ^{194}Ir (Balodis *et al.*, 1994; Garrett *et al.*, 1994). The case of ^{192}Ir has the advantage that both neighboring isotopes are stable, so that, in addition to the studies of radioactive decays and in-beam spectroscopy, it is possible to benefit from the excellent resolution achievable with (n,γ) reactions and from the powerful techniques of single-neutron transfer with both stripping and pickup reactions. For ^{190}Ir the target needed for (n,γ) studies is not stable, but it is possible to perform single-proton transfer as well as single-neutron transfer reactions to study the levels because ^{189}Os is stable.

One of the most striking observations from these projects is that there is abundant evidence for serious configuration mixing of the various 2qp states found, even at low excitation energies. For example, Kern *et al.* (1991) showed that for the ground state of ^{192}Ir no single 2qp configuration was consistent with all the experimental data; in order to explain properties such as the spin, parity, magnetic moment, and lack of (d,t) cross section, it was necessary to invoke a strongly mixed structure. As another example, if the 2qp states in ^{190}Ir were relatively pure there should be only about five or six levels populated strongly in *both* the single-neutron transfer and the single-proton transfer reactions. In practice, about twice this many were strongly populated in both reactions at low excitation energies (Garrett and Burke, 1995), indicating strong mixings. Furthermore, for all three of these iridium nuclides, the observed cross sections for individual levels could be better explained by including effects such as Coriolis mixing, but it was still not possible to obtain the good quality of agreement between experimental and calculated strengths that is seen in the well-deformed regions.

IV. SYSTEMATICS AND INTERPRETATION

An important tool for understanding the spectroscopy of individual nuclei is to study the systematics, i.e., the variation with increasing Z and N of certain observables associated with intrinsic states and their resulting rotational bands: absolute excitation energy, relative ener-

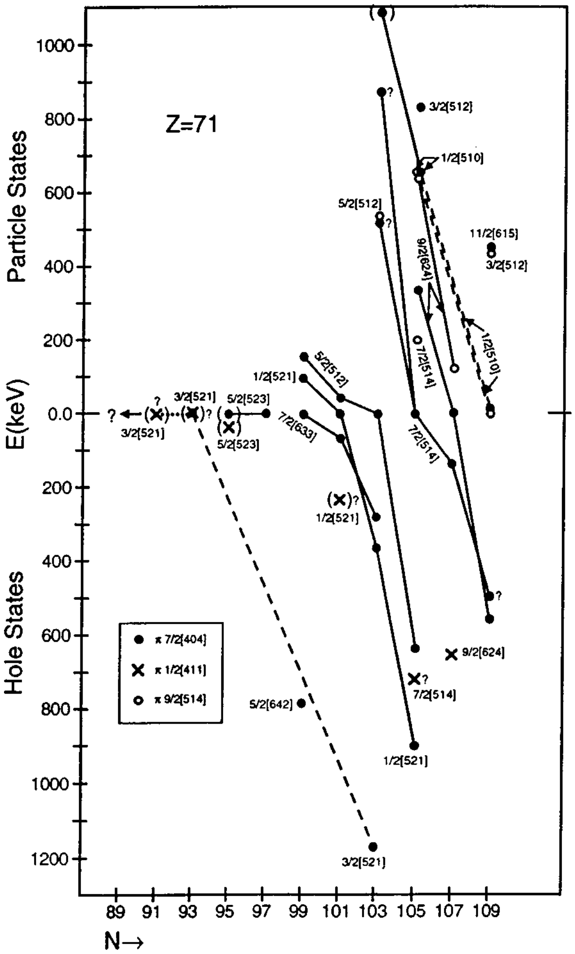

FIG. 8. Same as Fig. 7, for $Z=71$; also three π orbitals instead of one.

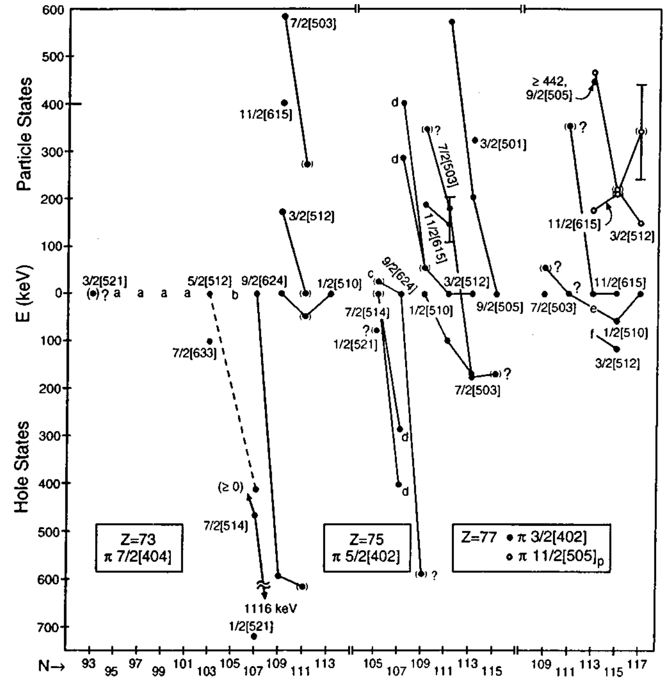

FIG. 9. Same as Fig. 7, for $Z=73$, 75, and 77. Key: (a) $1/2[541]_\pi$; (b) $9/2[514]_\pi$; (c) energy could also be >79 keV; (d) either $3/2[512]_\nu$ (particle) or $7/2[514]_\nu$ (hole); (e) $E \geqslant 26$ keV; (f) $E \geqslant 83$ keV.

gies between bandheads and between even and odd sequences of spin, isomerism, and multi-quasiparticle states, etc. In Secs. IV.A through IV.D we shall investigate these systematics in turn.

A. Introduction to Table III

All intrinsic states (Headly *et al.*, 1998) characterized by 2qp configurations are summarized in Table III. The Nilsson configurations of the protons are listed in column 1 and for each proton configuration the coupled neutron configurations are listed in column 2. $E_{\mathrm{T}}, K_{\mathrm{T}}$ and $E_{\mathrm{S}}, K_{\mathrm{S}}$, the triplet and singlet bandhead energies and spins of the "Gallagher-Moszkowski doublet" for a given Ω_p, Ω_n pair, will be separated by energy $\Delta E(S-T)$ in a predictable way. The 2qp states in Table III are classified in this manner, with $K_{\mathrm{T}}/K_{\mathrm{S}}$ in column 3, and E_{T}, E_{S}, and $\Delta E(S-T)$ in columns 5–7 for a given nucleus ^{A}X in column 4. Uncertainties in spins, parities, and energies are taken from Headly *et al.* (1998). Energies may appear more than once if a particular state has several alternative configurations proposed.

The right half of Table III is devoted to a theoretical analysis of the wave functions and excitation energies of the $K_{\mathrm{T}}, K_{\mathrm{S}}$ partners, using three different and successively more detailed calculational methods. For both K_{T} and K_{S}, columns labeled E_1 designate a zeroth-order approximation for the bandhead energies, determined by averaging the empirical π (proton) and ν (neutron) orbital energies observed in $(A-1)$ and $(A+1)$ nuclei which comprise the 2qp configuration: $E_T=E_S=E_{\Omega}^{p}+E_{\Omega}^{n}$. The triplet and singlet energies are thus degenerate in first order until an interaction is introduced in the model. This has been done in the columns labeled E_2, where the full Pyatov-Struble phenomenological model has been employed [see Eq. (28) in Sec. III.D]. Results are presented in columns E_1 and E_2 only for 2qp configurations where experimental data are present and reasonable input data exist. Columns E_3 and "$\{p+n\}$, %" designate results of the quasiparticle-plus-phonon model described in Sec. VI below. A key at the end of the table identifies the p#, n# abbreviations, including p17–p21 and n23,n24, which are not listed in the experimental data (Headly *et al.*, 1998) but come from present calculations.

B. Systematics of proton-neutron two-quasiparticle configurations

The systematics of p-n 2qp configurations in odd-odd nuclei reveal the variation in excitation energy of an intrinsic state over an isotopic or isotonic chain. This in turn can show the relative effect of the p and n orbitals on the 2qp energy as Z and N change. However, extracting such systematics from the available data in Table III is not so straightforward, contrary to the situation in odd-A nuclei (Jain *et al.*, 1990), for several reasons. First, and most obvious, is the scarcity of data for every configuration listed. Our survey contains 101 nuclei in which at least one state has been assigned either a 2qp or a shell-model characterization, and a total of 792 such characterizations, or fewer than 8 per nucleus on average—clearly, a very small fraction of all the possible 2qp states have been located to date. Comparing individual nuclei, we find that ^{152}Eu contains the most 2qp assignments with 37, followed by ^{176}Lu with 36 and ^{154}Eu with 32; only 8 nuclei have $\geqslant 20$ observed intrinsic states. The fraction of 2qp states that can be grouped into doublets with both K_{T} and K_{S} observed is also very small. Out of the 447 configuration/nucleus combinations presented, there are only 115 cases in which confident assignments of K_{T}, K_{S}, E_{T}, and E_{S} have been made, i.e., just over one per nucleus on average. The 2qp configuration most frequently observed is the 7/2[523] $\pm$5/2[523], $6^+/1^+$ doublet, with K_{T} or K_{S} measured a total of 15 times in 14 nuclei (but with only one instance of both K_{T} and K_{S} observed).

One reason for the small number of observed intrinsic states is the current focus in nuclear spectroscopy on high-spin states. This results in many levels observed per band but very few bandheads populated. Especially in the most p- or n-deficient nuclei, or in nuclei containing superdeformed bands, the ratio of total observed states to bandheads with confident assignments can be quite high: ^{158}Tm, 35/2; ^{168}Ta, 28/1; ^{178}Re, 71/1, ^{180}Re, 110/2; ^{194}Tl, 117/3.

Another limitation in studying the energy systematics of odd-odd nuclei comes from the method of assignment of 2qp configurations. Especially for nuclei near the limits of Z or N, where only one or several 2qp states have been identified, the configuration assignments have often been made from model expectations rather than from experimental data. For example, they may have been made indirectly through comparison with the ground-state assignments of odd-A neighbors, or purely from the use of a Nilsson diagram and appropriate Fermi level for prolate deformation $\epsilon \sim 0.2$–0.3 (e.g., in the case of isomers). In the former instance it is known that the ground state $K_{\mathrm{gst}} = \Omega_p \pm \Omega_n$ of an odd-odd nucleus, $_Z X_N$, is not always the same as the sum $\Omega_p(_Z X_{N\pm1}) \pm \Omega_n(_{Z\pm1} X_N)$, and in the latter case there are often two or more combinations of p and n orbitals which lie near each other on a Nilsson diagram that can lead to the same K^{π}_{gst}. A third indirect method of 2qp assignment, used particularly in high-spin work, is to compare an unknown band with those in neighboring odd-odd nuclei, if the level spacing and excitation energies appear similar. These indirect methods can lead to a potentially circular analysis in following the systematics of a given 2qp state: the systematics are used to assign new 2qp configurations, and then the larger data set is used to study "improved" systematics.

In Figs. 7–9 we plot the energy systematics of various 2qp configurations in medium-heavy odd-odd nuclei where significant data exist. The systematics are presented by fixing both Z and the π (proton) orbital, varying N, and following the energy of several coupled ν(neutron) orbitals (labeling the curves), looking only at resultant K_{T} states. This is done because the number of observed K_{T} states in a nucleus is normally greater than the number of K_{S} states; in Table III, 59% of states are K_{T}. Configurations are further distinguished according to their particle or hole nature relative to the ground state, determined separately for protons and neutrons from their position in the level scheme of neighboring odd-A nuclei (Figs. 15 and 16 in Jain *et al.*, 1990). This means that only those 2qp states are plotted for which the π or ν orbital is the odd-A ground state, or where both π and ν are holes or particles. (In the latter two cases the 2qp assignment has been made indirectly.) Long dashed lines indicate missing data points, and parentheses and question marks are taken from Headly *et al.* (1997). Significantly fewer data are available for fixed-N-and-ν-orbital/varying-Z combinations; we therefore do not show the plots of these systematics.

For fixed Z and varying N in Figs. 7–9, the π orbital of the ground state remains mostly the same, except in certain nuclei for N in the vicinity of 87. Similarly, for fixed N and varying Z, the ν orbital of the ground state remains essentially constant; in both cases this behavior mirrors the odd-A trend.

From Fig. 8 we see that the Lu isotopic chain and in particular the $7/2[404]_{\pi}$ orbital offer the most extensive systematics in this mass region. Using the Lu data as a representative example, we see that the general trend for a given 2qp configuration with increasing N is to begin as a particle excitation (pg, gp, or pp for the $\pi\nu$ configuration with $p \equiv$ particle, $g \equiv$ ground state, and $h \equiv$ hole configuration), decrease in energy as each additional pair of neutrons is added to the nucleus, and eventually become the ground state and then a hole (hg, gh, or hh) excitation as the ν Fermi level passes by. For $N = 89$–93 and 95,97, however, the same 2qp state is proposed as the ground-state configuration ($3/2[521]_{\nu}$ and $5/2[523]_{\nu}$, respectively). This feature occurs a total of seven times throughout Figs. 7–9 and reflects the odd-A behavior of the $7/2[404]_{\pi}$ orbital ($Z = 71$,73 ground state), and $3/2[521]_{\nu}$ ($N = 89$–93), $5/2[523]_{\nu}$ ($N = 95$,97), $3/2[512]_{\nu}$ ($N = 111$,113,117) and $1/2[521]_{\nu}$ ($N = 101$,103) orbitals, which remain the ground state over ranges in Z or N. This behavior in turn indicates a reordering of close-lying Nilsson orbitals as a result of changing deformation. The addition of each successive pair of neutrons to the nucleus (especially near closed shells) changes the deformation and mass, which also affect the 2qp energy through the π orbital.

Occasionally a particle (hole) state in Figs. 7–9 can be seen to increase (decrease) in energy as N or Z increases; see, e.g., $Z = 67$, 7/2[523] + 3/2[521](h); $Z = 77$, 11/2[505] + 11/2[615](p); and $Z = 63$, 5/2[413] $-$3/2[521] (p and h). This interesting feature is illustrated by the 11/2[505] + 11/2[615] 2qp state in $Z = 77$, $N = 111$–115 nuclei (Fig. 9), whose energy increases with N. The $11/2[505]_{\pi}$ orbital decreases sharply in energy in the range $N = 108$–116, while the $11/2[615]_{\nu}$ orbital remains fairly constant in energy for $Z = 76$, $N = 109$–115. This would imply that the 2qp energies do not follow the observed upward trend. The moment of inertia is probably decreasing between ^{190}Ir and ^{194}Ir, which would increase E_{rot} slightly but not enough to explain the large increase in total energy; the quasiparticle-plus phonon model predicts an increase in E_{rot} of 27 keV between ^{192}Ir and ^{194}Ir. But this model can offer us no further explanation for the rise in energy because the calculated energies were determined by a parameter-fitting procedure which included the experimental energies as input; if the fitting procedure had not been done, the 2qp energy in ^{194}Ir would not have increased relative to that in 2qp ^{192}Ir.

C. Coexistence of nuclear shapes

Different shapes and their corresponding spectroscopies often overlap. Most often this occurs in the shape-transition regions. For example, at the very beginning of the rare-earth region, one expects to find evidence for strong octupole correlations and possibly octupole deformation. As we proceed toward higher mass number the normal quadrupole deformation becomes dominant. However, there is a region in which both octupole-quadrupole and normal quadrupole deformation may coexist. In view of the evidence in even-even nuclei around $A\sim192$, it is possible that coexistence of prolate and oblate shapes (although so far unobserved) may occur in nuclei in the vicinity of ^{192}Ir (see Sec. III.E). Finally, it should also be noted that in all cases where superdeformation is observed there is coexistence with another shape, usually either the spherical shape or the normal quadrupole-deformed shape.

1. Octupole-quadrupole-deformed odd-odd rare earths

One of the most important recent developments in the study of nuclear shapes and spectroscopy has been the observation of octupole deformation. Just beyond the double spherical closed shells in ^{132}Sn, the $f_{7/2}$ and $\imath_{13/2}$ neutron orbitals and the $d_{5/2}$ and $h_{11/2}$ proton orbitals are very close together and also close to the Fermi surface. This combination of orbitals gives rise to very-low-energy $J^{\pi}=3^{-}$, 2qp configurations in even-even nuclei and a wide variety of spin-parity 4qp orbitals in odd-odd nuclei, which form the microscopic basis for possible stable octupole deformation (Sheline, 1989). Substantial evidence for reflection-asymmetric shape has been observed for nuclei in the $A\sim150$ region.[1] Simultaneously, theoretical studies have suggested that the best candidates for static reflection-asymmetric shape should occur when $N\sim88$ and $Z\sim56$, i.e., $A\sim144$ (Leander *et al.*, 1985; Sobiczewski *et al.*, 1988). Thus the experimental and theoretical evidence for the region of stable octupole deformation is somewhat in disagreement. This disagreement may be the result of very inadequate data in the highly neutron-excess region proposed as octupole deformed in the theoretical studies.

Experimental evidence for octupole shape in odd-odd nuclei would be the existence of parity doublet bands with members connected by strong $E1$ transitions. These parity doublet bands have the same spins but opposite parities and lie close together in energy. In addition, the magnetic moments of equivalent states with opposite parities are expected to be the same. Finally, in the case of odd-odd nuclei, one expects that the Newby shifts of the $K=0$ parity doublet bands will have the same absolute value but opposite signs (Sheline *et al.*, 1991). Additional evidence may also include the reversal of the odd-even staggering of the differential radii observed for the Eu isotopes (Sheline and Sood, 1989a), similar to the observations in the actinide region (Coc *et al.*, 1985, 1987; Borchers *et al.*, 1987; Ahmad *et al.*, 1988).

The strongest evidence for octupole shape has been found in two odd-odd nuclei, namely, ^{152}Eu and ^{154}Eu. Although a recent theoretical paper (Afanasjev and Ragnarsson, 1995) has called into question the existence of octupole deformation in these nuclei, these two cases are so striking (Headly *et al.*, 1998) that there should be little doubt about the existence of octupole deformation. Theoretical calculations, based on the quasiparticle-plus-phonon model and presented in Sec. VI, also support this claim.

2. Superdeformation

The earliest examples of superdeformed (SD) shapes (at low spins) were observed in fission isomers in the actinides (Polikanov, 1968; Brack *et al.*, 1972; Bjørnholm and Lynn, 1980) and also to some extent in light nuclei where an α-cluster model was invoked (Chandra and Mosel, 1978). However, the observation of SD shapes at high spins has been the most striking development in nuclear structure physics in recent years (Twin *et al.*,1986).

Four regions of high-spin SD bands are now well established: $A\sim80$, 130, 150, and 190, with many examples known in each mass region (Han and Wu, 1996; Singh *et al.*, 1996; Headly *et al.*, 1998). The deformation is always nearly 2:1 in axis ratio in the $A\sim80$ and 150 regions; however, it is slightly less in the other two mass regions. Only six examples of odd-odd SD nuclei in the mass region considered here are known so far: ^{144,148}Eu, ^{150,152}Tb, and ^{192,194}Tl. It is interesting to note that as many as six SD bands (the largest number known, in a few cases) are observed in ^{194}Tl, about which very little spectroscopic information is known at normal deformation. This suggests that a common mechanism must be operative which leads to the stabilization of the SD bands irrespective of whether these bands belong to an even-even or an odd-odd nucleus. All the properties displayed by the SD bands of odd-odd nuclei are also common with other SD bands. This brings into focus the universality of the properties of SD bands (Jain and Dudeja, 1996). Some of the well-known general features

---

[1]This includes the work of Phillips *et al.* (1986), Sheline and Sood (1986), Urban *et al.* (1987), Sheline *et al.* (1988), Phillips *et al.* (1988), Sheline and Sood (1989b), Sood and Sheline (1989c), Sheline and Sood, 1990, Vermeer (1990), Urban *et al.* (1991).

of SD bands include the identical band phenomenon (see Baktash *et al.*, 1995 and references therein) and unusual feeding and decay patterns (Carpenter *et al.*, 1996). It may be emphasized that the data on SD bands in odd-odd nuclei do not display any new additonal features; this in itself is probably an important observation. It has recently been suggested that these bands may represent unique examples of regular motion in a region of nonlinearity (Jain *et al.*, 1996, 1997; Dudeja *et al.*, 1997) which may explain the universality of the phenomenon.

D. Isomerism

One of the unique features of odd-odd spectra is the frequent occurrence of long-lived isomers. Several of these isomers do not have any observable isomeric (gamma) transition to the ground or other lower-lying states, thus rendering their energy placement, and quite often their spin-parity assignment, uncertain. Their characterization can sometimes be determined by examining the beta transitions which are their dominant mode of decay. Presently available information on isomers with $t_{1/2}>1$ sec for odd-odd isotopes in ${}_{61}$Pm$-{}_{77}$Ir nuclei with $89\geqslant N\geqslant 119$ is summarized in Table IV, which lists the observed $t_{1/2}$, assigned spin-parity, and the experimental excitation energy (in keV) for each known isomer. Multiple isomers are at present identified in 45 odd-odd nuclei of the region, with ten cases exhibiting three isomers each. The listed information is taken mainly from Nuclear Wallet Cards (1995) issued by the National Nuclear Data Center, Brookhaven, supplemented by more up-to-date data from Headly *et al.* (1998). As can be seen in this table, in 11 of the 45 nuclides it is not even known which of the known isomers is the nuclear ground state. The situation in odd-odd nuclei is markedly different from that observed in their odd-mass neighbors (Sood and Sheline, 1987a, 1987b). In the odd-mass nuclei the excitation energies and spin-parities of all known isomers are well determined, and, in all cases, the excited isomer has a much smaller half-life than its ground state. Further, every known isomer in odd-mass nuclei is seen to decay by an isomeric (gamma) transition. In contrast, in almost half the known cases, excited isomers in odd-odd nuclei have a half-life longer than the lower-lying ground state, and in more than one-third of the cases the dominant decay mode of the excited isomer is through an isobaric beta transition. The category includes the still outstanding puzzle about the origin (nucleosynthesis) of "nature's rarest stable isotope" ^{180m}Ta (Käppeler *et al.*, 1989), which species is actually an isomer with $t_{1/2}>1.2\times10^{15}$ y at an excitation energy of 75.3 keV above the 8.15 h ground state. In ^{186}Re, an isomer with $t_{1/2}=2\times10^{5}$ y is placed about 150 keV above its 3.8 d ground state. Structure considerations predict (Sood and Sheline, 1987a, 1987b) the occurrence of several as yet unidentified isomers in odd-odd deformed nuclei. It is to be remembered that we have arbitrarily restricted our discussion to isomers with $t_{1/2}\geqslant 1$ sec; in principle, these considerations apply equally to shorter-lived isomers, particularly those with half-lives in milli- or microseconds.

Interpretation of the isomers listed in Table IV may now be sought in terms of the Alaga rules for K-forbiddenness taken together with the model-dependent bandhead energies of the expected 2qp structures in the respective nucleus. The interpretation is made easier if an allowed unhindered "au" beta branch ($\log ft\leqslant 5.2$) is observed from the isomer. Consider the beta decay of the three isomers of ^{166}Lu, as shown in Fig. 10 (Sood and Sheline, 1990a; 1992). The observed beta branches with $\log ft<5.2$ from each of the three isomers unambiguously indicate a 5/2[523] neutron constituent in each isomer; this, taken together with the observed isomeric transition characteristics and the expected 2qp structures, leads to the specified configurations of each isomer in ^{166}Lu.

Similar considerations led Sood *et al.* (1986) to deduce the character and location of the 21-min high-spin isomer in ^{158}Ho. The "au" beta decay ($\log ft=4.47$) of this isomer to an 8^+ level in ^{158}Dy unambiguously establishes a 7/2[523] proton constituent in this isomer with positive parity and spin = (8 ± 1); examination of the available 2qp configuration space then leads to the assignment $9^+\{7/2[523]+11/2[505]\}$ for this isomer. Analysis of the possible 2qp configurations for the 67-keV, 27-min 2^- isomer in ^{158}Ho by Sood *et al.* (1986) highlighted another important indicator of the structure of isomers with a given energy and spin parity. They found that, based on the GM rule, any low-lying isomer must be the triplet ($K_{\rm T}$) member of the GM doublet unless a lower-lying triplet has been identified or is expected within the limited energy range. This condition rendered the earlier-suggested 2qp configurations {1/2[411]-5/2[523]} and {7/2[523]-3/2[651]} for the 2^- isomer unacceptable, since either of these suggestions would have required a triplet $K_>$ band [3^- or 5^-] to lie between the 5^+ ground state and the 67 keV 2^- isomer; no such bands were seen, nor were expected to be missed, in the reported studies.

An outstanding puzzle about some of these isomers is the absence, or unusually large hindrance, of isomeric (gamma) transitions. For instance, a 6.7-min, 3^+ isomer at (220 ± 130) keV in ^{168}Lu can be expected to decay by $E3$ transition to the 6^- ground state, while no such transition has been experimentally seen. Similarly, a 9.3-h, 46-keV 0^- isomer in ^{152}Eu does not decay to the 3^- ground state, whereas an M3 transition should connect these two states. The 2^- isomers, in both ^{158}Ho and ^{160}Ho, have hindrance factors (in Weisskopf units) of 10^4 and 10^5, respectively, for $\Delta I=3$ decays to the 5^+ ground states. This large hindrance factor for $\Delta I=3$ transitions in the two Ho isotopes, as well as also the absence of a $\Delta I=3$ transition connecting the 0^- isomer and 3^- ground state in ^{152}Eu, are attributed in part to the observation that the excited isomers are significantly less deformed than the respective ground states (Alkhazhov *et al.*, 1986, 1988; Neugart *et al.*, 1988; Sood *et al.*, 1992). However, the absence of a $\Delta I=3$ transition is

TABLE IV. Long-lived ($t_{1/2}>1$ sec) isomers in odd-odd rare earths. Entries in each box successively are the half-life, spin-parity I^π, and excitation energy (in keV).

$N_\downarrow/Z_\rightarrow$	$_{61}$Pm	$_{63}$Eu	$_{65}$Tb	$_{67}$Ho	$_{69}$Tm	$_{71}$Lu	$_{73}$Ta	$_{75}$Re	$_{77}$Ir
89		13.5y 3^- 0 9.3h 0^- 46 96m 8^- 148	21.5h 0 ? 9.0h 3^- ? 22.7h 7^- ?		4.0m 2^- ? ~20s (5^+) ?	36s(1^-) ? 40s (4^-) ?			
91	4.1m 1^+ 7.5m 4^- 13.8m (8)?	8.6y 3^- 0 46m 8^- 145	5.4d 3^- 0 24.4h 7^- 50 5.3h 0^+ 88	11.3m 5^+ 0 27m 2^- 67 21.3m 9^+ (180)	9.4m 1^- 0 74.5s(5) 100	1.4m (1^-) ? 1.5m (4^-) ? 1.9m ? ?			
93	1.7m (0,1) ? 2.7m(3,4)?		180y 3^- 0 10.5s 0^- 110	25.6m 5^+ 0 5.0h 2^- 60 3s 9^+ ≤225	21.7m 1^- 0 24.3s 5^+ 192			4.4s 6^+ ? 7.1s ? ?	
95				15m 1^+ 0 67.0m 6^- 106	2.0m 1^+ ? 5.1m 6^- ?	2.7m 6^- 0 1.4m 3^- 34 2.1m 0^- 43		4.4s (3^+) (0) 2.1s (7^+) (14)	
97				29m 1^+ 0	38m 6^- 140	5.5m 6^- 0	6.7m 3^+ 220	15s (5) ? 55s (2) ?	8s (3^+)(0) 5s (7^+)(193)
99				26.8h 0^- 0	1200y 7^- 6	2.0d 0^+ 0	0.7s 4^- 93		
101				3.0m 3^+ 0	132s 6^+ 59	6.7d 4^- 0	3.7m 1^- 42		
103				2.8m 6^+ 0	43s 1^+ 120	3.3y 1^- 0	142d 6^- 171		
105					5.4m 4^- 0 ? (1) 59	N 7^- 3.6h 1^- 123	9.3m 1^+ ? 2.4h 7^-		
107					23.1m 9^- 120	28.4m 1^+ N 9^- 75	8.2h 1^+ 0 12.7h 2^+ ?	64.0h 7^+ ?	
109						114d 3^- 0 15.8m 10^- 520	38.0d 3^- 0 169d 8^+ 188	16.6h 5^+ ? 2.0h 2^- ?	
111							98.6h 1^- 0	2×10^5y 8^+ 149	
113						17.0h 1^- 0	11.8d 4^+ 0	18.6m 6^- 172	1.2h 7^+ 26 3.3h 11^- 175
115							3.1m 2^- 0	73.8d $4^{(-)}$ 0 3.2h 6^- 120	1.5m $1^{(+)}$ 57 241y 9^+ 155
117								192h 1^- 0	171d (11^-) (190)
119[a]								52s 0^- 0	1.4h (11^-) 410

[a]Neutron number 119 not in Headly *et al.*, 1998.

also noted in several other isomer pairs, e.g., ^{154}Pm, ^{158}Tm, ^{160}Lu, ^{162}Lu, ^{168}Lu, ^{172}Re, ^{186}Ir, etc. This puzzling feature stands as an interesting challenge to theorists.

1. High-K four-quasiparticle states

Next to the 2qp states, one expects higher-lying four-quasiparticle (4qp) configurations to appear as intrinsic excitations in odd-odd nuclei. However, in view of the high level density and a large number of 2qp states with low K values, the best hope of locating the 4qp excitations is to look for high-K bands. An examination of the available single-particle orbitals reveals that the highest K value expected for 2qp states in well-deformed nuclei is $K=10$ arising from the configuration 9/2[514] +11/2[615]; experimentally we do find a 15.8-min, 519.6-

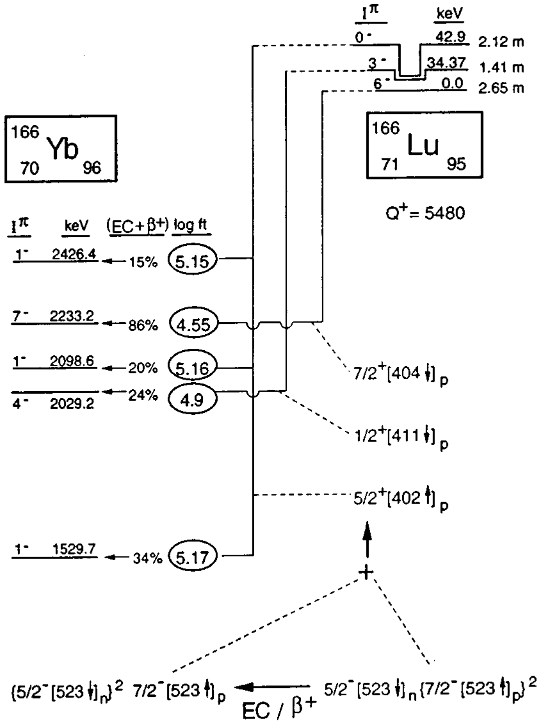

FIG. 10. Allowed unhindered beta decays of the three ^{166}Lu isomers. The bottom line gives the configuration of the orbitals involved in the transition and the configuration of the "spectator" proton for each isomer decay is indicated above it. Note that the 0^- decay populates three 1^- levels in ^{166}Yb with comparable intensity and similar logft values.

keV 10^- level in ^{182}Ta corresponding to this configuration. Thus any intrinsic excitations with $K>11$ in nuclei with A up to 180 should correspond to 4qp configurations. The earliest reference to the observation of a 4qp state was made by Helmer and Reich (1968), who suggested that a $K^\pi=16^+$ state in ^{178}Hf was a possible example of a 4qp state. Later, Khoo *et al.* (1975) found a $K^\pi=14^-$ 4qp isomer in ^{176}Hf, a nuclide with many 4qp states now known; they also stressed the usefulness of 4qp states in understanding the nature of residual interaction. At present such bands have been identified in only four odd-odd nuclei; observation of 4qp bands in ^{176}Ta and ^{178}Ta were reported in the late seventies (Buja-Bijunas and Waddington, 1978; Dubbers *et al.*, 1979) and in ^{180}Re and ^{182}Re in the eighties (Slaughter *et al.*, 1984; Kreiner *et al.*, 1988; Venkova *et al.*, 1990). The proposed 4qp configurations for these bands are listed in Table V. It is to be noted that these configuration assignments have been suggested as likely candidates based on the availability of orbitals, decay patterns, consideration of gyromagnetic ratios where available, etc. Obviously many other 4qp states are expected to occur in the 1–2 MeV energy range. In particular, such 4qp states in the vicinity of known high-spin isomers in neighboring even-even and odd-mass nuclei can reasonably be expected to be long- lived isomers and hence promising candidates for searches through heavy-ion reaction studies.

V. FEATURES OF ROTATIONAL STRUCTURES

The rotational bands of deformed odd-odd nuclei exhibit several unusual features and anomalies which, in addition to the GM splitting and Newby shifts discussed in Sec. III, make their study a fascinating subject. In the simplest possible picture, such variety and complexity can be attributed to the presence of two valence nucleons outside an even-even core and the interaction between them. On the other hand, one would also expect the rotational bands of odd-odd nuclei to be more exact and rigid due primarily to considerable quenching of the pairing correlations in such a system. These expectations are not completely belied. The rotational bands that are not sensitive to Coriolis effects do exhibit a behavior so exact that the variable-moment-of-inertia (VMI) model appears to provide a very good description of such bands (Jain and Goel, 1993). We mention only briefly some important features of the rotational spectra of odd-odd nuclei.

Several features of rotational bands are basically signature effects. The signature quantum number introduced in Sec. III.B in connection with $K=0$ bands is easily generalized to include nonzero K values. For $r=+1$ (or signature $\alpha=0$) members of the rotational bands, I is even, whereas for $r=-1$ (or signature $\alpha=1$) members, I is odd. A signature-dependent term in the Hamiltonian affects the odd and the even spins differently in some specific rotational bands such as those having either Ω_p or Ω_n, or both, equal to one-half. A direct Coriolis coupling is then possible between rotational bands.

The nondiagonal Coriolis term can, in a single step, cause mixing only among bands with $\Delta K=\pm 1$. However, step-by-step interaction in bands with $\Delta K=\pm 1$ can result in higher-order Coriolis mixing with significant effects. We shall present examples of such mixing.

A. Configuration-mixing features

Whenever one of the nucleons is in an $\Omega=1/2$ orbital, the GM doublet formed has $\Delta K=1$; accordingly the two bands are expected to be Coriolis admixed. This effect can be very significant in the cases wherein $K_T=K_< =|\Omega_p-\Omega_n|$ such that the same-I levels of the two bands lie close. A particularly impressive instance of this type, discussed by O'Neil and Burke (1972), appears in the ^{174}Lu spectrum. The mixing of $K^\pi=3^+$ and $K^\pi=2^+$ bands having a configuration 1/2[541]±5/2[512] is so strong (almost 50%) that the $I(I+1)$ spacing, and even the spin ordering, in the lower band is totally lost. The suggested configuration assignments were made on the basis of the "fingerprinting" capability of the transfer reaction studies.

Under special circumstances, either one or both of the odd nucleons may get decoupled leading to a semidecoupled or a doubly decoupled structure. Such rotational structures were first discussed by Toki *et al.* (1977, 1979) in the context of 2qp-plus-axially-asymmetric-

TABLE V. Four-quasiparticle states currently suggested in odd-odd rare-earth nuclei.

${}^{A}_{Z}X_N$	$t_{1/2}$	E_x (keV)	K^π	Configuration $\Omega[Nn_3\Lambda]$	Ref.
${}^{176}_{73}\mathrm{Ta}_{103}$	3.8 μs	1309+x	13^-	$p5/2[402]$: $n7/2[633]$: $n5/2[512]$: $n9/2[624]$ $p9/2[514]$: $n7/2[514]$: $n1/2[521]$: $n9/2[624]$	(Browne, 1990)
${}^{178}_{73}\mathrm{Ta}_{105}$	60 ms	1470.6+y	15^-	$\{p9/2[514]$: $n9/2[624]\}\otimes 9.6$ μs 1333 keV 6^+ in ^{176}Hf $\{p7/2[404]+p5/2[402]\}$ 61% $\{n7/2[514]+n5/2[512]\}$ 39%	(Browne, 1994b)
${}^{180}_{75}\mathrm{Re}_{105}$ [a]	70 ns	1496.0+z	11^-	$p5/2[402]$: $p9/2[514]$: $p1/2[541]$: $n7/2[514]$	
	—	1630.4+z	10^+	$p5/2[402]$: $p7/2[404]$: $p1/2[541]$: $n7/2[514]$	(Browne, 1994a)
	—	1750.8+z	11^-	$p5/2[402]$: $p7/2[404]$: $p1/2[541]$: $n9/2[624]$	
${}^{182}_{75}\mathrm{Re}_{107}$	82 ns	2256.5	16^-	$p9/2[514]$: $n9/2[624]$: $n7/2[514]$: $n7/2[503]$	(Jain *et al.*, 1988)

[a] Kreiner *et al.* (1987) suggest the *pnnn* configuration $K^\pi=13^-\{p9/2[514]$: $n7/2[514]$: $n1/2[521]$: $n9/2[624]\}$ for the 70 ns ^{180}Re isomer and the assignments 14^+ and 15^- for the other two levels.

rotor calculations. The existence of such bands in prolate deformed nuclei was discussed by Kreiner and Mariscotti (1979).

Bands involving a $\Omega=1/2$ orbital coupled to another orbital having $\Omega\neq 1/2$ may lead to a semidecoupled structure. In such a situation, a normal $\Delta I=1$ band splits into two $\Delta I=2$ chains, each labeled by a different signature. One of the two chains may closely match with the $\Omega\neq 1/2$ band in the neighboring odd-A nucleus.

In the special case wherein both the valence nucleons occupy predominantly $\Omega=1/2$ orbitals with large decoupling parameters, we come across the doubly decoupled bands. To date such bands have been identified (Kreiner, 1990; Olivier *et al.*, 1990) only in Ta, Re, and Ir isotopes. A diagonal signature-dependent matrix element in the Hamiltonian for the special case of $\Omega_p=\Omega_n=1/2$ leads to a constant shifting of even-I states relative to odd-I states in the $K=0$ band. A nondiagonal Coriolis matrix element connects the $K=0$ and the $K=1$ bands by a term

$$-\frac{\hbar^2}{2\Im}[a_p+(-1)^{I+1}a_n][I(I+1)]^{1/2} \tag{31}$$

which is both signature and I dependent. For large values of the decoupling parameters, it leads to two widely separated $\Delta I=2$ bands. The essential condition is that both participating particles decouple individually. Accordingly a clear fingerprint of a doubly decoupled band is that its level energies follow qualitatively the observed spacings of the ground-state band in the even-even core nucleus.

Another interesting property of a doubly decoupled band, pointed out by Olivier *et al.* (1990), is that its population is independent of the angular momentum induced in the system. This conclusion is based on the fact that an essentially identical population of the ^{174}Re doubly decoupled band is obtained using a wide variety of projectile/target combinations. A possible explanation offered for this phenomenon is the suggestion that a doubly decoupled band, lying not too far above the yrast band, acts as a trap for deexcitation of the compound system in the heavy-ion-induced reactions.

The particle-particle coupling term $(j_p^+j_n^-+j_p^-j_n^+)$ has also been observed to play a crucial role in some cases and to change significantly the character of a rotational band. We illustrate this point using as an example the $K=0^+$, 5/2[413]-5/2[642] band in ^{160}Tb, which has an empirical Newby shift $E_{\mathrm{N}}=3$ keV and therefore marginally favors the odd-spin members. Normally one would expect the even-spin members to be energetically favored in this band. This apparent contradiction is resolved by the 2qp-plus-rotor calculations (Goel *et al.*, 1991), which yield $E_{\mathrm{N}}=-8.5$ keV. Calculations have shown that the observed $K=0$ band has strong particle-particle coupling with the $K=0$, 3/2[411]-3/2[651] band. It is interesting to note that both $K=0$ bands have a positive Newby shift, whereas the resultant odd-even effect corresponds to a negative Newby shift, as shown in Fig. 11. This is the result of a strong mixing of the odd-spin members of the two $K=0$ bands; a 40–50 % mixing is calculated in the odd-spin members as compared to a

2–3% mixing in the even-spin members. This leads to a reversal in the final phase of staggering.

B. Odd-even staggering in the $K_< = |\Omega_p - \Omega_n|$ bands

It was surprising to observe the presence of an odd-even staggering in level energies of most of the $K_< = |\Omega_p - \Omega_n|$ bands where sufficient data were available (Jain *et al.*, 1988, 1989). The present data set (Headly *et al.*, 1998) identifies 194 intrinsic states having $K_< = |\Omega_p - \Omega_n|$ in the $A \geq 156$ nuclei. However, only 58 of these intrinsic states have a rotational band with four or more observed levels where the presence of an odd-even staggering in energy may be ascertained. The presence of an odd-even staggering in the $K=1$, 2, 3, and 4 bands implies the presence of higher-order Coriolis effects arising mainly from coupling with anomalous rotational structure in $K=0$ bands. The magnitude of staggering, of course, diminishes as we go to larger values of K; it is, however, remarkable that observable Coriolis effects remain in many bands having $K>1$.

The $K_<$ bands that arise from nucleons occupying high-j orbitals are observed to exhibit markedly enhanced odd-even staggering, even for large K values. These bands often involve an $i_{13/2}$ neutron and/or an $h_{11/2}$ proton. An illustrative and educative example is ^{182}Re, which has two such bands: $K^\pi = 2^+$, 5/2[402]-9/2[624] and $K^\pi = 4^-$, 1/2[541]-9/2[624]. Both configurations contain an $i_{13/2}$ neutron and display an unusually large energy staggering. The most interesting aspect of these bands is that the $K=4$ band exhibits a much larger staggering than the $K=2$ band. Detailed calculations based on a 2qp-plus-rotor model (Jain *et al.*, 1988, 1989) have helped in identifying the basic mechanisms responsible for the odd-even staggering. The most important of these is a mixing of the band with one or more Newby-shifted $K=0$ bands, which occurs directly for $K=1$ bands and through a chain of $\Delta K=1$ couplings for bands having $K>1$. We now understand that the $K_<$ bands are more irregular than the $K_>$ bands because only the former can be coupled directly to Newby-shifted $K=0$ bands, whereas the $K_>$ bands can be coupled to a $K=0$ band only in the special case of $\Omega_p = \Omega_n = 1/2$. In the case of ^{182}Re, the large odd-even staggering of the $K=0$, 1/2[541]-1/2[660] band is transmitted to the $K=4$ band through a higher-order Coriolis coupling.

C. Signature inversion in the $K_>$ bands of lighter rare earths

The possibility of a change of phase in the level staggering of rotational bands in doubly odd nuclei was first discussed by Kreiner and Mariscotti (1979, 1980); the currently observed features in the high-j configuration bands of lighter rare earths, however, differ from those predicted. A phase change in the level staggering is observed and is known as signature inversion.

The $K_> = (\Omega_p + \Omega_n)$ bands composed of high-j $i_{13/2}$ neutron plus $h_{11/2}$ proton configurations display two

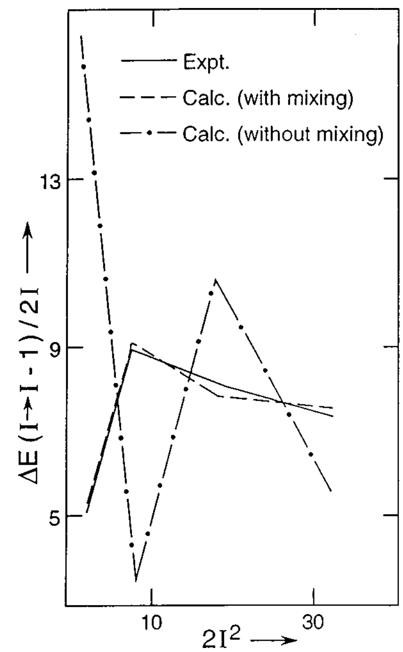

FIG. 11. Odd-even staggering in the $K=0^+$,5/2[413] −5/2[642] band in ^{160}Tb. Particle-particle coupling is shown to reverse the phase of odd-even staggering. See text for details.

prominent and interesting features. The bands in these nuclei exhibit a large odd-even staggering in their rotational energy spacings in contrast to other $K_>$ bands, which are known to exhibit a smooth behavior. Secondly, the favored signature in these bands is given by $\alpha_f = 1/2(-1)^{j_n - 1/2} + 1/2(-1)^{j_p - 1/2}$. However, the unfavored signature has been observed to lie lower in energy up to a critical spin in the range of $I=12$–18; the normal signature splitting is restored after the critical spin (Bengtsson *et al.*, 1982). In Fig. 12, we show the behavior of these bands in ^{152}Eu, ^{156}Tb, and ^{160}Ho; the point of signature inversion is indicated by an arrow in each case.

Attempts have been made to understand the phenomenon using several models, such as the cranked-shell model (Bengtsson *et al.*, 1984) the particle-rotor model (Hamamoto, 1990; Semmes and Ragnarsson, 1991; Jain and Goel, 1992; Goel, 1992; Goel and Jain, 1996), the angular momentum projection method (Hara and Sun, 1991), and the interacting boson-fermion model (Yoshida *et al.*, 1994).

Although triaxial deformation was initially suggested as the reason for signature inversion (Bengtsson *et al.*, 1984), we found that the phenomenon in ^{160}Ho could be explained within the framework of a 2qp-plus-axially-symmetric-rotor model. Using the database (Headly *et al.*, 1998), we can establish three general features of signature inversion (Jain *et al.*, 1993, Goel and Jain, 1997): (i) The point of signature inversion defined by a critical spin I_c shifts towards lower spin with increasing neutron number in a chain of isotopes; (ii) the point of inversion shifts towards higher spin with increasing proton number in a chain of isotones; and (iii) the magnitude of staggering before the inversion point becomes smaller with increasing neutron number in a chain of

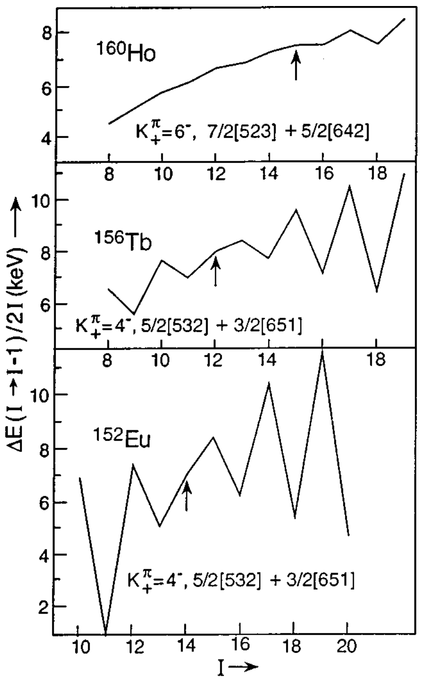

FIG. 12. Three typical examples of high-j configuration bands from the lighter rare earths which illustrate the pattern of signature inversion phenomena in the odd-even staggering. The point of inversion is indicated by an arrow in each case.

isotopes. Here we define the critical spin I_c as the point where the abnormal phase of staggering sets in as we move from the higher spin side of the bands to the bandhead. A study by Liu *et al.* (1995) has also pointed out similar systematics.

These features have been reasonably explained within the framework of the 2qp-plus-rotor model (Goel and Jain, 1997). Schematic calculations were carried out in the complete basis of $[h_{11/2}]_\pi \otimes [i_{13/2}]_\nu$; in addition to these, the $h_{9/2}$,1/2[541]$_\pi$ orbital was also included. It was found that the weak signature inversion, as observed for example in ^{160}Ho, could be understood without including the 1/2[541] orbital (Jain and Goel, 1992). However, it became necessary to include the 1/2[541] proton orbital to obtain the systematic features of signature inversion in a series of isotopes.

D. Smooth rotational behavior of the $K_> = (\Omega_p + \Omega_n)$ bands not involving a high-j neutron-proton configuration: the VMI model

The $K_> = (\Omega_p + \Omega_n)$ bands in odd-odd nuclei show a smooth dependence on angular momentum because the Coriolis mixing is minimal. These bands are therefore readily amenable to analysis in terms of the variable-moment-of-inertia (VMI) model (Mariscotti *et al.*, 1969; Goel and Jain, 1990). In the analysis we must exclude those $K_>$ bands whose configurations involve a high-j neutron/proton orbital and therefore display a large odd-even staggering. It is also possible to apply the VMI model to those $K_< = |\Omega_p - \Omega_n|$ bands which display minimal odd-even staggering (Goel and Jain, 1990; Jain and Goel, 1993). Mallman-like curves (Mallman, 1959; Scharff-Goldhaber *et al.*, 1976) for odd-odd nuclei agreed with the empirical values very well (Jain and Goel, 1993).

A remarkable observation is the strong configurational dependence of $\Im_K$ as well as its variation with spin. In almost all cases where sufficient data are available, it is possible to correlate the behavior of odd-odd rotational bands with the neighboring odd-A core nuclei (having either one proton or one neutron fewer) and to identify the neutron or proton configuration that is responsible for such behavior (Goel and Jain, 1990; Jain and Goel, 1993). The nearly identical behavior of most of the odd-odd rotational bands when compared to the neighboring odd-A bands involving the same neutron or proton configuration assumes special importance in view of the recent identification of identical bands in superdeformed and normally deformed nuclei (Jain, 1984; Stephens *et al.*, 1990; Ahmad *et al.*, 1991; Baktash *et al.*, 1992).

E. Effect of residual p-n interaction at high rotational frequencies

The importance of the residual p-n interaction in modifying the high-spin behavior was stressed by Toki, Yadav, and Faessler (1979), who studied its role in a triaxial rotor-particle calculation for odd-odd nuclei. It was pointed out that the residual p-n interaction could reverse the phase of energy staggering at high spin.

The effect of p-n interaction at high rotational frequency was more recently studied by Kvasil, Jain, and Sheline (1990) in a cranked HFB approach. A simple zero-range delta interaction with a spin-spin term was introduced in the model in a manner similar to the pairing interaction. Its influence on high-spin band crossing was then studied in the case of a simple model in which the valence neutron and proton occupied an $i_{13/2}$ and a $h_{11/2}$ orbital, respectively. Both the Wigner and the spin-spin part of the interaction were explicitly included in the calculations.

The results of these calculations show that the crossing of the lowest 2qp excitation of an odd-odd nucleus with the four-quasiparticle excitation, where a neutron pair is broken, exhibits a shift towards higher rotational frequency as soon as the residual interaction is switched on. It may be pointed out that, in a similar kind of calculation, the effect of a residual p-n interaction was studied within the framework of the particle-rotor model by Semmes and Ragnarsson (1992). Although the study was motivated by the signature inversion phenomenon, it was found that the point of inversion shifts to higher angular momenta when the p-n interaction was switched on. Since the point of inversion in this model represents crossing of two bands with opposite staggering behavior, it supports our findings (Kvasil, Jain, and Sheline, 1990). The importance of including the Wigner term was also emphasized by Semmes and Ragnarsson (1992). However, in a cranked Nilsson-plus-BCS calculation by Matsuzaki (1991), the effects of the residual p-

n interaction were found to be insufficient to reproduce the experimental data on signature splitting and signature inversion.

VI. MICROSCOPIC TREATMENT OF LOW-LYING STATES IN ODD-ODD DEFORMED NUCLEI

A. Microscopic model including vibrational degrees of freedom

In most of the theoretical analyses of low-lying states in odd-odd nuclei only the p-n interaction is taken into account and the coupling of external nucleons with the even-even core vibrations is neglected. On the other hand this coupling leads to the appearance of vibrational admixtures in the low-lying states of nuclei. In the case of odd-A deformed nuclei it is well known that vibrational components are very important, especially for the description of beta and gamma transition rates (see, for example, Kvasil *et al.*, 1992). The importance of vibrational admixtures in low-lying states of odd-odd nuclei has also been predicted in some phenomenological models (Paar, 1979; Brant *et al.*, 1987; Afanasjev *et al.*, 1988; Balantekin *et al.*, 1988; Chou *et al.*, 1988) and in microscopic approaches (see Kvasil *et al.*, 1992; Nosek *et al.*, 1992). The experimental observation of vibrational states of deformed odd-odd nuclei (e.g., Balodis *et al.*, 1988) indicates that a theoretical treatment of vibrational components is needed.

The basic Hamiltonian of the quasiparticle-plus-phonon model is the same as was introduced in Sec. III, Eqs. (3) and (4). The treatment of the intrinsic part of the Hamiltonian differs. The intrinsic part of the Hamiltonian is now written as

$$H_{\rm intr}=H_{\rm av}+H_{\rm pair}+H_{\rm res}, \qquad (32)$$

where the terms have their usual meaning. The short-range pairing interaction is approximated by the monopole pairing term

$$H_{\rm pair}=-\sum_{\tau\in n,p} G_\tau \sum_{qq'\in\tau} a^\dagger_{q+}a^\dagger_{q-}a_{q'-}a_{q'+}. \qquad (33)$$

In the framework of the quasiparticle-plus-phonon model, the long-range residual interaction $H_{\rm res}$ responsible for low-lying nuclear excitation can be decomposed into the multipole-multipole isoscalar and isovector form (Soloviev and Vogel, 1967; Soloviev, 1971; Kvasil *et al.*, 1991)

$$H_{\rm res}=-\frac{1}{2}\sum_{\lambda\mu}\sum_{\tau\tau'}(\kappa_0^{\lambda\mu}+\vec{\tau}\cdot\vec{\tau}'\kappa_1^{\lambda\mu})Q^\tau_{\lambda\mu}Q^\tau_{\lambda-\mu}, \qquad (34)$$

with the multipole operator

$$Q^\tau_{\lambda\mu}=\sum_{qq'\in\tau,\sigma_1\sigma_2}\delta_{\sigma_1K_1-\sigma_2K_2,\mu}\langle q_1\sigma_1|r^\lambda Y_{\lambda\mu}|q_2\sigma_2\rangle \times a^\dagger_{q_1\sigma_1}a_{q_2\sigma_2}. \qquad (35)$$

In Eqs. (33) to (35), τ represents the neutron and proton for which $\tau=-1$ and $\tau=+1$, respectively; $a^\dagger_{q_\sigma}$ is the particle creation operator for the single-particle state $q\sigma$, $\sigma=\pm$ characterizes the symmetry of each given single-particle state with respect to time reversal; G_τ is the pairing strength constant; $\kappa_0^{\lambda\mu}$ and $\kappa_1^{\lambda\mu}$ are the multipole isoscalar and isovector strength constants, respectively; $\langle q_1\sigma_1|r^\lambda Y_{\lambda\mu}|q_2\sigma_2\rangle$ are the single-particle matrix elements for the multipole operator. The eigenfunctions of the total Hamiltonian have the form of linear combinations of the basis vectors $|IMK\alpha_\rho\rangle$ already introduced in Sec. III, Eq. (10).

Using the Valatin-Bogolyubov transformation (Soloviev, 1971; Bohr and Mottelson, 1975; Ring and Schuck, 1980), from single-particle operators $a^\dagger_{q\sigma}$ to the quasiparticle operators $\alpha^\dagger_{q\sigma}$, and the random-phase approximation (RPA) equations for one-phonon excitations of the even-even core, we can write the intrinsic Hamiltonian of Eq. (32) schematically in the form (see Kvasil *et al.*, 1991, 1992 for details)

$$H_{\rm intr}=H_{Ev-Ev}+H_{\rm QB}+H^{\rm pair}_{\rm QB}+H_{\rm BB}, \qquad (36)$$

where H_{Ev-Ev} involves the $\alpha^\dagger\alpha$-type and $Q^\dagger_{\lambda\mu i}Q_{\lambda\mu i}$-type terms, and $Q^\dagger_{\lambda\mu i}$ are the phonon creation operators that create even-even core vibrational quanta with multipolarity λ and projection μ. The index i numerates phonons with given λ and μ solutions of the RPA equations (see, for example, Soloviev, 1971). $H_{\rm QB}$ and $H^{\rm pair}_{\rm QB}$ involve the terms of $Q^\dagger_{\lambda\mu i}\alpha^\dagger\alpha$ type originating from $H_{\rm res}$ and $H_{\rm pair}$, respectively. $H_{\rm BB}$ contains the terms of $\alpha^\dagger\alpha\alpha^\dagger\alpha$ type. The phonon operator $Q^\dagger_{\lambda\mu i}$ is

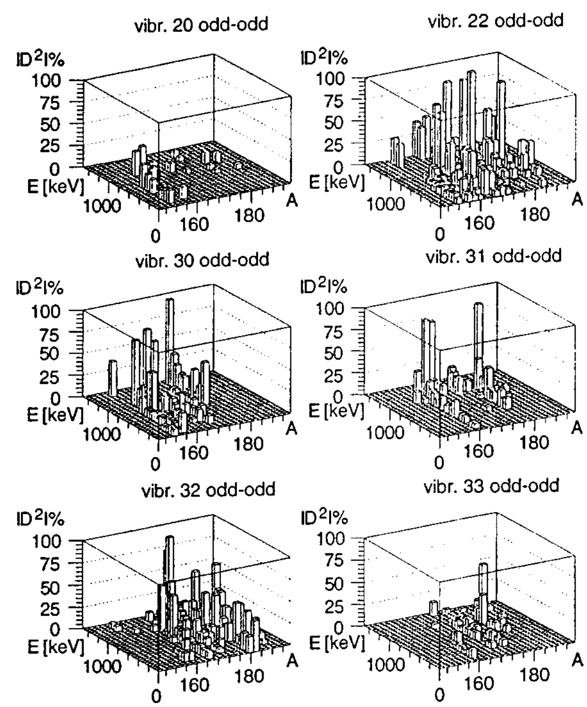

FIG. 13. A three-dimensional plot of the calculated vibrational phonon admixtures $|D^{\nu\gamma_0}_{sr\lambda\mu i}|^2$ in percent versus the intrinsic excitation energy in keV and the mass number A for low-lying states in odd-odd nuclei. Specific vibrations are labeled by the quantum numbers λ and μ. Thus the 20 and 22 vibrations correspond to the beta and gamma vibrations respectively.

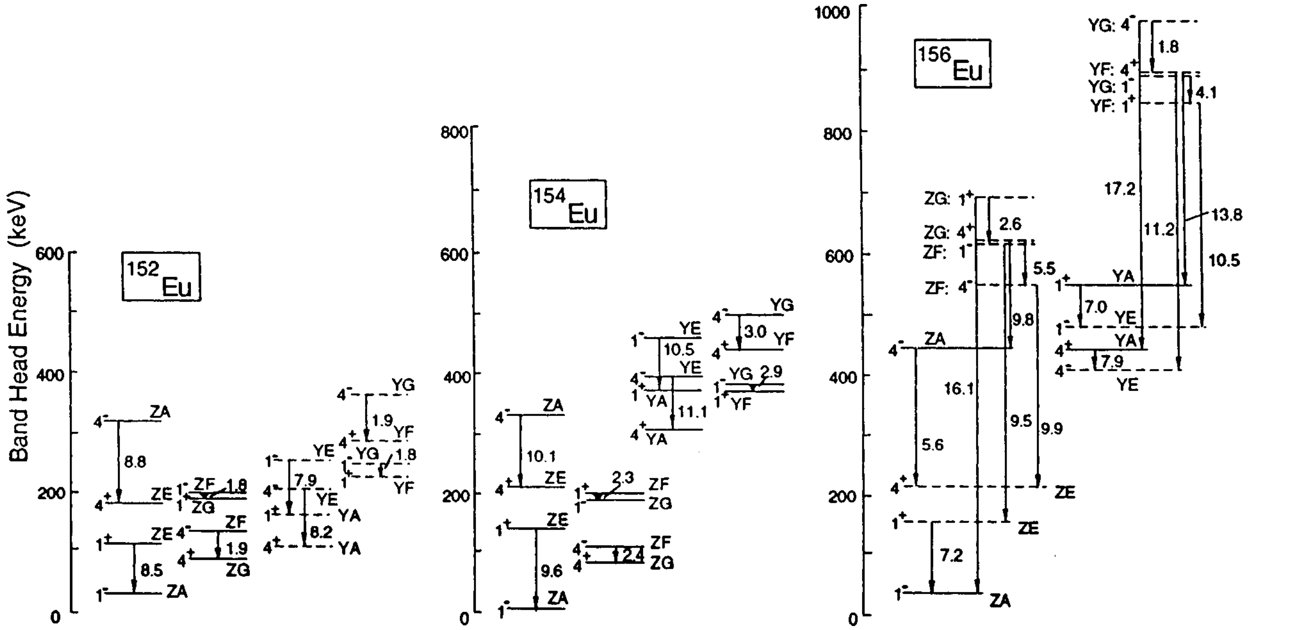

FIG. 14. Calculated energies and squared $E3$ intrinsic matrix elements (with no geometrical factors included) for the various $K^\pi=1^\pm$ and $K^\pi=4^\pm$ bands (16 in all) expected in the low-energy spectra of the odd-odd ${}_{63}$Eu isotopes with $A=152$ (left), 154 (middle), and 156 (right). The partial Nilsson configurations are abbreviated. For protons they are Z:5/2[413] and Y:5/2[532]; for neutrons, A:3/2[532], E:3/2[651], F:3/2[532] and G:3/2[402].

given in the framework of the RPA by the linear combination of 2qp components, which can be schematically written as

$$Q^\dagger_{\lambda\mu i}=\frac{1}{2}\sum_{q_1q_2}\{\psi^{\lambda\mu i}_{q_1q_2}\alpha^\dagger_{q_1}\alpha^\dagger_{q_2}-\phi^{\lambda\mu i}_{q_1q_2}\alpha_{q_1}\alpha_{q_2}\}. \tag{37}$$

In other words, from the point of view of an odd-odd nucleus, H_{Ev-Ev} in Eq. (36) represents the vibrating even-even core and $(H_{\rm QB}+H_{\rm QB}^{\rm pair})$ represent the coupling of the odd neutron and odd proton with the vibrating even-even core. $H_{\rm BB}$ in Eq. (36) also involves the $\alpha^\dagger\alpha\alpha^\dagger\alpha$ part of proton-neutron interaction between odd particles originating from $H_{\rm res}$ and $H_{\rm pair}$. In the quasiparticle-plus-phonon approach we restrict the $H_{\rm BB}$ term to only this p-n interaction and simultaneously generalize it so that

$$V_{pn}=\frac{1}{2}\sum_{rr'ss'}\langle r\sigma_r,s\sigma_s|V_{pn}|r'\sigma_{r'},s'\sigma_{s'}\rangle \times a^\dagger_{r\sigma_r}a_{r'\sigma_{r'}}a^\dagger_{s\sigma_s}a_{s'\sigma_{s'}}. \tag{38}$$

This is then used to describe GM splittings and N shifts instead of only the p-n interaction originating from $H_{\rm res}$ and $H_{\rm pair}$. In Eq. (38), $a^\dagger_{r\sigma_r}$ and $a^\dagger_{s\sigma_s}$ are the single-particle creation operators for protons and neutrons ($q\equiv r,s$), respectively. So $H_{\rm BB}$ in Eq. (36) represents the $\alpha^\dagger\alpha\alpha^\dagger\alpha$-type part of V_{pn} given by

$$\begin{aligned}H_{BB}\approx&\frac{1}{2}\sum_{rr'ss'}\langle r\sigma_r,s\sigma_s|V_{pn}|r'\sigma_{r'},s'\sigma_{s'}\rangle\\&\times\{(u_ru_{r'}u_su_{s'}+v_rv_{r'}v_sv_{s'})\alpha^\dagger_{r\sigma_r}\alpha_{r'\sigma_{r'}}\alpha^\dagger_{s\sigma_s}\alpha_{s'\sigma_{s'}}\\&-(v_rv_{r'}u_su_{s'}+u_ru_{r'}v_sv_{s'})\sigma_r\sigma_{r'}\alpha^\dagger_{r-\sigma_r}\alpha_{r'-\sigma_{r'}}\\&\times\alpha^\dagger_{s-\sigma_s}\alpha_{s'-\sigma_{s'}}\},\end{aligned} \tag{39}$$

where u_q,v_q are the amplitudes from the Valatin-Bogolyubov transformation.

The intrinsic wave function $|\psi_{\rho\gamma}(\sigma K^\pi)\rangle$ of the odd-odd nuclear state is expected to have both 2qp proton-neutron components and 2qp-plus-phonon components,

$$\begin{aligned}|\psi_{\rho\gamma}(\sigma K^\pi)\rangle&\\=&\Bigg\{\sum_{rs}C^{\rho\gamma}_{rs}A^\dagger_\gamma(r\sigma_r,s\sigma_s;\sigma K)\\&+\sum_{r\sigma_rs\sigma_s\gamma'\lambda\mu i\sigma'\sigma_\mu}D^{\rho\gamma}_{rs\lambda\mu i}A_{\gamma'}(r\sigma_r,s\sigma_s;\sigma'K')\\&\times Q^\dagger_{\lambda\mu i}\delta_{\sigma'K'+\sigma_\mu\mu,\sigma K}\Bigg\}|0\rangle,\end{aligned} \tag{40}$$

where $A^\dagger_\gamma(r\sigma_r,s\sigma_s;\sigma K)$ is the 2qp (r,s) proton-neutron creation operator symmetrized with respect to signature γ,

$$\begin{aligned}A^\dagger_\gamma(r\sigma_r,s\sigma_s;\sigma K)=&\frac{1}{\sqrt{1+\delta_{K0}}}\alpha^\dagger_{r\sigma_r}\alpha^\dagger_{s\sigma_s}\delta_{\sigma_rK_r+\sigma_sK_s,\sigma K}\\&\times[1-(1+\gamma\delta_{K0}\delta_{\sigma_s,-1}\delta_{\sigma_r,+1})].\end{aligned} \tag{41}$$

The first term on the right-hand side of Eq. (40) represents the sum over 2qp p-n components. The second sum in Eq. (40) represents the 2qp-plus-phonon components of a given intrinsic state. The amplitudes $C_{rs}^{\rho\gamma}$ and $D_{rs\lambda\mu i}^{\rho\gamma}$ are obtained from the variational method with the normalization condition for the state $|\psi_{\rho\gamma}(\sigma K^{\pi})\rangle$ as the Lagrange condition (Kvasil *et al.*, 1991, 1992),

$$\delta\{\langle\psi_{\rho\gamma}(\sigma K^{\pi})|H_{\mathrm{intr}}|\psi_{\rho\gamma}(\sigma K^{\pi})\rangle - \eta_{\rho\gamma}(\langle\psi_{\rho\gamma}(\sigma K^{\pi})|\psi_{\rho\gamma}(\sigma K^{\pi})\rangle-1)\}=0, \quad (42)$$

where amplitudes $C_{rs}^{\rho\gamma}$ and $D_{rs\lambda\mu i}^{\rho\gamma}$ are the variational variables. The physical meaning of the $\eta_{\rho\gamma}$ is the intrinsic excitation energy of the state $|\psi_{\rho\gamma}(\sigma K^{\pi})\rangle$. The variational condition (42) provides the expressions for amplitudes $C_{rs}^{\rho\gamma}$ and $D_{rs\lambda\mu i}^{\rho\gamma}$ as well as for energy $\eta_{\rho\gamma}$. The expressions for the case of the diagonal approximation of the p-n interaction can be found in Kvasil *et al.*, (1992). Knowing the intrinsic energy $\eta_{\rho\gamma}$ for both members, $|\psi_{\rho=p,n}(K=|\Omega_n\pm\Omega_p|\rangle$, of the GM doublet for a given p-n configuration ($\rho\equiv rs\equiv pn$), one can calculate the GM splitting,

$$\Delta E_{\mathrm{GM}}=\eta_{\rho\gamma}\delta_{K,|\Omega_n-\Omega_p|}-\eta_{\rho\gamma}\delta_{K,\Omega_n+\Omega_p}, \quad (43)$$

and for the case of $K=0$ bands, the N shift:

$$\Delta E_{K=0}=\delta_{K0}(\eta_{\rho\gamma=-1}-\eta_{\rho\gamma=+1}). \quad (44)$$

If the coupling $H_{\mathrm{QB}}+H_{\mathrm{QB}}^{\mathrm{pair}}$ of odd particles with the vibrating even-even core is neglected in Eq. (36), the quasiparticle-plus-phonon model is reduced to the standard model of independent quasiparticles with the corresponding GM splitting energy,

$$\Delta E_{\mathrm{GM}}=\langle p+,n-|V_{pn}|p+,n-\rangle - \langle p+,n+|V_{pn}|p+,n+\rangle \quad (45)$$

and N shift

$$\Delta E_{K=0}=2\langle p+,n-|V_{pn}|p-,n+\rangle, \quad (46)$$

where the signs (+ or −) specify the spin state.

B. Vibrational components

The quasiparticle-plus-phonon model briefly described above was used to calculate the energies and structures of low-lying intrinsic states in a wide region of deformed odd-odd rare-earth nuclei. The calculation for each odd-odd nucleus involved the following steps:

(i) calculation of the Nilsson-model single-particle energies and wave functions;

(ii) calculation of the Nilsson single-particle matrix elements of the multipole operators $Q_{\lambda\mu}$ of Eq. (35);

(iii) quasiparticle-plus-phonon calculation for an even-even core [structures and energies of the even-even core vibration phonons given by Eq. (37)];

(iv) calculation of the residual p-n interaction matrix elements in the Nilsson basis;

(v) quasiparticle-plus-phonon calculation for a given odd-odd nucleus yielding the amplitudes $C_{rs}^{\rho\gamma}$, $D_{rs\lambda\mu i}^{\rho\gamma}$, and the energies $\eta_{\rho\gamma}$.

The Coriolis coupling arising from the rotational part of the Hamiltonian was neglected. Quadrupole and hexadecapole deformation parameters as well as other parameters of the deformed Nilsson average field were taken from Gareev *et al.* (1973). Pairing strengths (taking into account so-called blocking effects) were taken from Soloviev (1971), and Fermi levels of proton and neutron systems in each nucleus were approximated by single-particle energies of ground states in the neighboring odd-A nuclei (Jain *et al.*, 1990). The residual p-n interaction V_{pn} was used in the standard phenomenological form with Gaussian radial dependence. Parameters of V_{pn} were obtained by a least-squares fit (G_{TP}) of all known GM splittings, as reported in this review.

Only the isoscalar parts of the long-range residual interaction, Eq. (34), were used (i.e., $\kappa_1^{\lambda\mu}=0$), since the isovector parts have no substantial influence on low-lying intrinsic states in deformed nuclei (see, for example, Soloviev, 1971). The strengths $\kappa_0^{\lambda\mu}$ for $\lambda=2,3$ were calculated from the experimental bandhead energies of the quadrupole and octupole one-phonon states in the corresponding even-even cores (Sood *et al.*, 1991). When an experimental value of the quadrupole or octupole bandhead energy in an even-even core was not known, we adopted a corresponding strength parameter from a neighboring isotope or isotone.

The results of these quasiparticle-plus-phonon calculations are partly presented in Table III. These results are given in columns denoted by $E3$ and $\{p+n\}$%. In column $E3$, the differences $E_{I=K,K\rho\gamma}-E_{I_0=K_0,K_0\rho_0\gamma_0}$ are given, where the indexes ρ_0 and γ_0 concern the ground state. These values are then compared directly with the experimental values in columns E_{T} or E_{S}. The contribution of the rotational term to the bandhead energy is thus included in these values. A uniform value of 9 keV was assumed for the inertial parameter $\hbar^2/2\mathfrak{I}$.

The column in Table III labeled $\{p+n\}$% contains first the percentage of the major p-n 2qp component. Then the column $\{p+n\}$% gives the indexes and percentages of any minor components of the given state that contributes 10% or more to the wave function.

This quasiparticle-plus-phonon model for odd-odd nuclei is a microscopic model without any parameter optimization. All parameters were determined from the characteristics of even-even cores. Therefore precise agreement between calculated and experimental energies cannot be expected. Since there are approximations in the model (e.g., restriction to separable multipole-multipole residual interactions, neglecting nondiagonal matrix elements of V_{pn} and others), the accuracy of the calculated energies cannot be better than tens of keV [the same as in Soloviev (1971) for odd-A nuclei]. Nevertheless, quasiparticle-plus-phonon calculations give important insight into the question of the vibrational collectivity of low-lying bandheads in deformed odd-odd nuclei.

As indicated in column $\{p+n\}$%, most of the low-lying intrinsic states in rare-earth odd-odd nuclei have 2qp character or a mixture of two or several 2qp states with only small core phonon admixtures.

In order to see how large the vibrational admixtures of a given multipolarity ($\lambda\mu$) are in low-lying states in an odd-odd nucleus with a given mass A, the dependence of the square of the phonon amplitude in the intrinsic wave function was analyzed as a function of the mass number A and the excitation energy. This dependence for quadrupole ($\lambda=2$) and octupole ($\lambda=3$) phonon admixtures is shown in Fig. 13 for different projections of μ.

Comparisons of the strengths of vibrational components in low-lying states in odd-odd or odd-A nuclei with the corresponding phonon energies in the even-even cores have also been made, and these results along with Fig. 13 reveal the following generalizations:

(i) The states below 0.9 MeV in odd-odd deformed nuclei have no significant vibrational components larger than 40%.

(ii) The vibrational components built on the quadrupole and octupole phonons in the low-lying states in odd-odd nuclei are larger when the quadrupole or octupole phonon energies in the even-even core are less.

(iii) At the onset of the deformation region ($A \approx 155$), vibrational components of the low-lying states are mostly formed from the octupole phonons $\lambda\mu=30$, while at the end of this region ($A\approx185$) they are built from the $\lambda\mu=32$ octupole phonons. This clearly demonstrates the importance of octupole correlations both at the beginning and at the end of the deformation region. The $\lambda\mu=31$ and $\lambda\mu=33$ octupole phonons are less important over the whole deformed region and their components are smaller.

(iv) Quadrupole γ vibrations with $\lambda\mu=22$ are spread over many low-lying states in odd-odd rare earths, while β vibrations and/or pairing vibrations ($\lambda\mu=20$) are relatively unimportant.

(v) Comparison of vibrational modes in odd-odd nuclei with vibrational modes in odd-A nuclei shows that the fragmentation of vibrational strength in the low-lying states of odd-odd nuclei is greater than in the odd-A case. In odd-odd nuclei the major part of the vibrational strength in general probably lies at higher energies than in odd-A and even-even nuclei.

C. Level structures of ^{152,154,156}Eu according to the quasiparticle-plus-phonon model

Recent neutron capture experiments (Balodis *et al.*, 1991) have led to a much more complete level scheme of ^{156}Eu, in which parity doublet structures have also been suggested with the implication of the existence of reflection asymmetry in ^{156}Eu. Very recently, however, Afanasjev and Ragnarsson (1995) have questioned the existence of octupole deformation not only in ^{156}Eu but also in ^{152}Eu and ^{154}Eu.

Using the quasiparticle-plus-phonon model with both quadrupole and octupole phonons, it has been possible to calculate the level structure of ^{152}Eu, ^{154}Eu, and ^{156}Eu. A comparison of the level structures for just the $K^{\pi}=1^{\pm}$ and $4^{\pm}$ bands (16 in all) is shown in Fig. 14.

The results in Fig. 14 establish that, whereas the level patterns of the three odd-odd Eu isotopes are similar, there are significant qualitative differences between ^{156}Eu and either ^{154}Eu or ^{152}Eu. Thus, for example, both in ^{152}Eu and in ^{154}Eu, octupole connections are seen to exist only between nearest opposite-parity but same-K band pairs. The pair configurations utilize the same $K=5/2$ proton and either the 3/2[521],3/2[651] or the 3/2[532], 3/2[402] sets of neutron orbitals in Fig. 14. This supports their interpretation as parity doublets. In the case of ^{156}Eu, the four bands with the same K, resulting from a given $K=5/2$ proton coupled to each of the $K=3/2$ neutron orbitals mentioned above, have significant $E3$ interconnections. $E3$ transition strengths between pairs of opposite-parity bands far apart in energy (reminiscent of octupole vibrations) are larger than the corresponding strengths between closer-lying pairs in each instance in Fig. 14. This strong cross connection between two pairs of each quartet, far apart in energy, observed in ^{156}Eu but absent in ^{152}Eu and ^{154}Eu, is contrary to the expectations for parity doublets, which are for strong $E3$ interconnections between close-lying parity-doublet partners and not for connections between other states.

While the evidence for octupole deformation is quite strong both experimentally and theoretically for ^{152}Eu and ^{154}Eu, in spite of suggestive level patterns for ^{156}Eu observed experimentally, the theoretical results are not consistent with octupole deformation for ^{156}Eu.

VII. CONCLUSIONS

This present review has endeavored to cover all the important aspects of odd-odd nuclei, experimental as well as theoretical. Primarily, it summarizes the present status of our understanding of the intrinsic and rotational level structures in medium-heavy deformed odd-odd nuclei. A brief summary of the experimental methods, old and new, their applicability and utility has been presented and suggestions made for odd-odd nuclei that are especially deserving of additional study.

The residual p-n interaction plays an important role in the evolution of intrinsic level structures and is one of the focal points of the present study. Empirical values of the GM splittings and Newby shifts have been extracted from the data and compared with the calculations based on a new parametrization of the residual p-n interaction. Despite an extended database, which has grown at a very slow pace over the past two decades, our understanding of the residual interaction seems to have improved marginally. Of particular concern is our lack of understanding of the Newby shift, which we consider as one of the challenging problems in low-energy nuclear physics. It appears that a quantum jump in the database coupled with a fresh intiative may be needed to resolve this problem.

The rotational bands observed in odd-odd nuclei have been found to display many new features such as odd-even staggering patterns and signature inversion phenomena. We conclude that higher-order Coriolis coupling plays an important role in explaining these phenomena, and a reasonable understanding of most of these features has been achieved. The residual *p-n* interaction can also play an important role in band crossing at high rotational frequencies and may delay the band crossing; this, however, still needs to be studied in greater detail.

The systematics of the 2qp intrinsic states, presented in this review, reveal several similarities with those for odd-*A* nuclei, as is expected. However, the systematics of odd-odd nuclei are certainly more complex and difficult to study because of the three-dimensional aspect of the problem (neutron-proton energy). The incompleteness of the systematics strongly suggests the need for more data on odd-odd nuclei.

Another important aspect of the present review has been the calculation of 2qp intrinsic level structures by using the empirical intrinsic level spacings for odd-*A* neighboring nuclei. Similar calculations were carried out using the quasiparticle-phonon model and results compared with the experimental data. A study of the vibrational phonon admixtures in wave functions emphasizes the importance of octupole phonons near the onset of the deformation region ($A \approx 155$) and at the end of this region ($A \approx 185$). It was found that the major part of the vibrational strength (mostly quadrupole gamma phonons) lies at higher energies in odd-odd nuclei than in odd-*A* and even-even nuclei. The quasiparticle-plus-phonon calculations for ^{152,154,156}Eu support the claim for octupole shape in the first two isotopes but not in ^{156}Eu.

Other topics of importance discussed in this review are shape coexistence features involving octupole and superdeformed shapes. Some higher-mass transitional nuclei like Au isotopes display features that may be related to the coexistence of oblate-prolate shape. A brief discussion of isomers and 4qp states was also presented.

This review outlines the key issues, both theoretical and experimental, that make the study of odd-odd nuclei an important area for further research. It is hoped that the new generation of detector arrays and the radioactive ion-beam facilities will extend the data and level assignments of odd-odd nuclei.

ACKNOWLEDGMENTS

We thank Dr. B. Singh for reading the manuscript, for helpful discussions, and for several useful comments. This work was supported in part by the U.S. National Science Foundation, Contract PHY92-07336, at Florida State University; by the Natural Sciences and Engineerings Research Council of Canada, at McMaster University; by the Department of Science & Technology, Government of India, at University of Roorkee; by the Department of Atomic Energy, Government of India, at Banaras Hindu University; and by the U.S. Department of Energy (under Contract W-7405-Eng-48) at Lawrence Livermore National Laboratory. It was also supported by Charles University under Contract No. GAUK-27 and the granting agency of the Czech Republic, under Contract No. GACR 202/94/0461. One of us (A.K.J.) acknowledges the hospitality of McMaster University, where this work was concluded.

REFERENCES

Afanasjev, A. V., T. V. Guseva, and Yu. Ya. Tamberg, 1988, Izv. Akad. Nauk SSSR, Ser. Fiz. **52**, 130.

Afanasjev, A. V. and I. Ragnarsson, 1995, Phys. Rev. C **51**, 1259.

Ahmad, I., M. P. Carpenter, R. R. Chasman, R. V. F. Janssens, and T. L. Khoo, 1991, Phys. Rev. C **44**, 1204.

Ahmad, S. A., W. Klempt, R. Neugart, E. W. Otten, P.-G. Reinhard, G. Ulm, and K. Wendt, 1988, Nucl. Phys. A **483**, 244.

Alaga, G., 1955, Phys. Rev. **100**, 432.

Alaga, G., 1957, Nucl. Phys. **4**, 625.

Alkhazov, G. D., A. E. Barzakh, I. Ya. Chubukov, V. P. Denisov, V. S. Ivanov, N. B. Buyanov, V. N. Fedoseyev, V. S. Letokhov, V. I. Mishin, and S. K. Sekatsky, 1988, *New techniques and results of collinear laser spectroscopy… Proceedings of the 5th International Conference on Nuclei Far from Stability*, Rosseau Lake, Canada, 1987, AIP Conf. Proc. No. 164, edited by I. S. Towner (AIP, New York), p. 115.

Alkhazov, G. D., E. E. Berlovich, H. Wagner, K. Dorchel, V. N. Panteleev, E. V. Peau, A. G. Polyakov, V. I. Tikhonov, V. Heddrich, and H. Hünermann, 1986, Sov. J. Nucl. Phys. **44**, 734.

Arnold, S.F., 1990, *Mathematical Statistics* (Prentice Hall, New Jersey), Chap. 12, p. 405.

Baktash, C., J. D. Garrett, D. F. Winchell, and A. Smith, 1992, Phys. Rev. Lett. **69**, 1500.

Baktash, C., B. Haas, and W. Nazarewicz, 1995, Annu. Rev. Nucl. Part. Sci. **45**, 485.

Balantekin, A. B., I. Bars, and F. Iachello, 1981, Nucl. Phys. A **370**, 284.

Balodis, M. K., and the ^{194}Ir Collaboration, 1994, in *Proceedings of the 8th International Symposium on Capture Gamma-Ray Spectroscopy and Related Topics*, Fribourg, Switzerland, edited by J. Kern (World Scientific, Singapore), p. 355.

Balodis, M. K., A. V. Afanas'ev, P. T. Prokof'ev, and Yu. Ya. Tamberg, 1988, Izv. Akad. Nauk SSSR, Ser. Fiz. **52**, 2117 [Bull. Acad. Sci. USSR, Phys. Ser. **52**, No. 11, 35 (1998)].

Balodis, M. K., N. D. Kramer, P. T. Prokofjev, A. V. Afanasjev, T. V. Guseva, J. J. Tambergs, K. Schreckenbach, W. F. Davidson, D. D. Warner, J. A. Pinston, P. H. M. Assche, and A. M. J. Spits, 1991, Nucl. Phys. A **523**, 261.

Balodis, M. K., P. T. Prokofjev, L. Simonova, R. Hoff, and R. Georgii, 1995, abstract submitted to the 35th Annual National Conference on Nuclear Spectroscopy, St. Petersburg, Russia (June, 1995), unpublished.

Bengtsson, R., H. Frisk, F. R. May, and J. A. Pinston, 1984, Nucl. Phys. A **415**, 129.

Bengtsson, R., J. A. Pinston, D. Barneoud, E. Monnand, and F. Schussler, 1982, Nucl. Phys. A **389**, 158.

Bennour, L., J. Libert, M. Meyer, and P. Quentin, 1987, Nucl. Phys. A **465**, 35.

Bjørnholm, S., and J. E. Lynn, 1980, Rev. Mod. Phys. **52**, 725.

Bohr, A., and B. R. Mottelson, 1975, *Nuclear Structure*, Vol. II (Benjamin, New York).

Boisson, J. P., R. Piepenbring, and W. Ogle, 1976, Phys. Rep. **26**, 99.

Borchers, W. R., R. Neugart, E. W. Otten, H. T. Duong, G. Ulm, K. Wendt, and the ISOLDE Collaboration, 1987, Hyperfine Interact. **34**, 25.

Brack, M. J., J. Damgaard, A. S. Jensen, H. C. Pauli, V. M. Strutinsky, and C. Y. Wong, 1972, Rev. Mod. Phys. **44**, 320.

Brant, S., V. Paar, D. Vretenar, G. Alaga, H. Seyfarth, O. Schult, and M. Bogdanivic, 1987, Phys. Lett. B **195**, 111.

Browne, E., 1990, Nucl. Data Sheets **60**, 227.

Browne, E., 1994a, Nucl. Data Sheets **71**, 81.

Browne, E., 1994b, Nucl. Data Sheets **72**, 221.

Bruder, A., J. Cl. Dousse, S. Drissi, M. Gasser, V. A. Ionescu, J. Kern, B. Perny, M. Rast, and Ch. Rhême, 1987a, Nucl. Phys. A **467**, 1.

Bruder, A., S. Drissi, V. A. Ionescu, J. Kern, and J. P. Vorlet, 1987b, Nucl. Phys. A **474**, 518.

Buja-Bijunas, L., and J. C. Waddington, 1978, Can. J. Phys. **56**, 872.

Bunker, M. E., and C. W. Reich, 1971, Rev. Mod. Phys. **43**, 348.

Burke, D. G., G. Kajrys, and D. Beachey, 1989, Nucl. Phys. A **492**, 68.

Burke, D. G., P. C. Sood, P. E. Garrett, Tao Qu, R. K. Sheline, and R. W. Hoff, 1993, Phys. Rev. C **47**, 131.

Burke, D. G., B. Zeidman, B. Elbek, B. Herskind, and M. Olesen, 1966, K. Dan. Vidensk. Selsk. Mat. Fys. Medd. **35**, 2.

Carpenter, M. P. *et al.*, 1996, in *Proceedings of the Workshop on Gammasphere Physics*, edited by M. A. Deleplanque, I. Y. Lee, and A. O. Macchiavelli (World Scientific, Singapore), p. 1.

Chandra, H., and U. Mosel, 1978, Nucl. Phys. A **298**, 151.

Chou, W.-T., W. A. Olivier, R. Aryaeinejad, W. C. McHarris, and Olaf Scholten, 1988, in *Proceedings of the Conference on High-Spin Nuclear Structure and Novel Nuclear Shapes*, April, Argonne National Laboratory, Argonne, Illinois; ANL-PHY-88-2, p. 292.

Coc, A., C. Thibault, F. Touchard, H. T. Duong, P. Juncar, S. Liberman, J. Pinard, M. Carre, J. Lermé, J. L. Vialle, S. Büttgenbach, A. C. Mueller, A. Pesnelle, and the ISOLDE Collaboration, 1987, Nucl. Phys. A **68**, 1.

Coc, A., C. Thibault, F. Touchard, H. T. Duong, P. Juncar, S. Liberman, J. Pinard, J. Lermé, J. L. Valle, S. Büttgenbach, A. C. Mueller, and A. Pesnelle, 1985, Phys. Lett. **163B**, 66.

De Pinho, A. G., and J. Picard, 1965, Nucl. Phys. **65**, 426.

Drissi, S., J. Kern, and E. Hagn, 1990, Nucl. Phys. A **512**, 413.

Dubbers, F., L. Funke, P. Kemnitz, K. D. Schilling, H. Strusney, E. Will, G. Winter, and M. K. Balodis, 1979, Nucl. Phys. A **315**, 317.

Dudeja, M., S. S. Malik, and A. K. Jain, 1997, Phys. Lett. B **412**, 14.

Elbek, B., and P. O. Tjǿm, 1969, Adv. Nucl. Phys. **3**, 259.

Elmore, D., and W. P. Alford, 1976, Nucl. Phys. A **273**, 1.

Frisk, H., 1988, Z. Phys. A **330**, 241.

Gallagher, C. J., Jr., 1960, Nucl. Phys. **16**, 215.

Gallagher, C. J., Jr., and S. A. Moszkowski, 1958, Phys. Rev. **111**, 1282.

Gareev, F. A. *et al.*, 1973, Part. Nuclei **4**, 357.

Garrett, P. E., and D. G. Burke, 1993, J. Phys. G **19**, 1021.

Garrett, P. E., and D. G. Burke, 1994, Nucl. Phys. A **568**, 445.

Garrett, P. E., and D. G. Burke, 1995, Nucl. Phys. A **581**, 267.

Garrett, P. E., D. G. Burke, Tao Qu, V. Paar, and S. Brant, 1994, Nucl. Phys. A **579**, 103.

Garrett, P. E., N. Warr, H. Baltzer, S. Boehmsdorff, D. G. Burke, M. Délèze, S. Drissi, J. Gröger, C. Günther, J. Kern, S. J. Mannanal, J. Manns, U. Müller, J.-P. Vorlet, and T. Weber, 1996, Nucl. Phys. A **611**, 68.

Girshick, F., K. Krien, R. A. Naumann, G. L. Struble, R. G. Lanier, L. G. Mann, J. A. Cizewski, E. R. Flynn, T. Nail, and R. K. Sheline, 1981, Phys. Lett. **98B**, 29.

Goel, A., 1992, Ph.D. thesis (University of Roorkee).

Goel, A., and A. K. Jain, 1990, Mod. Phys. Lett. A **5**, 2403.

Goel, A., and A. K. Jain, 1996, Pramana, J. Phys. **46**, 51.

Goel, A., and A. K. Jain, 1997, Nucl. Phys. A **620**, 265.

Goel, A., A. K. Jain, R. W. Hoff, and R. K. Sheline, 1991, Pramana, J. Phys. **36**, 105.

Hamamoto, I., 1990, Phys. Lett. B **235**, 221.

Han, X. L., and C.-L. Wu, 1996, At. Data Nucl. Data Tables **63**, 117.

Hara, K., and Y. Sun, 1991, Nucl. Phys. A **531**, 221.

Headly, D. M., R. K. Sheline, P. C. Sood, R. W. Hoff, A. K. Jain, and D. G. Burke, 1998, At. Data Nucl. Data Tables, in press.

Helmer, R. G., and C. W. Reich, 1968, Nucl. Phys. A **114**, 649.

Heyde, K., 1994, in *Capture Gamma Spectroscopy and Related Topics*, Proceedings of the 8th International Symposium, edited by J. Kern (World Scientific, Singapore), p. 13.

Hoff, R.W., 1994, in *Capture Gamma Spectroscopy and Related Topics,* Proceedings of the Eighth International Symposium, edited by J. Kern (World Scientific, Singapore), p. 132.

Hoff, R. W., H. G. Börner, K. Schreckenbach, G. G. Colvin, F. Hoyler, W. Schauer, T. von Egidy, R. Georgii, J. Ott, S. Schründer, R. F. Casten, R. L. Gill, M. Balodis, P. Prokofjevs, L. Simonova, J. Kern, V. A. Khitrov, A. M. Sukhovoj, O. Bersillon, S. Joly, G. Graw, D. Hofer, and B. Valnion, 1996, Phys. Rev. C **54**, 78.

Hoff, R. W., A. K. Jain, J. Kvasil, P. C. Sood, and R. K. Sheline, 1990, in *Exotic Nuclear Spectroscopy*, edited by W. C. McHarris (Plenum, New York), p. 413.

Jain, A. K., 1984, Z. Phys. A **317**, 117.

Jain, A. K., M. Dudeja, S. S. Malik, and Z. Ahmed, 1997, Phys. Lett. B **392**, 243.

Jain, A. K., and M. Dudeja, 1996, J. Korean Phys. Soc. Suppl. **29**, s361.

Jain, A. K., and A. Goel, 1992, Phys. Lett. B **277**, 233.

Jain, A. K., and A. Goel, 1993, Int. J. Mod. Phys. E **2**, 451; **2**, 923(E).

Jain, A. K., A. Goel, and R. Agrawal, 1993, Proc. Nucl. Phys. Symp. (Dept. of Atomic Energy, India) **36B**, 64.

Jain, A. K., J. Kvasil, R. K. Sheline, and R. W. Hoff, 1988, Phys. Lett. B **209**, 19.

Jain, A. K., J. Kvasil, R. K. Sheline, and R. W. Hoff, 1989, Phys. Rev. C **40**, 432.

Jain, A. K., R. K. Sheline, P. C. Sood, and K. Jain, 1990, Rev. Mod. Phys. **62**, 393.

Jain, K., and A. K. Jain, 1992, Phys. Rev. C **45**, 3013.

Jain, S. R., A. K. Jain, and Z. Ahmed, 1996, Phys. Lett. B **370**, 1.

Jones, H. D., 1969, Ph.D. thesis (Florida State University).

Jones, H. D., N. Onishi, T. Hess, and R. K. Sheline, 1971, Phys. Rev. C **3**, 529.

Käppeler, F., H. Beer, and K. Wisshak, 1989, Rep. Prog. Phys. **52**, 945.

Kern, J., A. Raemy, W. Beer, J.-Cl. Dousse, W. Schwitz, M. K. Balodis, P. T. Prokofjev, N. D. Kramer, L. I. Simonova, R. W. Hoff, D. G. Gardner, M. A. Gardner, R. F. Casten, R. L. Gill, R. Eder, T. von Egidy, E. Hagn, P. Hungerford, H. J. Scheerer, H. H. Schmidt, E. Zech, A. Chalupka, A. V.

Murzin, V. A. Libman, I. V. Kononenko, C. Coceva, P. Giacobbe, I. A. Kondurov, Yu. E. Loginov, P. A. Sushkov, S. Brant, and V. Paar, 1991, Nucl. Phys. A **534**, 77.

Khoo, T. L., F. M. Bernthal, R. A. Warner, G. F. Bertsch, and G. Hamilton, 1975, Phys. Rev. Lett. **35**, 1256.

Koch, H. R., H. G. Börner, J. A. Pinston, W. F. Davidson, J. Faudou, R. Roussille, and O. W. B. Schult, 1980, Nucl. Instrum. Methods **175**, 401.

Kreiner, A. J., 1990, in *Exotic Nuclear Spectroscopy*, edited by W. McHarris (Plenum, New York), p. 393.

Kreiner, A. J., J. Davidson, M. Davidson, D. Abriola, C. Pomar, and P. Thieberger, 1987, Phys. Rev. C **36**, 2309; **37**, 1338(E).

Kreiner, A. J., D. Hojman, J. Davidson, M. Davidson, M. Debray, G. Falcone, D. Santos, C. W. Beausang, D. B. Fossan, R. Ma, E. S. Paul, S. Shi, and N. Xu, 1988, Phys. Lett. B **215**, 629.

Kreiner, A. J., and M. A. J. Mariscotti, 1979, Phys. Rev. Lett. **43**, 1150.

Kreiner, A. J., and M. A. J. Mariscotti, 1980, J. Phys. G **6**, L13.

Kvasil, J., A. K. Jain, and R. K. Sheline, 1990, Czech. J. Phys. **40**, 278.

Kvasil, J., V. O. Nesterenko, and I. Hrivnacova, 1991, Czech. J. Phys., Sect. B **41**, 345.

Kvasil, J., R. K. Sheline, V. O. Nesterenko, I. Hrivnacova, and D. Nosek, 1992, Z. Phys. A **343**, 145.

Lasijo, R. S., R. K. Sheline, and Y. Tanaka, 1977, Atom Indonesia **3**, 21.

Leander, G. A., W. Nazarewicz, P. Olanders, I. Ragnarsson, and J. Dudek, 1985, Phys. Lett. **152B**, 284.

Liu, Y., Y. Ma, H. Mang, and S. Zhou, 1995, Phys. Rev. C **52**, 2514.

Mallman, C. A., 1959, Phys. Rev. Lett. **2**, 507.

Mannanal, S. J., B. Boschung, M. W. Carlen, J. Cl. Dousse, S. Drissi, P. E. Garrett, J. Kern, B. Perny, Ch. Rheme, J. P. Vorlet, C. Günther, J. Manns, and U. Müller, 1995, Nucl. Phys. A **582**, 141.

Massmann, H., J. O. Rasmussen, T. E. Ward, P. E. Haustein, and F. M. Bernthal, 1974, Phys. Rev. C **9**, 2312.

Mariscotti, M. A., G. Scharff-Goldhaber, and B. Buck, 1969, Phys. Rev. **178**, 1864.

Matsuzaki, M., 1991, Phys. Lett. B **269**, 23.

Motz, H. T., E. T. Jurney, O. W. B. Schult, R. H. Koch, U. Gruber, B. P. Maier, H. Baader, G. L. Struble, J. Kern, R. K. Sheline, T. von Egidy, T. Elze, E. Bieber, and A. Bäcklin, 1967, Phys. Rev. **155**, 1265.

Neiburg, L. A., P. T. Prokofjev, and Yu. Ya. Tomberg, 1972, Izv. Akad. Nauk. SSSR, Ser. Fiz. **36**, 2555 [Bull. Acad. Sci. USSR, Phys. Ser. **36**, 2220 (1972)].

Nesbet, R. K., 1963, J. Math. Phys. **4**, 1262.

Neugart, R., W. Arnold, W. Borchers, W. Neu, G. Ulm, and K. Wendt, 1988, in *New Techniques and Results of Collinear Laser Spectroscopy*, *Proceedings of the 5th International Conference on Nuclei Far From Stability*, Rosseau Lake, Canada, 1987, AIP Conference Proceedings No. 164, edited by I. S. Towner (AIP, New York), p.126.

Newby, N. D., Jr., 1962, Phys. Rev. **125**, 2036.

Nosek, D., J. Kvasil, R. K. Sheline, P. C. Sood, and J. Nosková, 1994, Int. J. Mod. Phys. E **3**, 967.

Nosek, D., J. Kvasil, F. Sterba, and P. Holan, 1989, Czech. J. Phys., Sect. B **39**, 494.

Nosek, D., R. K. Sheline, P. C. Sood, and J. Kvasil, 1992, Phys. Rev. C **46**, 2311.

Nosek, D., F. Sterba, and P. Holan, 1985, Acta. Univ. Crolinae-Mathematica et Physica **26**, 3.

Nuclear Wallet Cards, 1995, edited by J. K. Tuli (National Nuclear Data Center, Brookhaven, NY).

Olivier, W. A., W.-T. Chou, A. Rios, W. C. McHarris, and R. Aryaeinejad, 1990, in *Exotic Nuclear Spectroscopy*, edited by W. McHarris (Plenum, New York), p. 379.

O'Neil, R. A., and D. G. Burke, 1972, Nucl. Phys. A **195**, 207.

Paar, V., 1979, Nucl. Phys. A **331**, 16.

Peker, L. K., 1960, Izv. Akad. Nauk SSSR, Ser. Fiz. **24**, 365 [Bull. Acad. Sci. USSR, Phys. Ser. **24**, 350 (1960)].

Perny, B., J. Cl. Dousse, M. Gasser, J. Kern, R. Lanners, Ch. Rhême, and W. Schwitz, 1988, Nucl. Instrum. Methods Phys. Res. A **267**, 120.

Phillips, W. R., I. Ahmad, H. Emling, R. Holzmann, R. V. F. Janssens, T.-L. Khoo, and M. W. Drigert, 1986, Phys. Rev. Lett. **57**, 3257.

Phillips, W. R., R. V. F. Janssens, I. Ahmad, H. Emling, R. Holzmann, T.-L. Khoo, and M. W. Drigert, 1988, Phys. Lett. B **212**, 402.

Polikanov, S. M., 1968, Sov. Phys. Usp. **11**, 22.

Pyatov, N. I., 1963, Izv. Akad. Nauk SSSR, Ser. Fiz. **27**, 1436.

Ragnarsson, I., and P. B. Semmes, 1988, Hyperfine Interact. **43**, 425.

Ring, P., and P. Schuck, 1980, *The Nuclear Many-Body Problem* (Springer, New York).

Ritz, W., 1908, Phys. Z. **9**, 521.

Scharff-Goldhaber, G., C. B. Dover, and A. L. Goodman, 1976, Annu. Rev. Nucl. Sci. **26**, 239.

Scharff-Goldhaber, G., and K. Takahashi, 1967, Izv. Akad. Nauk SSSR, Ser. Fiz. **31**, 38 [Bull. Acad. Sci. USSR, Phys. Ser. **31**, 42 (1967)].

Semmes, P. B., and I. Ragnarsson, 1991, in *High-Spin Physics and Gamma-Soft Nuclei*, edited by J. X. Saladin, C. M. Vincent, and R. A. Sorensen (World Scientific, Singapore), p. 500.

Semmes, P. B., and I. Ragnarsson, 1992, in *Future Directions in Nuclear Physics with* 4π *Gamma Detection Systems*, edited by J. Dudek and B. Haas (AIP, New York), p. 566.

Shahabuddin, M. A. M., J. C. Waddington, D. G. Burke, O. Straume, and G. Løvhøiden, 1978, Nucl. Phys. A **307**, 239.

Sheline, R. K., 1989, Phys. Lett. B **219**, 222.

Sheline, R. K., A. K. Jain, and K. Jain, 1988, Phys. Rev. C **38**, 2952.

Sheline, R. K., J. Kvasil, C. F. Liang, and P. Paris, 1991, Phys. Rev. C **44**, R1732.

Sheline, R. K., and P. C. Sood, 1986, Phys. Rev. C **34**, 2362.

Sheline, R. K., and P. C. Sood, 1989a, Prog. Theor. Phys. **81**, 1057.

Sheline, R. K., and P. C. Sood, 1989b, Mod. Phys. Lett. A **4**, 1329.

Sheline, R. K., and P. C. Sood, 1990, Int. J. Mod. Phys. A **5**, 2677.

Sheline, R. K., C. E. Watson, B. P. Maier, U. Gruber, R. H. Koch, O. W. B. Schult, H. T. Motz, E. T. Jurney, G. L. Struble, T. von Egidy, T. Elze, and E. Bieber, 1966, Phys. Rev. **143**, 857.

Singh, B., R. B. Firestone, and S. Y. Frank Chu, 1996, Nucl. Data Sheets **78**, 1.

Singh, R. N., and P. C. Sood, 1982, J. Phys. G **8**, 231.

Slaughter, M. F., R. A. Warner, T. L. Khoo, W. H. Kelly, and C. McHarris, 1984, Phys. Rev. C **29**, 114.

Sobiczewski, A., Z. Patyk, S. Cwiok, and P. Rozmei, 1988, Nucl. Phys. A **485**, 16.

Soloviev, V. G., 1971, *Theory of Complex Nuclei* (Nauka, Moscow; translation Pergamon, Oxford, 1976).

Soloviev, V. G., and P. Vogel, 1967, Nucl. Phys. A **92**, 449.

Sood, P. C., and D. G. Burke, 1995, Phys. Rev. C **51**, 2226.

Sood, P. C., D. M. Headly, and R. K. Sheline, 1991, At. Data Nucl. Data Tables **47**, 89.

Sood, P. C., D. M. Headly, R. K. Sheline, and R. W. Hoff, 1994, At. Data Nucl. Data Tables **58**, 167.

Sood, P. C., R. W. Hoff, and R. K. Sheline, 1986, Phys. Rev. C **33**, 2163.

Sood, P. C., and R. S. Ray, 1986, Pramana, J. Phys. **27**, 537.

Sood, P. C., and R. K. Sheline, 1987a, Phys. Rev. C **35**, 1958.

Sood, P. C., and R. K. Sheline, 1987b, Nucl. Instrum. Methods Phys. Res. B **24/25**, 473.

Sood, P. C., and R. K. Sheline, 1989a, At. Data Nucl. Data Tables **43**, 259.

Sood, P. C., and R. K. Sheline, 1989b, Mod. Phys. Lett. A **4**, 1711.

Sood, P. C., and R. K. Sheline, 1989c, Phys. Rev. C **40**, 1530.

Sood, P. C., and R. K. Sheline, 1990a, Phys. Scr. **42**, 25.

Sood, P. C., and R. K. Sheline, 1990b, Pramana, J. Phys. **35**, 329.

Sood, P. C., and R. K. Sheline, 1992, in *Spectroscopy and Structure of Molecules and Nuclei*, edited by N. R. Johnson and M. El Sayed (World Scientific, Singapore), p. 69.

Sood, P. C., R. K. Sheline, and R. S. Ray, 1987, Phys. Rev. C **35**, 1922.

Sood, P. C., and R. N. Singh, 1982, Nucl. Phys. A **373**, 519.

Stephens, F. S., M. A. Deleplanque, J. E. Draper, R. M. Diamond, A. O. Macchiavelli, C. W. Beausang, W. Korten, W. H. Kelly, F. Azaiez, J. A. Becker, E. A. Henry, S. W. Yates, M. J. Brinkman, A. Kuhnert, and J. A. Cizewski, 1990, Phys. Rev. Lett. **65**, 301.

Struble, G. L., J. Kern, and R. K. Sheline, 1965, Phys. Rev. **137**, B772.

Struble, G. L., R. G. Lanier, L. G. Mann, R. T. Kouzes, D. Mueller, R. A. Naumann, F. Girshick, I. C. Oelrich, and W. H. Moore, 1978, Phys. Rev. Lett. **40**, 615.

Tanaka, Y., R. S. Lasijo, R. K. Sheline, and Y. Oda, 1979, Prog. Theor. Phys. **62**, 1266.

Toki, H., H. L. Yadav, and A. Faessler, 1977a, Phys. Lett. **66B**, 310.

Toki, H., H. L. Yadav, and A. Faessler, 1977b, Phys. Lett. **71B**, 1.

Toki, H., H. L. Yadav, and A. Faessler, 1979, Z. Phys. A **292**, 79.

Thompson, R. C., A. Ikeda, P. Kleinheinz, R. K. Sheline, and P. J. Daly, 1975, Phys. Lett. **55B**, 447.

Twin, P. J., B. M. Nyako, A. H. Nelson, J. Simpson, M. A. Bentley, H. W. Cranmer-Gordon, P. D. Forsyth, D. Howe, A. R. Mokhtar, J. D. Morrison, J. F. Sharpey-Schafer, and G. Sletten, 1986, Phys. Rev. Lett. **57**, 811.

Urban, W., R. M. Lieder, J. C. Bacelar, P. P. Singh, D. Alber, D. Balabanski, W. Gast, H. Grawe, G. Hebbinghaus, J. R. Longman, T. Morek, R. F. Noorman, T. Rzaca-Urban, H. Schnare, M. Thoms, O. Zell, and W. Nazarewicz, 1991, Phys. Lett. B **258**, 293.

Urban, W., R. M. Lieder, W. Gast, G. Hebbinghaus, A. Krämer-Flecken, K. P. Blume, and H. Hübel, 1987, Phys. Lett. B **185**, 331.

Venkova, Ts., R. M. Lieder, T. Morek, W. Gast, G. Hebbinghaus, A. Krämer-Flecken, J. Schäffler-Kräh, W. Urban, G. Sletten, H. Kluge, and K. H. Maier, 1990, Nucl. Phys. A **514**, 87.

Vergnes, M. N., and R. K. Sheline, 1963, Phys. Rev. **132**, 1736.

Vermeer, W. J., M. K. Khan, A. S. Mowbray, J. B. Fitzgerald, J. A. Cizewski, B. J. Varley, J. L. Durell, and W. R. Phillips, 1990, Phys. Rev. C **42**, R1183.

Wallmeroth, K., G. Bollen, A. Dohn, P. Egelhof, U. Krönert, M. J. G. Borge, J. Campos, A. Rodriguez Yunta, K. Heyde, C. de Coster, J. L. Wood, H.-J. Kluge, and the ISOLDE Collaboration, 1989, Nucl. Phys. A **493**, 224.

Ward, T. E., P. E. Haustein, J. B. Cumming, and Y. Y. Chu, 1974, Phys. Rev. C **10**, 1983.

Yoshida, N., H. Sagawa, and J. Otsuka, 1994, Nucl. Phys. A **567**, 17.

Yu, C. H., D. M. Cullen, D. Cline, M. Simon, D. C. Radford, I. Y. Lee, and A. O. Macchiavelli, 1996, in *Proceedings of the Workshop on Gammasphere Physics*, edited by M. A. Deleplanque, I. Y. Lee, and A. O. Macchiavelli (World Scientific, Singapore), p. 254.

Zylicz, J., P. G. Hansen, H. L. Nielsen, and K. Wilsky, 1967, Ark. Fys. **36**, 643.